Order Number 9325125

The mechanism of formation and the structure of microemulsions

Lyons, George Bernard, Ph.D.

City University of New York, 1993

U·M·I
300 N. Zeeb Rd.
Ann Arbor, MI 48106

A

The MECHANISM of FORMATION and the STRUCTURE of MICROEMULSIONS

b y

George Bernard Lyons

A dissertation submitted to the Graduate Faculty in Chemistry in partial fulfillment for the degree of Doctor of Philosophy, the City University of New York.

This manuscript has been read and accepted for the Graduate Faculty in Chemistry in satisfaction of the dissertation requirement for the degree of Doctor of Philosphy.

04/20/1993
Date

Helen J. Rosano
Chair of Examining Committee

4/22/93
Date

Executive Officer

David C. Locke

John Arento

Charles J. Conte
Supervisory Committee

The City University of New York

Abstract

The MECHANISM of FORMATION and the STRUCTURE of MICROEMULSION SYSTEMS

by

George Lyons

Adviser: Dr. Henri L. Rosano

The subject of this dissertation is the formation and structure of microemulsion systems. At the initiation of this dissertation there was some disagreement as to whether microemulsion systems are thermodynamically or kinetically stable systems. We assume that each one of the microemulsion systems investigated in Chapter 2 and 3 are thermodynamically stable systems. Once this assumption was postulated, the thermodynamic properties associated with microemulsion formation were determined for each microemulsion system investigated. For each system investigated in Chapter 2 and 3, the change in free energy associated with microemulsion formation are small negative numbers. This shows that the process is spontaneous for each system investigated. However the driving force in transforming an emulsion into a microemulsion is small. Therefore we conclude that the microemulsion systems prepared by the titration method in Chapter 2 and 3 are thermodynamically stable systems.

The remainder of this thesis is dedicated to investigating the size and structure of the microdroplets in oil-in-water microemulsion systems. In Chapter 4 the size of the microdroplets is measured by the technique of D.C. polarography. This technique depends on tagging the microdroplet with an oil soluble electroactive probe and measuring the diffusion current of this reducible species. Microdroplet radii were found to increase as the volume fraction of dispersed phase (oil) increased for the oil-in-water microemulsion systems and prepared at constant amount of primary surfactant and investigated by D.C. polarography .

In Chapter 5 the size of the microdroplets in two different oil-in-water microemulsion systems is measured by vapor pressure measurements. From the vapor pressure measurements two different regimes of phase behavior are found for these systems. One region occurs at low volume fraction of dispersed phase and the phase behavior is characterized by a vapor pressure lowering in this region. The microdroplets can be described as isolated and noninteracting particles in the low dispersed volume fraction region. At high volume fraction of dispersed phase the microdroplets in these systems begin to interact and the vapor pressure increases dramatically.

Acknowledgement

I do hereby wish to express my sincere desire to thank all of the different people who have helped me to complete this dissertation. It is impossible to mention everyone who has had some small hand in this great undertaking and all of those people who in any way connected to me have helped me build a greater foundation on which to build my life. Let me try to name some of the people who foremost come to mind in connection with the completion of this dissertation. I would like to first mention my friend and mentor, Dr. Henri Rosano, whose guidance and supervision was much appreciated. I would like to thank the members of my doctoral dissertation committee: Dr. John Arents, Dr. David Locke, and Dr. Charles Cante. I would like to mention some other names of people who you the reader will in most instances not recognize but to me these people shall always be remembered by me for for as long as I should come to prevail in this universe in whatever manner of being. I would like to thank Dr. Hilton Weiss, Dr. Albert Heurich, and Dr. Peter Skiff. I would also like to mention my brother Harold, Jr., or should I say Butchie, my good friend David Feingold, my amazing brother Bobby, and of course my daughter Jessica. All of these people have inspired me and made me realize the miracle and beauty that is life. Lastly I most certainly need to mention both of my parents, Dr. Harold Aloysius Lyons and Rita Wood Lyons.

Table of Contents

List of Figures

Chapter 1

Chapter 2

Chapter 3

List of Tables

Chapter 2

Chapter 3

Chapter 4

Chapter 5

CHAPTER 1: INTRODUCTION

1.1. Introduction

Usually, oil and water phases are immiscible. Pseudo one-phase systems consisting of oil, water, and surfactant are called emulsions. Emulsions are formed when oil, water, and surfactant are mixed together in the proper ratio so that one phase becomes dispersed as large particles in the other phase. Coarse emulsions are optically opaque and usually separate with time.

Emulsions are of two types: oil in water (o/w) or water in oil (w/o). These systems are stabilized by the presence of amphipathic molecules called surfactants. These molecules have the ability to adsorb at the oil/water interface and reduce the interfacial tension γ_i between the oil and water phases. Due to the size of the particles in the dispersed phase, on the order of 100 nm in diameter, these systems appear milky. In some cases, transparent mixtures of oil and water can be prepared with the proper combination of surface active materials. If the size of the dispersed particles can be diminished to one-quarter the wavelength of visible light, then these systems are transparent since they scatter very little visible light. The term microemulsion was first proposed by Schulman et al. (1) to describe these isotropic and transparent one-phase dispersions of oil, water, and surfactant.

The phenomenum of microemulsion formation is documented extensively. This chapter provides a brief review of many notable investigators who have contributed to comprehending both the mechanism of formation and the structure of microemulsion systems.

1.2. The Schulman Microemulsion

In 1943, Hoar and Schulman (2) noted that oil/alkali-metal soap (or cationic soap, such as cetyl trimethyl ammonium bromide)/ alcohol/ water systems of certain concentrations exist as transparent, electrically non-conducting dispersions, in which oil is the con-

tinuous phase. These transparent water-in-oil dispersions show a slight Tyndall effect. In agreement with the optical properties of these systems, the existence of an oleopathic hydro-micelle, analogous to the hydrophilic swollen micelle, was postulated. A spherical microdroplet core of dispersed water surrounded by a monolayer sheath of amphipathic molecules was visualized for the microstructure of these transparent water-in-oil systems. In this hypothetical "inverted" micelle, the hydrophobic and hydrophilic portions of the amphipathic molecules were believed to be oriented so that the inner, aqueous core was juxtaposed near the hydrophilic portion of the amphipathic molecule and the oil-continuous phase was in juxtaposition near the outer, hydrophobic portion of the amphipathic molecule. They referred to these water-in-oil dispersions as oleopathic hydro-micelle as opposed to the well-known swollen micelle. Additionally, they termed oil-in-water dispersions as hydrophilic swollen micelle. They further stated that two essential conditions necessary for the formation of these transparent oil-continuous systems are: (1) high soap/ water ratio, and (2) the presence of an alcohol, fatty acid, amine, or other non-ionized amphipathic substance in mole-fraction approximately equal to that of the soap. Dilution of these oil-continuous systems with excess water inverts them to oil-in-water emulsions which are milky for low soap/ oil ratios and transparent for high soap/ oil ratios.

In 1960, Schulman, Stoekenius, and Prince (1) referred to these oil-in-water or water-in-oil optically isotropic and transparent systems as "microemulsons." Using high-resolution electron microscopy, direct visual observation of the structures in microemulsion systems systems was obtained by Schulman, Stoekenius, and Prince. From these electron microscopic experiments the microemulsion systems investigated by these workers were found to have a microstructure consisiting of dispersed spherical droplets. From the direct visual examination of the optical image generated by electron beam in these experiments, spherical droplet diameters ranging from 75-1200 Å were clearly observed using high-resolution electron microscopy. Subsequently, Schulman and coworkers investigated the size of dispersed microdroplets in this microemulsion system by low-angle x-ray diffraction and light scatter-

ing. These workers reported that the droplet diameters observed in electron microscopy experiments agree with the diameters calculated from low-angle x-ray diffraction experiments (3) for the same microemulsion system.

1.3. Metastable Negative Interfacial Tension

The first attempt to explain the formation of microemulsion systems was presented by Schulman in 1960. According to Schulman (1,4-5), the basic physical chemistry criterion necessary for microemulsion formation was a metastable negative interfacial tension. Schulman suggested the metastable negative interfacial tension could be produced by a mixed interfacial film composed of surfactant and cosurfactant. For an oil-in-water microemulsion, Schulman noted that increased surface pressure is produced through penetration of the mixed film by the oil molecules at the oil/water interface (6-8). Microemulsion formation involves a large increase in interfacial area. Schulman suggested that the increase in surface pressure and resulting increase in interfacial area is the basis for microemulsion formation. Schulman hypothesized that a metastable negative interfacial tension would allow a negative free energy variation $-\gamma_i\, dA$ (where γ_i = interfacial tension and A = interfacial surface area), which could be used to break up the macro-droplets. According to Schulman, the interfacial film would help to stabilize the dispersed phase droplets and prevent phase separation. Schulman concluded that macroemulsions, on the other hand, form before the interfacial tension reaches zero. Unlike stable microemulsion systems, eventual phase separation will occur in macroemulsions. The total interfacial tension can be defined by equation (1.1).

$$\gamma_i = \gamma_{o/w} - \pi_i \qquad (1.1)$$

where $\gamma_{o/w}$ = interfacial tension without the addition of amphipathic molecules;

π_i = the spreading pressure induced by the amphipathic molecules;

and γ_i = the interfacial tension of the oil/water interface after amphipathic molecule (or mixed film) has been added.

Thus if π_i is greater than $\gamma_{o/w}$, Schulman concluded that there will be a negative interfacial tension γ_i and a microemulsion will form spontaneously since there is now free energy available to increase the interfacial area. According to Schulman (1,4-5), the equilibrium condition will be reached when $\pi_i = \gamma_{o/w}$ or at zero interfacial tension. However, if π_i is less than $\gamma_{o/w}$, Schulman concluded that a macroemulsion will form, since the interfacial tension is now positive.

The idea of a metastable negative interfacial tension necessary for microemulsion formation requires a high surface spreading pressure from the interfacial film. An essential feature of these systems is that molecules of the dispersed phase must penetrate or associate with the molecules forming the interphase. This results in an increase in surface spreading pressure. Duplex film (6-8) experiments have shown that large surface spreading pressures occur for systems capable of producing a microemulsion. To form a duplex film, a mixture of hydrocarbon and surfactant is spread on a Langmuir trough, creating two interfaces (i.e., oil/water and oil/air) which behave independent of one another. Since the interface would break up and spontaneously emulsify, the direct measurement of the metastable negative interfacial tension at the oil/water interface is impossible to determine. However if a counter tension is placed on the interfacial measuring device (for example a Wilhelmy plate) to support the interface and to prevent surface breakup, then the interfacial spreading pressure and metastable negative interfacial tension can be calculated indirectly by equation (1.2).

$$\gamma_i = \gamma_{o/w} - \pi_i = \gamma_{a/w} - \gamma_{o/a} - \pi_d \qquad (1.2)$$

where π_d = is the counter tension (collapse pressure) obtained by the pull on a Wilhelmy plate at a duplex film;

$\gamma_{a/w}$ = surface tension at aqueous/air interface;

and $\gamma_{o/a}$ = surface tension at oil/air interface.

Except for γ_i and π_i , all terms are experimentally determined. This allows π_i and γ_i to be

easily calculated. To illustrate the concept of the duplex film method, the following example is given. To produce a negative interfacial tension π_i would have to be greater than 50 dynes/cm if n-hexadecane is used as the oil phase (where $\gamma_{o/w}$ = 50 dynes/cm, $\gamma_{o/a}$ = 29 dynes/cm and $\gamma_{a/w}$ = 72 dynes/cm). Incorporating these values into eq (1.2) we have:

$$\gamma_i = 50 - \pi_i = 72 - 29 - \pi_d \qquad (1.2)$$

The measured collapse pressure π_d would then have to be greater than 43 dynes/cm. Values higher than 43 dynes/cm were found if stearic acid and n-hexadecane were spread on an aqueous phase containing 2-amino-2-methyl-1-propanol at a pH = 10.4. Spontaneous microemulsification should occur for this system and in fact this system is capable of producing a microemulsion. These data reinforce the idea that oil molecules are able to penetrate mixed interfacial films during microemulsion formation, reducing the interfacial pressure required for microemulsion formation.

In 1965 Prince modified Schulman's concept of metastable negative interfacial tension (9). Noting that the distribution of alcohol between the oil phase and the interface is different for each oil (10), Prince concluded that the oil/water surface tension in equation 1.2 should be replaced by the term $(\gamma_{o/w})_a$,where $(\gamma_{o/w})_a$ is the surface tension of water against oil plus its fraction of alcohol. Therefore the condition of metastable interfacial tension should be written according to equation 1.3:

$$\gamma_i = \gamma_{(o/w)a} - \pi_i \qquad (1.3)$$

It follows that negative interfacial tension may be achieved not so much by a great increase in surface pressure as by substantial depression in $(\gamma_{o/w})_a$. This depression is brought about by the spontaneous distribution of alcohol between the interface and the oil phase. Therefore the film pressure required to reduce the interfacial tension below zero was much lower than previously expected.

1.4. Mixed Film Theory

In 1955 Bowcott and Schulman (4) noted that from earlier results of monolayer penetration experiments (6-8) at the air/water interface, it is evident that alcohol molecules are penetrating between soap molecules and disordering the regular condensed two dimensional packing in the micelles to produce a liquid interphase. They concluded that this permits surface tension forces to act at the liquid interface and produce a curvature according to the diffference in tension between the hydrocarbon portion of the interphase molecules and the oil phase, and the polar portion of the interphase molecules and the water phase. They noted that the effect of forming a mixed film between a water soluble soap and an oil soluble amphipathic molecule is to lower the interfacial tension between the oil and water phases to only a fraction of a dyne/cm. This was considered the basis for spontaneous microemulsification. This theory was referred to as the Mixed Film Theory by Bowcott and Schulman. The Mixed Film Theory considered the balance between the hydrophilic and hydrophobic nature of the interphase. This theory stated that if the mixed monolayer is liquid then the phase continuity will be determined by the curvature brought about by two opposing surface tension forces: γ_{mo} , the interfacial tension between the mixed monolayer and the oil phase; and γ_{mw} , the interfacial tension between the mixed monolayer and the water phase. These two surface tension forces are juxtaposed on opposite sides of the interphase. The Mixed Film Theory predicts that the system will produce a w/o (water-in-oil) microemulsion when the interfacial tension between the mixed monolayer and aqueous phase is greater than the interfacial tension between the mixed monolayer and the oil phase. Likewise, if the interfacial tension between the mixed monolayer and the oil phase is greater than the interfacial tension between the mixed monolayer and the aqueous phase, the system will produce a o/w (oil-in-water) microemulsion. Summarizing briefly:

If $\gamma_{mw} > \gamma_{mo}$ then system will produce a w/o microemulsion.

If $\gamma_{mo} > \gamma_{mw}$ then system will produce a o/w microemulsion.

These ideas were illustrated using microemulsions of benzene/ water/ sodium oleate/and alchohol (where the alcohol was titrated into the system). Thus, to change a microemulsion from an oil-continuous to water-continuous system it is necessary to increase γ_{mo} relative to γ_{wo}. By decreasing the n-alkyl chainlength of the alcohol the nature of the interphase is more hydrophilic and less paraffinic (hydrophobic) for these mixed film systems. This effect can also be affected by using an oil with a larger interfacial tension with respect to water. They summarized the conditions governing the phase continuity of transparent oil/ water/ surfactant dispersions using the following four general rules:

1) If the interfacial film is ionized the system will be o/w, since the charges will by mutual repulsion orient the film molecules with their ionized groups outwards.

2) If the stabilizing agent is unionized and preferably soluble in oil, the system will be w/o.

3) If the stabilizing agent is unionized and preferably soluble in water, the system will be o/w.

4) Addition of salt to remove the diffuse layer and surface charge in case 1 will make the agent behave as in case 2 or 3.

1.5. Limitations of the Schulman Mechanism of Microemulsion Formation

As espoused by Schulman and Prince, the concept of a metastable negative interfacial tension and the ideas generated by the Mixed Film Theory have had a profound impact on the field of microemulsions. These two theories have undergone a substantial amount of discussion, refinement, and reformulation. These two theories provided the first impetus to explain the formation of these transparent dispersions and they provide a simple feeling for the balance of forces involved in microemulsion formation. However, there are many limitations to the Schulman arguments used to explain microemulsion formation. The concept of metastable negative interfacial tension fails to consider curvature effects for microemulsion formation. These two theories also neglect to mention entropy effects and they fail to

consider electrostatic surface energies or interaction energies between different droplets.

1.6. Shinoda Mechanism of Microemulsion Formation

Whereas the Schulman model of microemulsion formation focused on a transitory negative interfacial tension, Shinoda and Friberg (11-16) presented another theory to explain microemulsion formation. Their theory was concerned with the solubilization properties of oil/water/ and surfactant systems. For a system prepared with 10% nonylphenol-7.4-ethylene oxide/ 90% cyclohexane mixture and water, they noted that the solubilization of oil in water containing a certain amount of nonionic surfactant increases drastically at an optimum temperature below which solution splits into an oil phase and an aqueous surfactant phase. This temperature is referred to as the phase-inversion temperature (PIT) and is demarcated by the cloud point. At this temperature, a rather large amount of oil and all the water is dissolved by the surfactant phase. If we further increase the temperature, we eventually reach the solubilization limit of water. Beyond this temperature the water is no longer soluble in the surfactant phase. Above the solubilization limit temperature, the system splits into a water phase and a surfactant phase containing oil.

Shinoda and Friberg noted that surfactant dissolves in water in singly dispersed state up to the saturation concentration above which micelles are formed at temperatures above the melting point (or Kraft point) of the hydrated surfactant, and hydrated solid surfactant phase separates below the melting point. Somewhat above the Kraft point, water dissolves in nonionic surfactant phase infinitely at lower temperature and an aqueous micellar solution in equilibrium with excess oil phase is obtained. At an intermediate temperature, when the hydrophile/ lipophile of surfactant is just balanced the solubilities of water and oil in surfactant are both finite and a surfactant phase in equilibrium with excess water and oil is obtained. At higher temperatures, hydrocarbon will dissolve infinitely in surfactant phase and a reversed micellar solution is obtained in equilibrium with excess water phase. Reversed micelles may solubilize a finite volume of water at higher temperatures. Analogously, micelles may solubilize a finite volume of oil at lower temperatures. Surfactant

phase separates from excess water in solutions above the cloud point, because the hydrophilic/ lipophilic property of nonionic surfactant shifts to more lipophilic with a temperature increase.

Shinoda characterized the change in phase behavior of these oil, water, and surfactant systems. A transition in the behavior of the surfactant phase occurs as one increases the temperature or changes the HLB (Hydrophile-Lipophile Balance). Characteristically, these systems go from a two phase (lower surfactant and upper oil) to three phase (lower water, middle surfactant, and upper oil) to two phase system (lower water and upper surfactant). The behavior of these systems is illustrated most effectively by a Shinoda phase diagram. A Shinoda phase diagram corresponds to the situation where the system is constituted from equal volumes of oil and water. Shinoda and Friberg noted that with an increase in temperature the behavior of the surfactant phase undergoes a transition from a hydrophilic to lipophilic system. They described this process as a continuous change in the HLB (Hydrophile/ Lipophile Balance) of the surfactant phase. These workers also noted that the continuous change in the behavior of the nonionic surfactant phase that occurs by increasing the temperature can be affected by other methods. For example, decreasing the hydrophilic chainlength of a nonionic surfactant increases the lipophilic tendencies of the surfactant phase. The addition of a lipophilic cosurfactant can also increase the HLB of a surfactant phase. They also noted that the HLB of the nonionic surfactant phase increases by increasing the salt concentration of the system. However, these workers also noted that a temperature change usually does not affect the HLB of a hydrophilic, ionic surfactant. However, the continuous change from an aqueous micellar solution to middle surfactant phase, and finally, to nonaqueous reversed micellar solution can be affected by the addition of a lipophilic cosurfactant or by increasing the salt concentration in the oil/ water/ and ionic surfactant system.

The continuous change in the behavior of the surfactant phase described by Shinoda and Friberg can be extended to include the formation of microemulsion systems. In this

context we can consider both water-in-oil and oil-in-water microemulsion systems to correspond to the upper right and lower left of a Shinoda phase diagram respectively. Moreover, if a sufficient quanity of surfactant is available, the three-phase system may be replaced by a one-phase system.

1.7. Entropy Effects of Microemulsion Formation

Entropy effects for microemulsion formation were first mentioned by Ruckenstein and Chi (17-19). They considered the free energy of microemulsion formation to consist of three contributions (eq. 1.4):

$$\Delta G_m = \Delta G_1 + \Delta G_2 + \Delta G_3 \qquad (1.4)$$

ΔG_1 = the change in interfacial free energy;

ΔG_2 = the interaction free energy between droplets;

ΔG_3 = the effect caused by the entropy of dispersion.

ΔG_1 , the interfacial free energy, consists of the specific free energy of the uncharged surface and the specific free energy for the formation of the electrical double layer. A Debye-Huckel approximation was used to determine the specific free energy for the formation of the double electrical layer. A pairwise additivity of interaction potentials was assumed to calculate ΔG_2 , the interaction free energy between droplets. The pair potential was composed of a Van der Waals attraction potential and an electrical double layer repulsive potential. ΔG_3, the effect caused by the entropy of dispersion, is calculated using a Boltzmann relation for the entropy of mixing. A lattice model is used to represent the number of configurations in the Boltzmann relation of a liquid mixture formed from M molecules of the continuous phase and N molecules of the dispersed phase, where the N molecules are in the form of m equal-sized droplets. At constant values of the dispersed phase, the computational procedure involves calculating the variation of the free energy, ΔG_m , with the radius, R, of the droplet. The computer technique generated four different types of curves of the variation of ΔG_m with R. Two of these curves relate to negative free energy changes

for microemulsion formation, while the other two curves correspond to positive free energy changes for microemulsion formation. Microemulsions will form if negative values of ΔG_m are obtained. The value of R which yields the minimum value of ΔG_m^* (denoted by R^*) is the most stable droplet size for a given volume fraction of the dispersed phase. For cases where the free energy change is always positive, only emulsions which are thermodynamically unstable can be formed. However it is possible that a kinetically stable microemulsion could form in this case. Phase inversion occurs at that volume fraction for which values of ΔG^* for both types of microemulsions are equal.

The entropy effect generated by a very flexible, fluctuating interface has also been considered by Talmon and Prager (20). For microemulsion systems, the interface is very soft and may be randomly bent at large scales (100 Å). These workers demonstrated that, in the absence of other interaction effects, this entropy term may impose certain phase transitions; when the amount of surfactant is decreased, they predict that the microemulsion separates into two phases (oil rich and water rich). They developed a statistical thermodynamic model of microemulsions using a one-parameter free energy function (itself composed of three model parameters). The resulting one-parameter free energy function predicts the transition from a two-phase to three-phase to two-phase equilibria for these computer-modelled systems. Their model bears a strong resemblance to phase behavior which is characteristic of experimental microemulsion systems. This corresponds to phase behavior characterized by Shinoda and Friberg (11-16) where a continuous change from a two-phase to three-phase to two-phase system occurs with a concurrent change in the HLB (Hydrophile- Lipophile Balance). In this model they made the following simplifications:

1) Microemulsions were considered three-component systems, regardless of the number of components actually present.

2) The oil and water components are considered to be completely immiscible at the molecular level.

3) The entire internal interface separating the oil and water regions is covered by a surfactant monolayer.

4) The volume fraction of surfactant is negligible.

They represented the structure of microemulsions to be a random geometry of interspersed oil and water domains generated by Voronoi tesselation (21), with the surfactant monolayer adsorbed at the boundary between these two domains. Voronoi tesselation considers only those configurations of the internal surface between the oil and water domains generated by a two-step procedure. The first step involves subdividing the volume V of a microemulsion into random polyhedra by placing N = c V Poisson points completely at random within V (i.e., with no correlation between positions of different points), and then associating with each of these nuclei the polyhedral region (polytope) lying closer to it than any other. In the second step the polytopes are randomly selected to be filled with water or oil, with the probability of placement of water or oil corresponding to the volume fraction of oil or water. Clearly this generates a computer simulation model where by gradually increasing the oil to water ratio V_o / V_w , we can generate random three-dimensional structures which pass continuously from an oil-in-water geometry at low V_o / V_w to a bicontinuous geometry at intermediate V_o / V_w to a water-in-oil geometry at high V_o / V_w .

However there are some limitations to this theory. In the absence of independent estimates of the model constants the quantitative predictions of the theory are limited to statements about the compositions of individual microemulsion phases coexisting in three-phase equilibria. Also the model only considers free energy functions generated by entropy effects with no explicit energy terms included. This carries the implication that the predicted phase equilibria should be temperature independent, in contradiction to experimental fact. In actuality an explicit energy term is introduced in this model through the assumption (22) that all the surfactant in the system is adsorbed at the oil-water boundary. Such optimal performance of surfactant is the result of a delicate balance between the

hydrophilic and lipophilic moieties of the surfactant molecules, a balance which is sensitive not only to temperature but also to the concentration of cosurfactant and the salinity of the water component (23-24). The theory developed in this paper applies only to the narrow range of conditions in which the surfactant system is close to optimal to allow formation of a microemulsion, and even within this range one would expect the model parameters to vary with temperature, cosurfactant concentration, and salinity.

1.8. Curvature Effects of Microemulsion Formation

The Schulman description of microemulsion formation also ignores all energies associated with the curvature of the interface. Indeed, for many problems involving fluid/ fluid interfaces, curvature energies represent only a very minor correction and the interfacial energy γ_i dA dominates the behavior. However, for microemulsion systems we are dealing with interfaces where the interfacial energy nearly vanishes (i.e., γ_i approaches zero), and curvature effects become relevant. The rigidity and spontaneous curvature of the interface has been considered by Helfrich (25). In this paper by Helfrich, the curvature of the film is defined by the parameter 1/R and the rigidity of the film is defined by the parameter K (or alternatively, the film flexibility parameter may be defined as the inverse K^{-1} of the rigidity). For a curvature 1/R we expect an energy contribution per unit area of the film:

$$F = \gamma - \frac{K}{R_0 R} + \frac{K}{2R^2} \tag{1.5}$$

In this expression, the rigidity of the interface K has the dimensions of energy and $1/R_o$ is defined as the spontaneous curvature of the interface and can be of either sign (i.e., we count R_o as positive for direct micelles and negative for inverse micelles).

Mitchell and Ninham (26) have considered curvature effects for microemulsion systems. They developed a theory of self-assembly of surfactant molecules into micelles and bilayers and extended these ideas to include vesicles and microemulsions. In this theory the formation of surfactant aggregates is determined by the law of mass action. Keeping in mind possible complications due to phase transitions and interactions the strategy is then to

compare the chemical potentials of different aggregates to see which has the minimum chemical potential. In the simplest version of this theory (27-28) the chemical potential of the hypothetical N aggregate is then considered to be composed of four terms. The first term is a bulk term which measures the hydrophobic free energy of removing hydrocarbon tails from water into an assumed oil-like phase made up of tails which form the micelle interior. The interior is assumed to be fluid in estimating this free energy transfer. A second term, the surface term γa, is included to allow for the fact that the hydrophobic tails still have some contact with water (after being removed from water to aggregate), where a is the area per surfactant molecule and γ is an interfacial tension. Opposing this attractive energy in the second term is an additional term to account for repulsive head-group interactions. These interactions can be due to steric repulsion, hydration, electrostatic, and other forces. A third free energy term is included so as to account for curvature effects of the interface. Finally, a fourth term is included to account for the free energy of geometrical packing. This assumes that the interior of an aggregate is fluid-like and to a first approximation incompressible. This term introduces criteria where the critical tail-length of a fully extended surfactant molecule imposes geometrical constraints on the structure of the aggregates formed. For spherical and cylindrical micelles this condition $R \leq l_c$ (i.e., consistent with the definition of a fluid-like and incompressible aggregate).

This procedure assumes that the surfactant can be divided unambiguously into a head group and tail and that the partial volume v of the tail is prescribed so that for an aggregate of number N the tail region is Nv. The location of the interface which defines the radius is the surface which bounds the volume occupied by the hydrocarbon tails. Then for spherical micelles we have a volume defined by equation 1.6 and a head-group defined by the equation 1.7.

$$N v = \frac{4 \Pi R^3}{3} \tag{1.6}$$

$$N a_o = 4 \pi R^2 \tag{1.7}$$

The packing criterion for micelles imposes the condition that the average chainlength is R = l_c = 3 v/a_o. These two equations allow us to determine the packing criterion for spherical micelles (see equation 1.8 and 1.9).

$$l_c \leq R = 3\frac{v}{a_o} \tag{1.8}$$

$$\frac{v}{a_0\, l_c} \geq \frac{1}{3} \tag{1.9}$$

This model is then extended to include oil/ water/ surfactant systems. Microemulsions were treated in a similar manner to pure surfactant aggregates and the distribution determined by the law of mass action. In the case of multicomponent systems the determination of which mixed aggregates form is a little more complicated. Here the composition of the aggregates will be dependent on the overall composition of the mixture. For a given mixed composition of aggregates there will correspond a given minimum chemical potential at some specific composition of M oil molecules and N surfactant molecules. The minimization is taken with respect to the size and shape of different aggregates and is subject to the geometrical constrictions imposed by the geometrical packing in microemulsion droplets. An iterative process is used where a chemical potential is assumed for a given chemical species. The composition of the corresponding aggregate and overall composition of the corresponding solution follow. The procedure is repeated until the iteration yields the required minimum chemical potential for size, shape, and composition of aggregates.

In this paper, Mitchell and Ninham demonstrated the importance of geometrical packing of the surfactant film and its relation to microemulsion formation. They concluded that the nature of the aggregates formed depends on the packing ratio v /a_o l_c . The packing ratio v /a_o l_c is affected by many factors including hydrophilicity of head group, ionic strength of solution, pH, temperature, and the addition of lipophilic compounds such as cosurfactants. They noted that the packing ratio v /a_o l_c provides a measure of the hydrophilic-lipophilic balance, and that the incorporation of a cosurfactant into these surfactant aggregates produces a "wedge effect" which increases the mean volume per surfactant

molecule without affecting appreciably either a_o or l_c . Consequently $v/a_o l_c$ would increase with the addition of cosurfactant, leading successively to an increase in micelle size, the formation of long rod-shaped micelles and eventually the formation of the lamellar phase (also called the middle phase). If $v/a_o l_c$ increases with temperature hydrocarbon solubility in nonionic surfactant systems should increase with temperature until $v/a_o l_c$ reaches a value of 1 where phase inversion would be expected to occur. At higher temperatures, w/o microemulsions would be expected and the solubility of water would decrease as the temperature rises. These ideas agree favorably with the Shinoda concept associated with the P.I.T. (phase-inversion temperature) and the change in the hydrophilic-lipophilic balance of the surfactant phase (11-16).

For microemulsion films composed of nonionic surfactants, Robbins (22) has considered curvature effects in some detail. He develops his ideas in three consecutive steps. In the first step, using steric considerations, he estimates the optimal radius for a spherical microemulsion droplet. In the second step he estimates K/R_0 by analyzing the stress on each side of the surfactant film. Here the sign of K/R_0 is related to a classic rule of Bancroft (29) for ordinary emulsions. In a third step, Robbins writes the free energy of one droplet in the form of equation 1.10:

$$F_d = 4\gamma\Pi R^2 - \frac{4K\Pi R}{R_0} + \frac{4\Pi\lambda R^3}{3} \qquad (1.10)$$

where the first three terms can be derived from eq. 1.5 and the last term is related to the chemical potential of the inner constituent (e.g., water, if we are dealing with inverse micelles). He then restricts his attention to a microemulsion which is in equilibrium with one solvent (e.g., w/o microemulsion in equilibrium with water) and argues that $\lambda = 0$ at this point. He then derives the optimal radius R by minimization of F_d (by taking the first derivative of F_d with respect to R and setting equal to zero). He then reaches the condition:

$$\gamma = \frac{K}{2R_0R} \qquad (1.11)$$

Inserting his estimates for K/R_o and for R, he can now predict γ ; γ is the interfacial energy/ cm^2 for a flat interface ($R = \infty$), i.e., γ represents the interfacial tension between the w/o microemulsion and pure water.

1.9. De Gennes and Taupin Model of Microemulsion Formation

The question why some oil, water, and surfactant systems form periodic arrays of surfactant while other systems form isotropic dispersions called microemulsions has been addressed by De Gennes and Taupin (30). De Gennes and Taupin noted that the phase diagram of an oil, water, and surfactant system is usually dominated by a variety of regularly organized phases but that in some special cases these systems form isotropic microemulsions where no periodicity occurs. De Gennes and Taupin also noted that whereas the regularly organized phases are highly viscous, microemulsions are transparent fluids of low viscosity. De Gennes and Taupin observed that for these microemulsion systems the transparency was a consequence of the small size (approximately 100 Å) of the oil (or water) microregions while the low viscosity expressed the fluid character of their overall structure. In this paper the flexibility of the interfacial film was invoked to explain the variety of structures formed for these oil, water, and surfactant systems. These workers concluded that one essential parameter was the curvature elasticity K of the fluid interface. A second term ξ_K, the persistence length of the interface, was defined to increase exponentially with the curvature elasticity K.

De Gennes and Taupin suggested that oil, water, and surfactant systems can generate microemulsions in a large part of their phase diagrams when two main conditions are satisfied:

i) the surfactant is able to saturate the oil/water interface rather than building up pure micelles inside one of the bulk phases; and

ii) the interface is very flexible and the long-range interactions are weak enough so that any "macrocrystal" structure must melt.

Condition (i) is satisfied by systems that reach a state that approaches zero interfacial tension. This state is referred to as the "saturated state." Systems of this type that approach zero interfacial tension tend to increase the total interfacial area between oil and water. They lead to highly divided systems. Two different classes of oil, water, and surfactant systems are formed when highly divided systems are formed. In most cases the oil and water regions form a periodic array or "macrocrystal" when condition (i) is satisfied for an oil, water, and surfactant system. These regularly organized systems are characterized by rigid interfacial structures. In some favorable cases a microemulsion will form when both conditions (i) and (ii) are satisfied. Microemulsions are characterized by flexible interfacial structures and subsequently satisfy condition (ii).

In a model related to but different from the ideas developed by Talmon and Prager, De Gennes and Taupin defined the persistence length parameter ξ_k of the flexible interface so as to include entropy contributions to the free energy of microemulsion formation. Writing the free energy of microemulsion formation as (see eq. 1.12):

$$f = f_{bulk} + \gamma_{ow} A + n_s G(\Sigma) \qquad (1.12)$$

where f_{bulk} = the free energy of the bulk phase;

γ_{ow} = the interfacial tension of a bare interface (without surfactant);

A = the area of this interface;

n_s = the number of surfactant molecules;

and $G(\Sigma)$ = is the free energy contribution per surfactant molecule.

They assume that a given chemical potential μ_s of the surfactant imposes a certain surface area Σ_s per surfactant molecule. By differentiating equation 1.12 with respect to n_s and using the definition of the Langmuir surface pressure (equation 1.13) and the definition of the interfacial area of the surfactant molecule (equation 1.14), equation 1.15 is derived.

$$\Pi(\Sigma_s) = - \frac{\partial G}{\partial \Sigma} \qquad (1.13)$$

$$\Sigma_s = \frac{A}{n_s} \tag{1.14}$$

$$\mu_s = G(\Sigma_s) + \Pi(\Sigma_s)\,\Sigma_s \tag{1.15}$$

The result is then a certain $\gamma(\Sigma_s)$ which depends ultimately on μ_s.

Although a crude approximation, this model reduces the statistics of the interface to a "lattice gas model." The statistical behavior of a lattice gas model is well-known. When the coupling between adjacent cubes $\gamma\xi_k^2$ is weaker than kT, or more precisely (eq. 1.16):

$$\gamma \leq \gamma_c = \frac{\alpha kT}{\xi_k^2} \tag{1.16}$$

(where α = 0.44 for a simple cubic lattice), De Gennes and Taupin predict a single phase with oil and water mixed down to the scale ξ_k But when the inequality is reversed, phase separation is expected.

A number of significant properties emerge from the De Gennes and Taupin model and are of more general validity:

1) The persistence length ξ_k is expected to be rather large, and thus γ should be small; therefore, we are not very far from the Schulman criterion of metastable negative interfacial tension(1,14-15).

2) Phase separation occurs not because of specific interactions between droplets, but purely because of a balance between interfacial energy and interfacial entropy.

3) The region of phase separation corresponds to $\gamma > \gamma_c$.

4) The lattice gas model generates two-phase equilibria. However, the model is highly degenerate. Small perturbations on the structure of the free energy (induced by curvature effects or other corrections) might lead to three-phase equilibria. The first attempt at this perturbation effect was made by Talmon and Prager (30).

De Gennes and Taupin invoked the concept of the flexibility of the interfacial film to explain why some oil, water, and surfactant systems form periodic arrays of surfactant while other systems form isotropic microemulsions. These workers concluded that when the curvature elasticity K is above some critical value K_c the interfaces tend to build up periodic arrays resulting in organized phases. When K is below K_c the interface becomes extremely wrinkled and the resulting gain in entropy is larger than the loss in energy due to departure from a periodic array. This case K below K_c corresponds to microemulsion formation.

1.10. Rosano Mechanism of Microemulsion Formation

A theory on the formation of microemulsion systems has also been provided by Cavallo and Rosano (31). This theory predicted the behavior of microemulsion systems only up to a certain critical dispersed phase volume, referred to as the percolation threshold. A single total free energy minimum corresponding to a stable system was found by the model for phase volumes below the percolation threshold. Above the percolation threshold interaction beween microdroplets begins to occur. Above the percolation threshold the Cavallo and Rosano model predicts instability with no free energy minimum for these transparent systems.

This theoretical model proposed that the total free energy change per unit volume, G_T, for the formation of microdroplets in these transparent systems to consist of three different different free energy terms (see eq. 1.17):

$$G_T = G_{sh} + G_a + G_b \tag{1.17}$$

where G_{sh}, G_a, and G_b correspond to:

1) G_{sh}, the free energy of formation of the liquid crystal structure interfacial sheath made of oil phase, aqueous phase, and surfactant molecules;

2) G_a, the work required to expand the interface;

3) G_b, the interfacial bending energy.

This model does not consider the free energy contribution due to interactions between microdroplets in these transparent systems. G_{sh} is assumed in this publication to be at least of the order of magnitude of G_s, the energy of solvation between the dispersed oil phase and the hydrocarbon tails of the surfactant molecules. It was calculated to be 9×10^7 erg/cm^3 based on the free energy of mixing, ΔG_m, between octane and dodecane. For a spherical particle, the total free energy per unit volume for the formation of microdroplets can be represented by equation 1.18 (excluding the free energy due to interactions between microdroplets):

$$G_T = \frac{-4\pi r^3 G_s}{3} + 4\pi r^2 \left\{ \gamma_i + \frac{K_r}{2} \left(\frac{1}{r} - \frac{1}{r_0} \right)^2 \right\} \qquad (1.18)$$

where γ_i = interfacial tension;

K_r = rigidity constant of the interface;

r = radius of the microemulsion droplets;

G_s = energy of solvation between the dispersed oil phase and the hydrocarbon tails of the surfactant molecules;

and r_0 = natural radius of curvature.

As a first estimate, r_0 was assumed by Cavallo and Rosano to be 90 Å. 90 Å is a typical radius for a microemulsion system droplet as determined by Photon Correlation Spectroscopy (PCS). For the interfacial tension, it is well known that γ_i is very low (32) and it is reasonable to use 0.1 dyne/cm for these systems. In this paper the total free energy, G_T, was then plotted versus the radius of the microdroplets for different K_r values (see Figure 1.1). It was reported in this paper that when the interfacial rigidity, K_r, is above some critical value K_r^{limit} (3×10^{-10} ergs), a single free energy minimum was found. However, there is also a maximum in this free energy versus radius curve but it occurs at very large radii

and corresponds to $G_T > 0$. In this paper K_r^{limit} corresponds to the value of K_r in which the maximum in the free energy curve has a value of $G_T = 0$. When K_r is smaller than both K_{min} (where K_{min} corresponds to the G_T versus R curve where a horizontal inflection point occurs) and the critical value K_r^{limit}, a free energy minimum was found and G_T decreases monotonically and the theory predicts instability, leading to phase separation. At the critical K_r^{limit} value, a maximum and minimum was also found in the free energy curve. The radii of the maximum and minimum formed are denoted as R_{max} and R_c, respectively. Similar energy curves can be obtained for different r_0 values. The free energy curves of different r_0 at their K_r^{limit} values were plotted in Figure 1.2.

In general, when K_r is greater than K_r^{limit}, a negative free energy minimum and a positive free energy maximum was found. This corresponds to a monodispersed microemulsion system. In this region, the smallest R_{min}, the minimum formed is found to be equal to r_0 as it is limited by the natural radius of the interface. If K_r is decreased, R_{min} increases. This corresponds to microemulsification of more dispersed phase that results in an increase of the microdroplet size. In other words, for a microemulsion system, when the dispersed phase volume fraction is increased for a fixed amount of surfactant, the droplets increase in size but its interfacial rigidity decreases. Hence, the bigger the droplets are, the less rigid (or more flexible) they are. According to this model, when K_r is smaller than K_r^{limit}, the system becomes unstable. Experimentally, it is recognized that droplets beyond a certain critical size will start to interact. It is assumed that R_{min} at K_r^{limit} (called R_c) is the point where interaction between droplets begins. Therefore, K_r^{limit} must correspond to the percolation threshold, ϕ_c. So far, this model fits the experimental results for disperse volume fraction below ϕ_c. If a semi-log was used to plot K_r^{limit} against r_0, a straight line was obtained (see Figure 1.4). This demonstrates that K_r^{limit} is exponentially proportional to r_0 which should be constant for a particular system. However, if r_0 is changed by a change in temperature, K_r^{limit} will change too. Since K_r^{limit} corresponds to ϕ_c, ϕ_c will also change. This agrees with measurements of the conductivity of microemulsions which sug-

gested the existence of ϕ_c as a function of volume fraction, temperature, and globule size (33-37).

In a subsequent publication Chan and Rosano (38) discussed the mechanism of microemusion formation using a theoretical model that considers four different free energy terms. The free energy expression used in this paper is identical to the expression used by Cavallo and Rosano except that it also includes G_I, a free energy term for microdroplet interactions. This paper assumes that the microdroplet interaction term does not have to be considered when the microemulsion system is prepared with dispersed volume fractions less than the percoalation threshold. For microemulsions of dispersed volume fraction beyond ϕ_c, an interaction term has to be introduced in order to account for percolation between droplets. It is assumed that only when the droplet size is larger than R_c that interaction occurs. The upper limit of interaction is of size R_{max} because larger droplets would interact in such a way that the system becomes unstable. Therefore, the interaction between spherical microdroplets is simply the product of K_r^{limit} and the relative increase in surface area between spheres of radii R_c, and R_{max}, i.e., $16\pi^2 \left[\frac{r - r_c}{r_c}\right]^2 \left[\frac{r - r_{max}}{r_{max}}\right]^2$. The product of the relative increase in surface area corresponds to the probability function of interaction between two micro-spherical-drops. When G_T includes an interaction term, two energy minima are found for the same r_0. These new energy curves were plotted in Figure 1.4. The existence of two energy minima represents the interaction between droplets and accounts for the phenomenon of percolation. As measured by P.C.S. (36), the presence of the second energy minimum at a much higher radius also explains the sharp increase in particle size and polydispersity for dispersed volume fractions greater than percolation threshold, ϕ_c.

Chan and Rosano noted that Ruckenstein and Chi (17-19) had proposed a thermodynamic treatment to obtain information on the stability of microemulsions and the size of the droplets in stable systems. They noted that the Ruckenstein and Chi model considered the free energy to consist of the change in interfacial free energy, the interaction energy between droplets, and the effect caused by the entropy of dispersion. In a later paper

Ruckenstein concluded that the stability of microemulsions is due to:

1) lowering of the interfacial tension to very low values and

2) the free energy change due to the dilation effect and to entropy of dispersion of the globules which is negative, overcomes the small positive interfacial tension.

According to the Chan and Rosano results, a very low interfacial tension is not necessary. The free energy of formation of the interfacial sheath (negative) appears to be sufficient to counterbalance the work necessary to form and bend the interface.

The theoretical model proposed by Chan and Rosano to explain the mechanism of microemulsion formation agrees with De Gennes and Taupin that the interfacial sheath rigidity is high for monodispersed systems. As the rigidity of the interface decreases, the diameter of the droplet increases and the system becomes polydispersed due to interaction between droplets.

1.11. The Structure of the Interface

Lindman and Stilbs et al. (39-50) studied the microstructure of isotropic surfactant solutions containing oil and water (microemulsions). Some years ago it became evident that basic structural information on isotropic surfactant solutions was contained in the long-range (lateral) mobilities of the individual molecules and that, therefore, molecular self-diffusion studies should offer a convenient route to investigate microemulsion microstructure (39-40). With the advent of the Fourier transform (FT) version of the pulsed-gradient spin-echo (PGSE) NMR technique (41-43), it became feasible to measure rapidly and simultaneously the self-diffusion coefficients of several constituents in a complex mixture with high precision and over a broad range of molecular mobilities and composition. Therefore, a rather broad program for investigating the structure of microemulsion phases appearing in different surfactant systems was initiated (44). A comprehensive review of the principles and applications of the approach has been published (45).

In order to determine the self-diffusion coefficient by the FT PGSE NMR technique, a spin-echo is Fourier-transformed to resolve individual contributions of the echo in the frequency domain. From the variations of the signal amplitudes with time during which diffusion is monitored, the self-diffusion coefficient of a large number of components can generally be determined simultaneously. A detailed paper (41) describing the technique is available. The signal amplitudes of the different constituents decay proportional to their decay rate. Therefore, a rapid decay rate corresponds to rapid diffusion.

The use of self-diffusion coefficients for extracting information on solution structure is based on the relation between diffusivity and size of the diffusing objects. This is exemplified by the Stokes-Einstein equation, where for a spherical object there is an inverse proportionality between the self-diffusion coefficient and the radius. A molecule that is part of a big aggregate and has a long lifetime in the aggregate will diffuse slowly over macroscopic distances, as its translational mobility is governed by that of the entire aggregate. (On the other hand, the molecule may move rapidly within the aggregate and have a high, short-time self-diffusion coefficient, but this is not monitored by the present type of experiments.) If there is a certain probability for the studied molecule to exist in a nonaggregated state in the interaggregate solution, the self-diffusion coefficient will become higher than if it is confined entirely to the aggregate. In fact, the effective observable self-diffusion is the weighted average over the different environments the molecule samples as a function of time.

Based on such simple reasoning, molecular self-diffusion over macroscopic distances is very sensitive to confinement into closed domains. Therefore, multicomponent self-diffusion studies, as obtained most conveniently in the Fourier transform spin-echo NMR work, can easily distinguish between different structural models in many cases. These models include a water-in-oil, an oil-in-water, and a bicontinuous structural model.

Water-in-oil droplet structure: Since water is confined to closed domains for a water-in-oil structure, water diffusion will be slow for this type of structure. If surfactant

molecules occur only at the interface, their diffusion will be the same as that of the droplets themselves. Oil diffusion will be high as it forms the continuous domains. It will only be retarded with respect to the neat oil by an obstruction effect due to the droplets and by penetration between surfactant alkyl chains. Therefore, a water-in-oil structure predicts that $D_{oil} >> D_{water} \approx D_{surfactant} \approx D_{droplet}$.

Oil-in-water structure: In this case water diffusion occurs in a continuous medium and is retarded compared to neat water only by surfactant solvation and obstruction. Thus an oil-in-water structure predicts $D_{water} >> D_{oil} \approx D_{surfactant} \approx D_{droplet}$.

Bicontinuous structure: A large number of structures are possible in which both water and oil form domains that are continuous over macroscopic distances and where surfactant molecules are located at the interfaces between these domains. In particular, we may think of layered or channel-type structures. D_{water} and D_{oil} will both be high for continuous microemulsions, lowered by the values of the neat liquids only by obstruction and solvation/penetration effects. Surfactant diffusion will be hindered by the location at interfacial films but will be unrestricted. We expect $D_{surfactant}$ to be intermediate between the value of unassociated surfactant molecules (of the order of 10^{-9} m^2 s^{-1}) and its value for droplet-type structures (of the order of 10^{-11} m^2 s^{-1}).

A surprising result of this research was the discovery that some microemulsion systems do not fit the classic picture of oil-in-water or water-in-oil droplet structure. With butanol or pentanol as the cosurfactant for a microemulsion system composed of sodium octylbenzenesulfonate/ alcohol/ decane/& water (D_2O), D_{oil} and D_{water} are both high and of the same order of magnitude and differ only by a factor 2-3 over wide concentration ranges. This result suggests that this microemulsion system should be described by a bicontinuous structure and not by a droplet structure. $D_{surfactant}$ is of the order of 10^{-10} m^2 s^{-1}, as expected for a surfactant continuous structure, and is remarkably constant over wide ranges of water-to-oil ratio. D_{water} decreases at the highest water contents, but these changes are not dramatic. Characteristic of these nonclassical microemulsion systems is that a bicon-

tinuous structure persists over wide concentration ranges (40,45,47).

The structure of four-component systems is dramatically dependent on the cosurfactant (47). Changing the cosurfactant from butanol to decanol at constant composition changes D_{water} by two orders of magnitude, while D_{oil} remains quite constant. With a long chain alchohol as cosurfactant, the structure is of a distinct w/o droplet type. Ceglie et al. (48) have further demonstrated the cosurfactant effect and in particular demonstrated that a change of oil has little or no influence on the microemulsion structure.

The dramatic effect of salinity on phase diagrams and microemulsion structure was demonstrated for sodium dodecylsulfate/ butanol/ toluene/and water systems (49). Increasing the salinity of a system of water, salt, cosurfactant, surfactant, and oil may change the phase behavior from a Winsor type I (oil-in-water) to a Winsor type III (bicontinuous) to a Winsor type II (water-in-oil) system, and this is paralleled by dramatic changes in self-diffusion (50) from a region where $D_{water} >> D_{oil}$, via a region where $D_{water} \approx D_{oil}$, both being high, to a region where $D_{oil} >> D_{water}$. The change in the ratio D_{water}/D_{oil} is by a factor of ca. 10^4. $D_{surfactant}$ is around 10^{-11} m^2 s^{-1} or somewhat above in low- and high-salinity regions, whereas it rises to 10^{-10} m^2 s^{-1} in the intermediate region. Increasing addition of salt thus induces a transition from an oil-in-water structure to a bicontinuous structure (also surfactant continuous) and then to a water-in-oil structure (50).

Instead of increasing the salinity, a similar effect was found for nonionic surfactant systems by increasing the temperature (50). Systems studied include tetraethyleneglycol dodecylether/ hexadecane/and water, tetraethyleneglycol dodecylether/ decane/and water, and tetraethyleneglycol decylether/and water. The temperature-dependent phase behavior is accompanied by a self-diffusion behavior that is very sensitive to temperature. A transition from a w/o droplet structure to a bicontinuous structure to an o/w droplet structure is demonstrated by the self-diffusion coefficients of the constituent molecules as the temperature is increased.

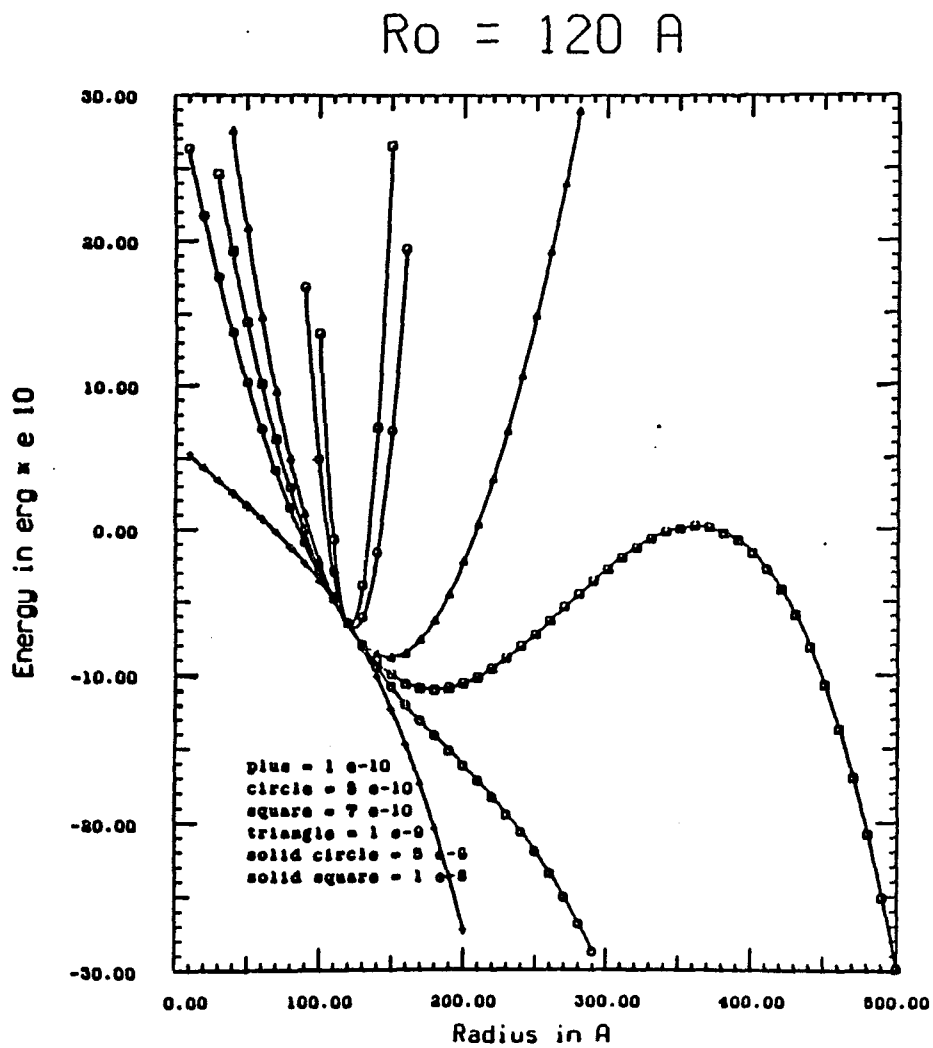
Ro = 120 A
30.00
20.00
10.00
0.00
-10.00
-20.00
-30.00
Energy in erg * e 10
0.00
100.00
200.00
300.00
400.00
500.00
Radius in A
plus = 1 e-10
circle = 5 e-10
square = 7 e-10
triangle = 1 e-9
solid circle = 5 e-9
solid square = 1 e-8

FIGURE 1.1

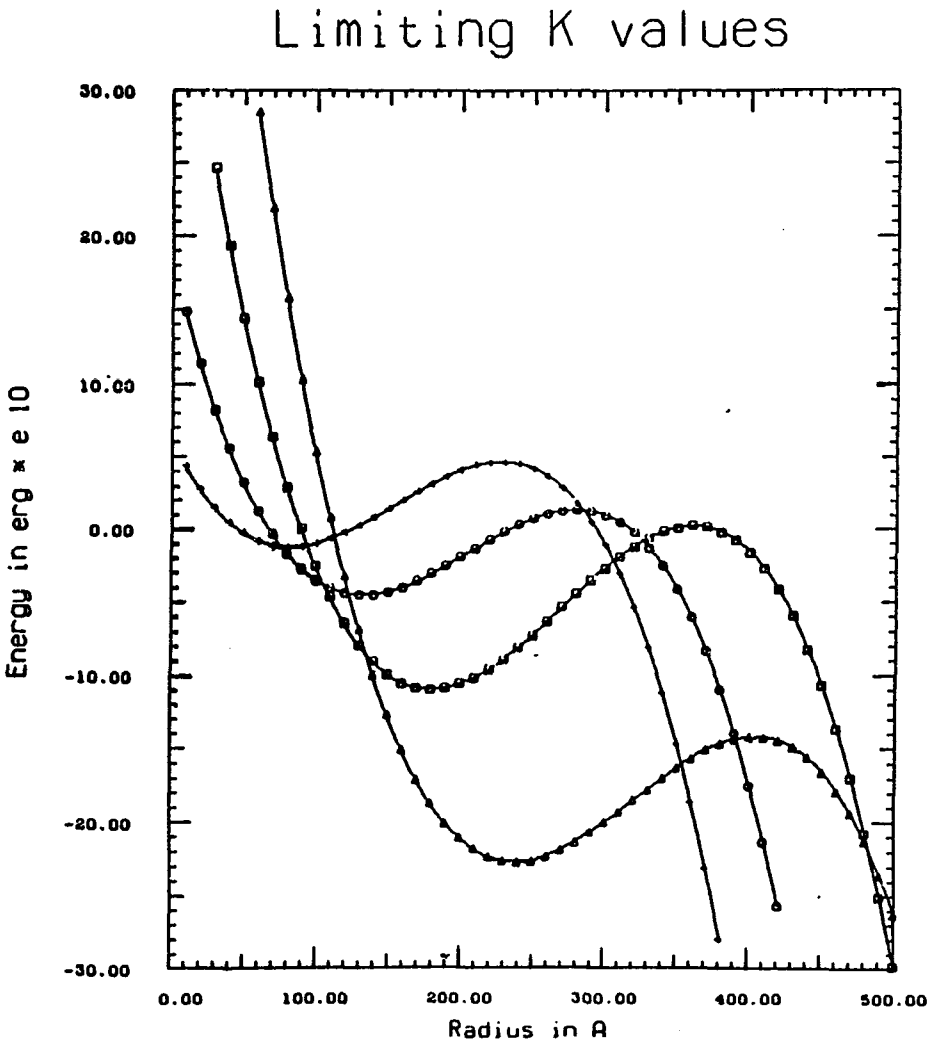
Limiting K values
30.00
20.00
10.00
0.00
-10.00
-20.00
-30.00
Energy in erg * e 10
0.00
100.00
200.00
300.00
400.00
500.00
Radius in A

FIGURE 1.2

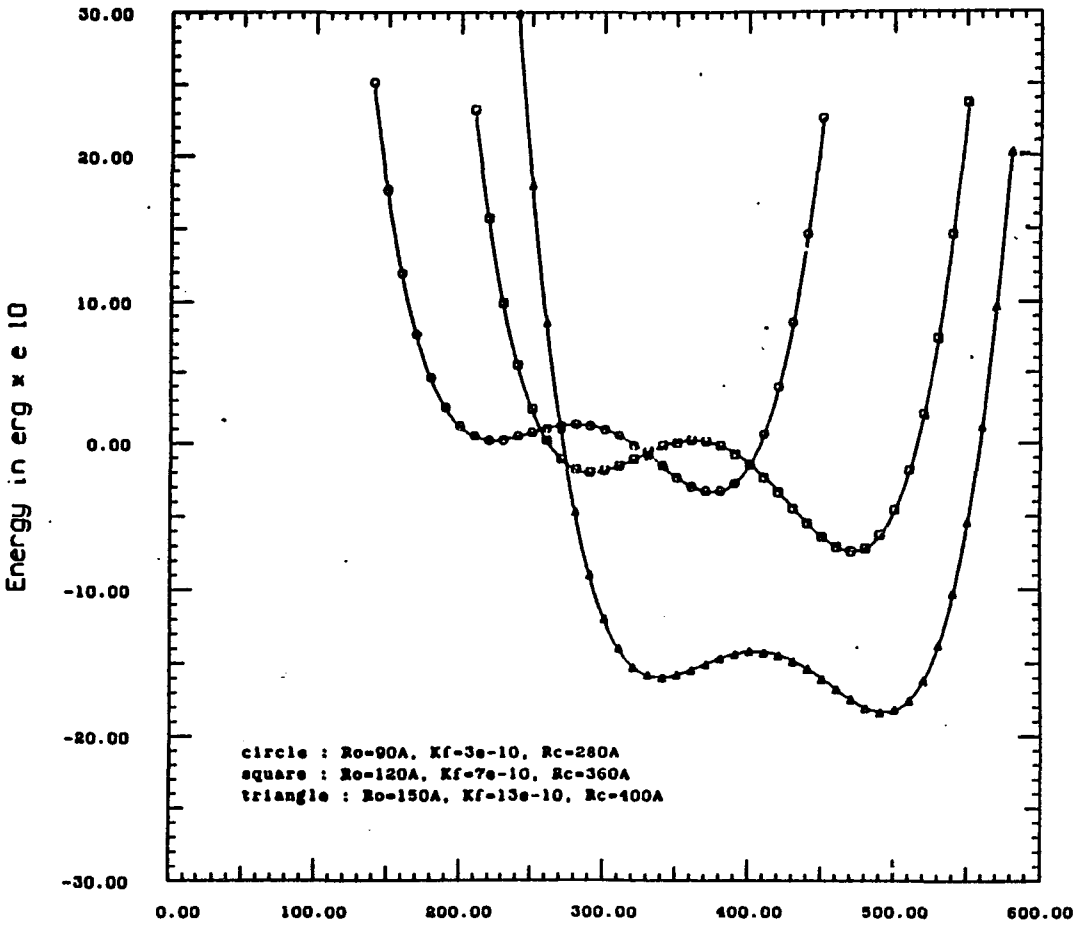
30.00
20.00
10.00
0.00
-10.00
-20.00
-30.00
Energy in erg x e 10
0.00
100.00
200.00
300.00
400.00
500.00
600.00
circle : Ro=90A, Kf=3e-10, Rc=280A
square : Ro=120A, Kf=7e-10, Rc=360A
triangle : Ro=150A, Kf=13e-10, Rc=400A

FIGURE 1.3

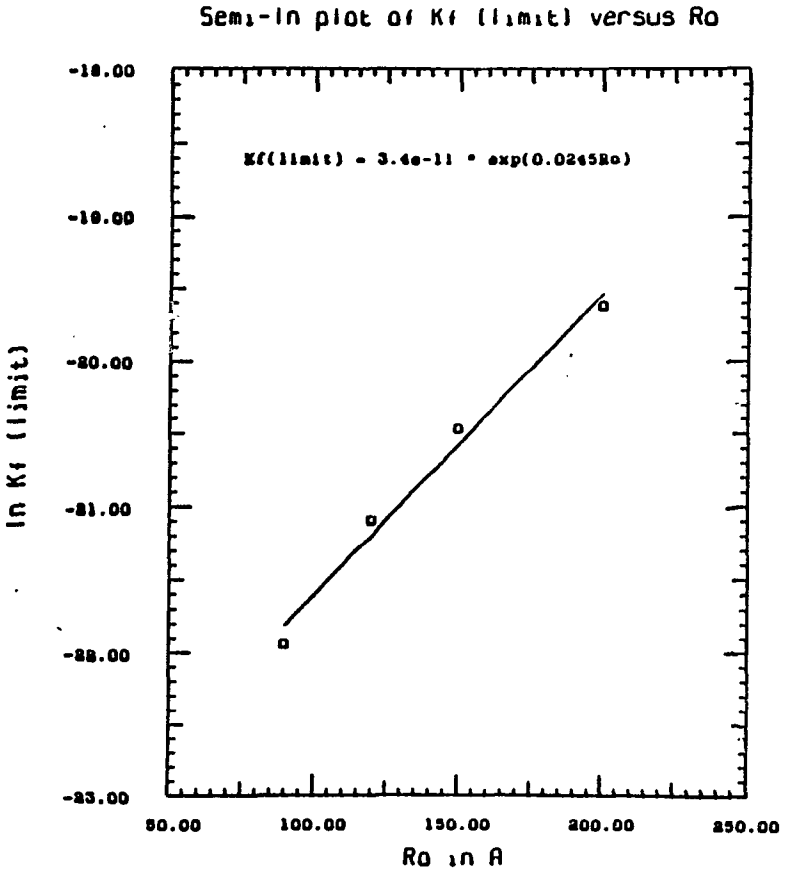
Semi-ln plot of Kf (limit) versus Ro
Kf(limit) = 3.4e-11 * exp(0.0245Ro)
-18.00
-19.00
-80.00
-81.00
-88.00
-83.00
ln Kf (limit)
50.00
100.00
150.00
200.00
250.00
Ro in A

FIGURE 1.4

References

1. Stoeckenius, W., Schulman, J. H., and Prince, L. M., *Kolloid Z.*,**169,** 170, (1960).

2. Hoar, T. P., Schulman, J. H., *Nature*, **152,** 102 (1943)

3. Stoeckenius, W., *J. Biophys. Biochem. Cytol.*, **5,** 491, (1959).

4. Bowcott, J.E., and Schulman, J.H., *Z. Elektrochem.*, **59,** 4, 283, (1955).

5. Schulman, J.H., *N.Y. Acad. Sci.*, **92,** 366, (1961).

6. Goddard, E.D., Schulman, J.H., *J. Colloid Sci.*, **8,** 309, (1953).

7. Shulman, J.H., Stoekenius, W., and Prince, L.M., *J. Phys. Chem.*, **63,** 1677, (1959).

8. Schulman, J.H., Matalon, R., and Cohen, M., *Discussions Faraday Soc.*, **11,** 117, (1951).

9. Prince, L.M., *J. Coll. Interface*, **23,** 165, (1967).

10. Cooke, C.E., Jr., and Schulman, J.H., *Proc. 2nd Scandinavian Symp. Surface Activity*, Stockholm, November, 1964.

11. Shinoda, K., Kuneida, H., Arai, T., and Saijo, H., *J. Phys. Chem.*, **88,** 5126, (1984).

12. Saito, H., and Shinoda, K., *J. Colloid & Interface Sci.*, **32,** 647, (1970). Shinoda, K., *Progress in Colloid & Polymer Sci.*, **68,** 1, (1983).

14. Shinoda, K., and Kuneida, H., *J. Colloid & Interface Sci.*, **42,** 381, (1972).

15. Friberg, S., Lapczynska, I., Gillberg, G., *J. Colloid & Interface Sci.*, **56,** 19, (1976).

16. Shinoda, K., and Friberg, S., *Adv. in Colloid and Interface Sci.*, **4,** 193, (1974).

17. Ruckenstein, E., *Chem. Phys. Letters*, **57,** 3517, (1978).

18. Ruckenstein, E., and Chi, J., *J. Chem. Soc., Faraday Trans.*, **2,** 71, 1690, (1975).

19. Ruckenstein, E., *J. Colloid & Interface Sci.*, **66,** 369, (1978).

20. Talmon, Y., and Prager, S., *J. Chem. Phys.*, **69,** 2984, (1978).

21. Talmon, Y., and Prager, S., *Nature (London)*, **267,** 333, (1977).

22. Robbins, M.L., in "*Micellization, Solubilization, and Microemulsions*," **Vol. 2,** edited by

K.L. Mittal, Plenum Press 1977, p. 713-753; also Scriven, L.E., ibid., p. 877-893.

23. Healy, R. N., Reed, R. L., and Stenmark, D. G., *Soc. Petrol. Eng. J.*, **16,** 147, (1967).

24. Winsor, P. A., *Chem. Rev.*, **68,** 1, (1968).

25. Helfrich, W., *Naturforsch. C*, **28,** 693, (1973).

26. Mitchell, D. J., and Ninham, B. W., *J. Chem. Soc., Faraday Trans. 2*, **77,** 601, (1981).

27. Tanford, C., *The Hydrophobic Effect*, John Wiley & Sons, New York, 1973.

28. Tanford, C., *J. Phys. Chem.*, **76,** 3020, (1972).

29. Bancroft, W.D., and Tucker, C.W., *J. Phys. Chem.*, **31,** 1680, (1927).

30. De Gennes, P.G., Taupin, C., *J. Phys. Chem.*, **86,** 2294, (1982).

31. Cavallo, J.L., Rosano, H.L., *J. Phys. Chem.*, **90,** 6817, (1986).

32. Rosano, H.L., Jon, D., Whittam, J.H., *JAOCS*, **59,** 8, 360, (1982).

33. Eicke, H.F., Kubick, R., Hasse, R., Zschokke, I., in "*Surfactant in Solution,*" Edited by Mittal, K., and Lindman, B., Plenum Press, (1984), p. 1533-1558.

34. Cazabat, A.M., Langevin, D., Meunier, J., Pouchelon, A., *J. Phys. Lett.*, **43,** 189, (1982).

35. Kim, M.W., Huang, J.S., *Phys. Rev.*, **A34,** 719, (1986).

36. Bhattachacharaya, S., Stokes, J., Kim, M.W., Webman, I., *Phys. Rev. Lett.*, **55,** 1884, (1985).

37. Van Dijk, H.A., *Phys. Rev. Lett.*, **55,** 1003, (1985).

38. Chan, S.Y., Rosano, H.L., *J. Dispersion Science Tech.*, **9,** 5 & 6, 523, (1988-1989).

39. Lindman, B., Kamenke, N., Kathopoulis, T.M., Brun, B., Nilsson, P.G., *J. Phys. Chem.*, **84,** 2485, (1980).

40. Stilbs, P., Moseley, M.E., and Lindman, B., *J. Magn. Resonance*, **40,** 401, (1980).

41. Stilbs, P., *Progr. N.M.R. Spectrosc., in press.*

42. Stilbs, P., and Moseley, M.E., *Chem. Scripta*, **15,** 176, (1980).

43. Stilbs, P., and Moseley, M.E., *Chem. Scripta*, **15**, 215, (1980).

44. Lindman, B., Stilbs, P., and Moseley, M.E., *J. Colloid Interface Sci.*, **83**, 569, (1981).

45. Lindman, B., Stilbs, P., and Moseley, M.E., in "*Microemulsions*," Friberg, S.E., and Botherel, P., eds., CRC Press, Cleveland, Ohio, in press.

46. Lindman, B., Ahlonas, T., Soderman, O., Waldenhaug, H., Rapacki, K., and Stilbs, P., *Faraday Disc., Chem. Soc.*, **76**, 317, (1983).

47 Stilbs, P., Rapacki, K., and Lindman, B., *J. Colloid Interface Sci.*, **95**, 583, (1983(.

48. Ceglie, A., Das, K.P., and Lindman, B., *J. Colloid Interface Sci., in press.*

49. Guering, P., and Lindman, B., *Langmuir*, **1**, 464, (1985).

50. Nilsson, P.G., and Lindman, B., *J. Phys. Chem.*, **86**, 271, (1982).

CHAPTER 2:

FREE ENERGY, ENTHALPY, and ENTROPY CHANGES during the FORMATION of a n-HEXADECANE/K Stearate/Water/1-Pentanol Microemulsion System

2.1. Introduction

Mixtures of oil and water in the presence of a surface-active agent usually form coarse emulsions which are optically opaque, or nearly so, and usually separate on standing. In some cases, transparent one-phase mixtures of oil and water can be prepared with the proper combination of surface-active materials. The term microemulsion (1) was first proposed by Schulman et al. (1) to descibe these systems. Previously, some confusion about the definition of the term microemulsion existed. The broadest definition of the term microemulsion may simply be a transparent dispersion of oil, water, and surfactant that forms spontaneously upon the addition of a cosurfactant. Terms such as swollen micellar solution (2), micellar emulsion (3,4), middle phase (5), unstable microemulsions (6), and spontaneous transparent emulsions (7) have also been used to describe these transparent one-phase systems. Friberg (8) suggested that thermodynamic stability of these systems, although generally accepted, is not always a valid criterion to define these systems. Studies with these systems as well as experience with technical microemulsions have demonstrated that a great number of systems do not have thermodynamic stability (4,8-15). Podzimek and Friberg (14) concluded that for o/w microemulsions with high oil content, thermodynamic stability appears to be an exception.

With the system discussed in this paper (n-hexadecane/ potassium stearate/ H_2O/ 1-pentanol) we reported that the system will clear spontaneously when the 1-pentanol was added dropwise to the coarse emulsion. If the equivalent volume of 1-pentanol necessary to clear the system by titration was predistributed between the oil and water phases no clearing was observed. When all of the 1-pentanol was added to the aqueous phase the system finally cleared after 5 min. of stirring (6). It is then postulated that the titration procedure was the best method to use since it produced spontaneous clearing. Moreover, it was assumed that the system was in an equilibrium thermodynamic state.

When preparing microemulsions by the "point" (titration) method various changes are often noted. Sometimes, there are dramatic viscosity increases just before the mixture becomes transparent. Also, mixtures may progress from a lactescent milk to a clear microemulsion, rapidly or slowly, as drops of cosurfactant are added.

These observations appear to indicate that the initial macroemulsion may be transformed into a Scriven (16) bicontinuous structure which eventually resolves into a microemulsion system.

2.2. Experimental Section

The n-hexadecane, stearic acid, KOH, and 1-pentanol were all reagent grade. Stearic acid/ n-hexadecane (1.0×10^{-3} mol/ ml) mixtures were placed into a round-bottom flask connected to a condenser and heated until a clear solution was obtained. n-Hexadecane (2.3 ml) containing 2.3×10^{-3} mol of stearic acid was then pipetted (with a hot pipet) into a variable volume of a 0.375 N KOH aqueous solution which had been placed in a thermostated 200 ml water-jacketed beaker. A Fisher Teflon magnetic stirrer was used to maintain gentle stirring during the titration. The system was titrated with 1-pentanol (the cosurfactant) by use of a microburet (0.02ml increments). A Bausch and Lomb Spectronic 20 spectrometer at 510 nm was used during the titration with 1-pentanol. As 1-pentanol was added the system remained opaque until the percent transmittance increased abruptly. Eventually,

addition of 1-pentanol will produce a decrease in transmittance (see Figure 2.1). Microemulsions of potassium stearate/ n-hexadecane/ water/& 1-pentanol were prepared by the same procedure but the volume of the aqueous KOH solution was increased from 10 to 60 ml. The same procedure was repeated at various temperatures from 25 to 50°C.

2.3. Results

At a given temperature and for a given volume of the aqueous phase the minimum volume of 1-pentanol needed to obtain maximum percent transmittance was determined from the titration curve. Graphs of milliliters of alcohol vs. volume of aqueous KOH gave straight lines (see Figure 2.2). A linear regression program was used to fit the data: slope (ml of 1-pentanol/ mL of aqueous phase) and intercept (mL of alcohol at 0 mL of KOH) were determined. Table 2.1 lists the results. From the slope and intercept, the mole fraction of alcohol in the interphase and the continuous aqueous phase were calculated (see equation 2.1 and 2.2).

$$X_i = \frac{n_i}{n_i + n_s} \tag{2.1}$$

where X_i = mole fraction of cosurfactant (1-pentanol) at the interface;

n_i = number of moles of cosurfactant at the interface;

n_s = number of moles of surfactant (potassium stearate) at the interface;

$$X_c = \frac{n_c}{n_c + n_a} \tag{2.2}$$

where X_c = mole fraction of cosurfacatant in continuous (aqueous) phase;

n_c = number of moles of cosurfactant in the continuous phase;

n_a = number of moles of water in the continuous phase;

The free energy change per mole for the adsorption of alcohol was calculated from equation 2.3:

$$\Delta G = - R T \ln \frac{X_i}{X_c} \tag{2.3}$$

The variation of ΔG vs. temperature allowed the determination of the entropy of formation of these systems (again with a regression method). See equation 2.4.

$$\left[\frac{\Delta G}{\Delta T}\right]_P = - \Delta S \tag{2.4}$$

The results are tabulated in Table 2.1. From Table 2.1, the entropy change accompanying alcohol adsorption was calculated by the linear regression method to be 77.8 J K^{-1} mol^{-1}. The interpolated ΔG and ΔH values at 30°C are -14.8 and +8.74 kJ/mol, respectively. The enthalpy change of transforming a coarse emulsion into a microemulsion was calculated using equation 2.5.

$$\Delta G = \Delta H - T \Delta S \tag{2.5}$$

where ΔG = free energy change for microemulsion formation;

ΔH = enthalpy change for microemulsion formation;

T = temperature;

and ΔS = entropy change for microemulsion formation.

In one experiment the volume of n-hexadecane was reduced from 2.3 to 1.15 mL. It was found that the volume of 1-pentanol to produce an abrupt rise in percent light transmittance was very similar in both cases. In a previous publication (6) it was reported that, when the microemulsion has been formed, excess short-chain alcohol finds its way inside the oil droplet, eventually increasing its radius and decreasing transmittance. It is concluded that the alcohol at the opaque/clear transition state is predominantly in the oil/ water interphase at the point where the percent transmittance increases abruptly.

From simple geometric considerations the formation of a microemulsion system corresponds to an explosive breaking up of macroemulsion droplets. For example, a droplet with a 120-nm radius will break into 1728 microdroplets with a 10-nm radius. This is why

it is desirable to prepare a fine emulsion initially before titration with the cosurfactant. From the above considerations the main factors involved in the preparation of a microemulsion system seem to be (1) the very low interfacial tension during the large increase of the interfacial area accompanying the transformation of coarse droplets into microdroplets, (2) an overall decrease in free energy accompanying the adsorption of the cosurfactant at the oil/ water interface, and (3) the formation of a flexible oil/ surfactant/ cosurfactant interface as evidenced by the positive value found for the entropy.

In Table 2.1, it can be seen that the ratio of the number of moles of 1-pentanol to potassium stearate varies from 3.6:1 to 6:1. From film penetration in monolayer experiments it is well-known that the presence of alcohols in the film produces low interfacial tension and an expanded monolayer (17). Microemulsion formation depends on this film penetration and will not occur without it. Previously, Di Meglio et al. (18) studied the system sodium dodecyl sulfate/ H_2O/ C_6H_{12}/ and 1-pentanol by the spin-labelling technique. These workers focused their attention to lamellar phases that appear in the vicinity of the oil-in-water microemulsion region. These lamellar phases were prepared with a smaller amount of cosurfactant than the corresponding microemulsion phase. Near the vicinity of the microemulsion region, Di Meglio et al. demonstrated that by increasing the swelling ratio (i.e., oil/ water ratio) or the cosurfactant concentration that the amplitudes of the undulations increase leading to a concomitant decrease in the rigidity of the interfacial film. From these results, it was concluded that the role of both the cosurfactant and the oil is to lower the rigidity of the interfacial film during the resolution of the lamellar system into a transparent, isotropic microemulsion.

The mutual solubility of 1-pentanol and 0.375 N KOH was determined by the Hill and Malisoff method (19). At 27°C, the mole fraction of 1-pentanol in 0.375 N KOH was found to be 8.73×10^{-3}. At this temperature, the mole fraction of 1-pentanol calculated from the slope of the curve in Figure 2.1 is approximately 2×10^{-3}. Let us now assume that the difference [6.73×10^{-3} mol] between these two values corresponds to 1-pentanol

associated to 2.3 x 10^{-3} mol of potassium stearate and is responsible for the formation of the dispersed oil phase. Interestingly, this corresponds to a 3:1 ratio of moles of 1-pentanol to mole of potassium stearate, comparable to the ratios tabulated in Table 2.1.

Entropy effects in microemulsion systems have been discussed by Ruckenstein and Chi (20), Talmon and Praager (21), and by De Gennes and Taupin. De Gennes and Taupin concluded that a microemulsion system would result from the melting of a macrocrystalline structure. It is appropriate to mention that in 1943 Schulman and McRoberts (17) pictured the role of the cosurfactant as increasing the disorder of the interfacial film necessary to produce high radii of curvature of the microemulsion particles.

Our results lead to the conclusion that the spontaneous formation of n-hexadecane/potassium stearate/ H_2O/1-pentanol very fine dispersions depends on the way the various components are added. These facts account for the small ΔG values found. Moreover, for the system investigated in this chapter we conclude that this process is entropy driven.

FIGURE 2.1

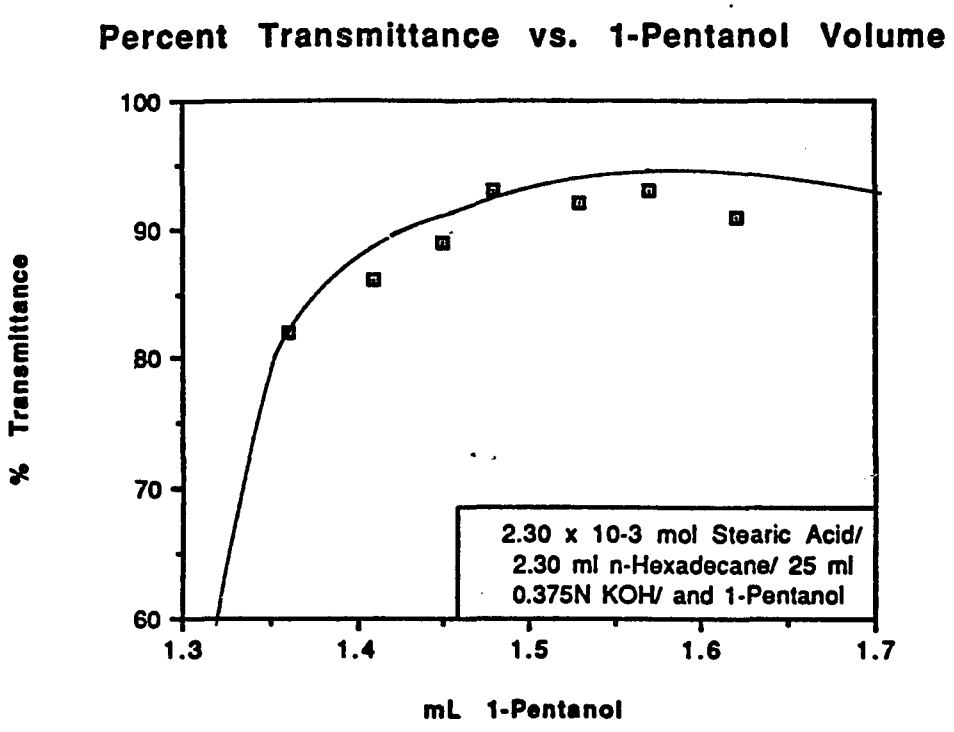
Percent Transmittance vs. 1-Pentanol Volume
% Transmittance
100
90
80
70
60
1.3
1.4
1.5
1.6
1.7
mL 1-Pentanol
2.30 x 10-3 mol Stearic Acid/
2.30 ml n-Hexadecane/ 25 ml
0.375N KOH/ and 1-Pentanol

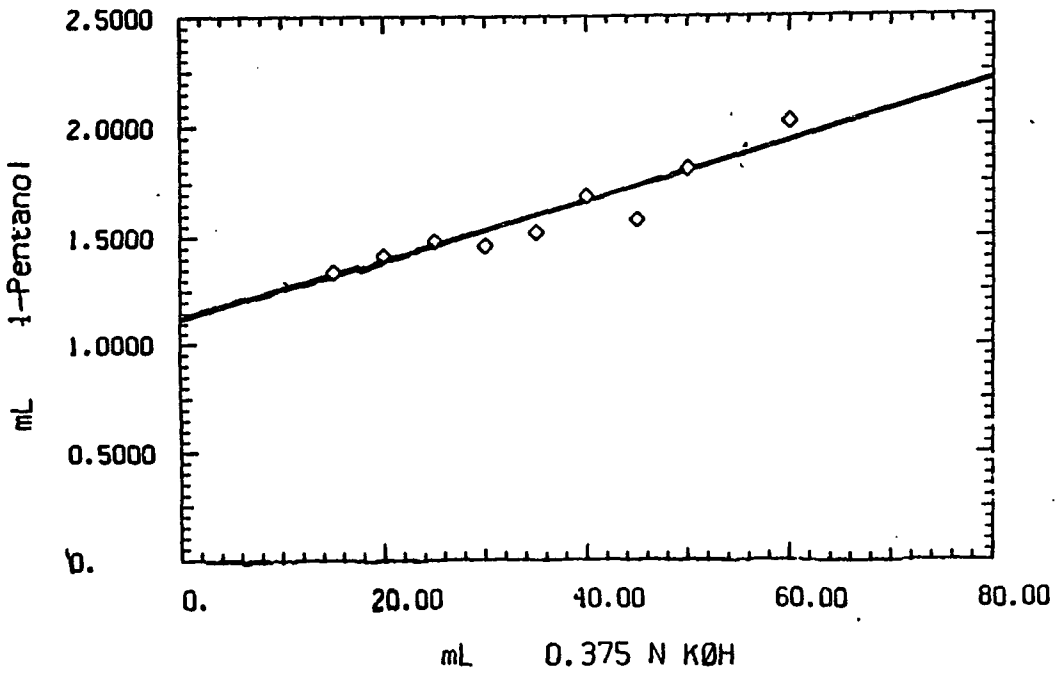
2.30mL nC16/0.0023molStearicAcid/0.375N KØH/& 1-Pentanol
2.5000
2.0000
1.5000
1.0000
0.5000
0.
mL 1-Pentanol
0.
20.00
40.00
60.00
80.00
mL 0.375 N KØH

FIGURE 2.2

Table 2.1			
Temp.	n-Hexadecane	Intercept	Slope
(°C)	(ml)	(ml 1-pentanol)	(ml of 1-pentanol per ml aqueous)
25	2.30	1.42	1.42×10^{-2}
30	1.15	0.901	1.14×10^{-2}
30	2.30	0.895	1.31×10^{-2}
35	2.30	1.14	1.16×10^{-2}
40	2.30	1.19	0.977×10^{-2}
43	2.30	0.882	1.73×10^{-2}
45	2.30	1.27	1.165×10^{-2}
50	2.30	1.50	1.73×10^{-2}

Table 2.1 Continued.				
Temp.	Molar ratio	X_i	X_c	ΔG
(°C)			($\times 10^{-3}$)	(kJ/mol)
25	4.17	0.807	2.88	-14.0
30	4.06	0.802	1.89	-15.3
30	3.59	0.782	2.17	-14.8
35	4.52	0.820	1.92	-15.5
40	4.76	0.827	1.62	-16.2
43	3.53	0.780	1.87	-15.9
45	5.08	0.836	1.86	-16.2
50	6.01	0.857	1.85	-16.5

References

1. Stoekenius, W., Schulman, J.H., and Prince, L.M., *Kolloid-Z.*, **169,** 170, 1960.
2. Shinoda, K., and Kuneida, H., *J. Colloid Interface Sci.*, **42,** 381, 1973.
3. Adamson, A.W., *J. Colloid Interface Sci.*, **29,** 261, 1969.
4. Gerbacia, W.E., Rosano, H.L., and Zajac, M., *J. Am. Oil Chem. Soc.*, **53,** 101, 1976.
5. Robbins, M.L., in "*Micellization, Solubilization, and Microemulsions*," Mittal, K.L., Ed., Plenum Press, New York, 1977; Vol. 2, pp 713-753; See also Scriven, L.E., ibid., pp. 877-893.
6. Rosano, H.L., Lan, T., Weiss, A., Whittam, J.H., Gerbacia, W.E., *J. Phys. Chem.*, **85,** 468-473, 1981.
7. Hoar, T.P., and Schulman, J.H., *Nature (London)*, **152,** 102, 1943.
8. Friberg, S.E., *Colloids Surf.*, **4, 201, 1982.**
9. Rosano, H.L., Lan, T., Weiss, A., Gerbacia, W.E.F., and Whittam, J.H., *J. Colloid Interface Sci.*, **72a (2), 1979.**
10. Rosano, H.L., Jon, D., and Whittam, J.H., *J. Am. Oil Chem. Soc.*, **59,** 360, 1982.
11. Rosano, H.L., *U.S. Patent* 4 146 499, 1979.
12. Gerbacia, W., Rosano, H.L., and Whittam, J.H., in "Colloid and Interface Science"; Kerker, M., Ed.; Academic Press: New York, 1976, Vol. II, pp 245-256.
13. Overbeek, J.Th., *Discuss. Faraday Soc.*, **65,** 7, 1978.
14. Podzimek, M., Friberg, S.E., *J. Dispersion Sci. Technol.*, **1,** 34, 1980.
15. Rosano, H.L., *J. Soc. Cosmet. Chem.*, **25,** 609, 1974.
16. Scriven, L.E., in "*Micellization, Solubilization, and Microemulsions*"; Mittal, K.L.. Ed.; Plenum Press: New York, 1977; p. 277.

17.Schulman, J.H., McRoberts, M., *Trans. Faraday Soc.*, **42,** 165, 1946.

18.Di Meglio, J.M., Dvolaitsky, M., Ober, R., and Taupin, C., *J. Phys. Lett. (Orsay, Fr.)*, **44,** L229-L234, 1983.

19.Hill, A.E., and Malisoff, W.M., *J. Am. Chem. Soc.*, **48,** 918, 1926.

20.Ruckenstein, E., Chi, J., *J. Chem. Soc., Faraday Trans.* **2,** 71, 1690, 1975.

21.Talmon, Y., Prager, J., *J. Chem. Phys.*, **69,** 2984, 1978.

22.De Gennes, P.G., Taupin, C., *J. Phys. Chem.*, **86,** 2294, 1982.

CHAPTER 3: The MECHANISM

OF

MICROEMULSION FORMATION

3.1. Introduction

Oil-in-water (O/W) emulsions of sodium long-chain sulfate/ n-hydrocarbons/ 5% NaCl were titrated to clarity (85% transmittance or better) with long-chain dimethylamine oxide. These data confirm that microemulsion formation appears to be dependent on specific interactions among the constituent molecules at the O/W interface. Six emulsions (5 O/W; 1 W/O) were titrated to clarity with cosurfactant. The volume of the continuous phase was varied from 10 to 60 ml. The mole fractions of cosurfactant/surfactant and cosurfactant/continuous phase were determined at various temperatures (15 to 55°C). At 30°C, free energy, enthalpy changes accompanying cosurfactant adsorption during microemulsion formation were found to vary from -19.6 to -6.4 kJ/mole and -25 to +18.7 kJ/mole, respectively. Entropy change of formation was positive in five cases (from 3.5 x 10^{-2} to 8.3 x 10^{-2} kJ/K mole) and -1.8 x 10^{-2} kJ/K mole in one case. The positive entropy values can be explained by an increase in compositional entropy, an increase in the disorder (or flexibility) of the interfacial film, or the formation of the mixed surfactant/ cosurfactant interface. Negative entropy values can be explained by a decrease in orientational entropy which may occur in the formation of hydrogen bonds between surfactant and cosurfactant. The measured entropy changes for microemulsion formation depend on the interplay between these different positive and negative entropy contributions to the entropy change of formation. The small measured values of free energy of formation help to explain why the manner of combining the various components may be important in the formation of these systems.

During the titration of an emulsion with a cosurfactant, the system often undergoes

viscosity changes before clearing. After each addition the system was allowed to equilibrate. Phase separation was observed, and it was concluded that O/W microemulsions may be described as hydropathic oleomicellar solutions.

While emulsions tend to be opaque and microemulsions are transparent, the most significant difference between them involves the factors responsible in their formation. Emulsion stability is usually dependent on the amount of work and surfactant added to a system. Increasing the amount of work and surfactant concentration usually imparts greater stability to emulsion systems. However this is not the case for microemulsions. Unlike emulsons, microemulsion formation depends on the specific interactions between the constituent molecules comprising the particular microemulsion system. If these interactions are not realized, neither work input or increased surfactant concentration will produce a microemulsion system. Arbitrary combinations of oil, aqueous, surfactant, and cosurfactant constituents will not always form a stable microemulsion. However, when the proper combination of specific component molecules (i.e. oil, water, surfactant, and cosurfactant) are used and the conditions are just right spontaneous formation occurs with very little mechanical work necessary (1).

It has been shown that some microemulsion systems may not be thermodynamically stable (2). These systems appear to be kinetically stable for long periods of time. This conclusion is based on the fact that for some microemulsion systems the order of mixing plays a major role in their possible formation. In these experiments, a constant total amount of cosurfactant was predistributed in various ratios between an aqueous phase and a surfactant phase containing oil and lipophillic surfactant. The two phases were then combined and allowed to equilibrate. This microemulsion system would spontaneously clear or microemulsify only when most of the cosurfactant was predistributed in the aqueous phase before combining the two corresponding phases. Therefore microemulsion systems could be described as belonging to one of two general phenomena, either a kinetically stable or thermodynamically stable dispersion of oil, water, surfactant, and cosurfactant.

Microemulsions are usually either O/W or W/O dispersions. In some cases microemulsions are best described by bicontinuous and not droplet structures. Two criteria must be considered for microemulsification: formation and stability.

3.1.1. Formation

It was originally suggested by Schulman et al. (3,4) that microemulsions form when the surfactant and cosurfactant, in just the right ratio, produce a mixed adsorbed film that reduces the interfacial tension γ_i below zero. They concluded that γ_i must have a metastable negative value, giving a negative free energy variation $-\gamma_i$ dA (where dA is the change in interfacial area) responsible for spontaneous dispersion.

The interfacial tension γ_i in the presence of the mixed film is given by equation 3.1:

$$\gamma_i = \gamma_{o/w} - \pi_i \qquad (3.1)$$

where $\gamma_{o/w}$ is the O/W interfacial tension without the film present and π_i is the interfacial surface pressure of the film. At equilibrium γ_i becomes zero. If this concept of zero interfacial tension is accepted, stabilization of the microemulsion is implied.

However, this model does not seem to be conceptually valid one, since $\gamma_i = 0$ would not require the dispersed phase to be distributed in spherical droplets as is found in the systems under discussion (5).

Rosano et al. (2) have considered the dynamic role of the cosurfactant in lowering the interfacial tension during the titration of a coarse emulsion into a transparent dispersion. It has been pointed out that during the addition of a cosurfactant to an emulsion of either O/W or W/O, excess cosurfactant accumulates at the oil/interface during transport, reducing the interfacial tension to well below the positive equilibrium value. The surfactant retards the cosurfactant interfacial transport; a prolonged low interfacial tension helps in the formation of a large increase in the interfacial area. Eventually, γ_i regains a small positive value responsible for the resolution of the system into microemulsion droplets.

3.1.2. Stability

Emulsion and microemulsion stability do not appear to be dependent only on the value of the γ_i, but mainly on the structure of the film surrounding each droplet (6,7). For a given oil/surfactant pair, cosurfactant steric requirements determine the volume of the dispersed phase that can be stabilized. These systems are oil and cosurfactant-dependent. Surfactant, cosurfactant, nature of the oil, and aqueous phase are four interacting variables that determine the size of the dispersed phase droplet when microemulsions are formed.

Only specific component combinations can produce transparent systems. In addition, the various components must be put together in just the right order to produce a microemulsion. Consequently, these experimental results lead to two basic questions.

1. Are these systems kinetically stable, since they may show occasional path dependency in their formation?

2. Are they thermodynamically stable, even though their occasional path dependency properties may reflect activation energy barriers that they must overcome during their formation?

This chapter discusses the thermodynamic properties and preparation associated with the formation of five O/W and one W/O microemulsion systems.

3.2. Experimental

3.2.1. Chemicals

N-Octane, n-decane, n-dodecane, n-tetradecane, and n-hexadecane were all 99%+ (gold label Aldrich Chemical Co., Milwaukee, Wis.). Sodium myristyl sulfate (Cyclo Chemicals Corporation, Miami, Fla.), sodium cetyl sulfate (Henkel Chemical Co., Fort Lee, N.J.), sodium dodecyl sulfate (Aldrich Chemical Co., Inc., Milwaukee, Wis.), potassium hydroxide, toluene, and 1-pentanol (Fischer Scientific Co., Fair Lawn, N.J.) were all reagent

grade. Octyl and nonylphenolethylene oxide compounds were all 100% active (GAF Corp., New York, N.Y.). Dodecyl, tetradecyl, and hexadecyldimethylamine oxide (Onyx Chemical Co., Jersey City, N.J.) were all 30% active. All chemicals were used as received. Freshly distilled water was used in all preparations, and all glassware was first thoroughly cleaned with a fresh sulfuric acid/potassium dichromate solution.

3.2.2. Method of Preparation of Transparent Systems

Rosano (8) has shown that in order to microemulsify a given volume V of dispersed phase, a sufficient number of surfactant molecules is a necessary requirement. It is hypothesized that surfactant molecules saturate the O/W interface and are needed to stabilize the dispersion. Oil, water, and surfactant are mixed in just the right ratio to form the best initial emulsion. The amount of surfactant required was estimated on basic geometric considerations. Assuming that monodisperse spherical droplets are formed, the total interfacial area A to be covered by surfactant, is given by equation 3.2.

$$A = n\sigma = 4\pi r^2 a \tag{3.2}$$

where n = number of surfactant molecules;

σ = cross-sectional area occupied by the surfactant molecules at the O/W interface;

r = radius of the dispersed phase droplets;

and a = total number of droplets composing the dispersed phase volume.

The total volume V of the dispersed phase is given by equation 3.3.

$$V = \frac{4\pi r^3 a}{3} \tag{3.3}$$

Combining equations 3.2 and 3.2, an equation relating the number of molecules of surfactant needed to cover the interfacial area to the volume of the dispersed phase is given by equation 3.4.

$$n = \frac{3V}{r\sigma} \tag{3.4}$$

The number of grams of surfactant is then given by equation 3.5.

$$g = \frac{Mn}{A} \tag{3.5}$$

where g = number of grams of surfactant;

n = number of molecules of surfactant;

M = gram molecular weight of the surfactant;

and A = Avogardro's number.

From equation 3.5, the minimum amount of surfactant required to produce the best initial emulsion was calculated. This emulsion was then titrated with a second surfactant (cosurfactant).

Microemulsion systems were prepared in water-jacketed beakers maintained at constant temperature, using the titration technique (8). An initial coarse macroemulsion was prepared from a oil/surfactant mixture added to an aqueous phase. The system was then titrated to clarity using a cosurfactant delivered from a microburet. Continuous stirring was maintained throughout the titration process to ensure homogeneous mixing. Percent transmittance was measured as the system started to clear with a Spectronic 20 spectrometer (Bausch & Lomb Co., Rochester, N.Y.) at 520 nm.

Another method employed in the preparation of microemulsions was to predistribute the cosurfactant in various ratios between an aqueous phase and an oil phase containing lipophillic surfactant before combining them. It was found that the manner and relative order of combining the components could affect the formation of the dispersion. From the results, it appears that the formation of these spontaneously forming transparent systems may be, in certain cases, path dependent (8). In this study, five O/W emulsions and one W/O emulsion were titrated to clarity (transmittance greater than 90%) with a cosurfactant. The systems investigated are shown in Table 3.1. Other oil-in-water microemulsions were

prepared with n-octane, n-decane, n-tetradecane, or n-hexadecane, 5% saline and sodium lauryl, sodium myristyl, or sodium cetyl sulfate. The systems were titrated to clarity with dodecyl, tetradecyl, or hexadecyldimethylamine oxides; see Table 3.2.

3.2.3. Viscosity and Percent Transmittance

In a water-jacketed beaker maintained at 30 °C, an emulsion consisting of 2.0 ml n-decane/0.5ml nonylphenol-1.5-ethylene oxide + 0.5 ml nonylphenol-4-ethylene oxide/and 35 ml water was titrated to clarity with nonylphenol-10-ethylene oxide. Upon each addition of nonylphenol-10-ethylene oxide, percent transmittance and viscosity (Brookfield Synchro-Lectric Model LVT, Stoughton, Mass.) were determined.

3.2.4. Phase Volume and Particle Size Determination

Volumes of upper and lower phases were determined for 15 individual systems prepared with 2.0 ml n-octane/ 0.5 ml nonylphenol-1.5-ethylene oxide + 0.5 ml nonylphenol-4-ethylene oxide /and 30 ml water. To each system a different amount of nonylphenol-9-ethylene oxide was added. Each of the systems was shaken thoroughly and stored in graduated cylinders for 30 days at room temperature (22 °C). The mean drop diameter of the lower phase was determined with a Sub-Micron Particle Analyzer, Model N4 (Coulter Electronics, Hialeah, Fla.).

3.3. RESULTS

3.3.1. Long-Chain Dimethylamine Oxide Microemulsions

Table 3.2 illustrates the specificity involved in microemulsion formation. It was observed that with sodium cetyl sulfate, n-octane produced a transparent gel. For sodium myristyl sulfate, transparent systems were more prevalent for all oils used except n-hexadecane. No microemulsions were formed when hexadecyldimethylamine oxide was used as a cosurfactant. With sodium lauryl sulfate, microemulsion systems were obtained, but again no transparent systems were found when n-hexadecane was used as the oil phase.

3.3.2. Thermodynamic Properties of Microemulsion Formation

Figure 3.1 represents a typical plot of the minimum volume of cosurfactant, at various volumes of aqueous phase and at constant temperature, required to titrate an emulsion into a microemulsion. For this system (system 3 in Table 3.1), the octylphenol-9-ethylene oxide cosurfactant is added dropwise to an initial emulsion composed of 2.0 ml n-hexadecane/ 0.5 ml nonylphenol-1.5-ethylene oxide + 0.5 ml nonylphenol-4-ethylene oxide/and a variable volume of water. At the specified temperature and the specified volume of continuous phase (water), the minimum volume of cosurfactant needed to titrate the system is plotted. The system spontaneously clears after the minimum volume of cosurfactant has been added. For example, at 45 °C, if an initial emulsion containing 30 ml of water was titrated, the system remained milky until 1.5 ml of nonylphenol-9-ethylene oxide had been added. Beyond this volume of cosurfactant, the system remained clear. The same process was repeated at constant temperature with various volumes of water (continuous phase). A straight line was obtained, as shown in Figure 3.1. The value of the slope (milliliters of cosurfactant per milliliter of continuous phase) and the intercept (milliliters of cosurfactant at zero milliliters water) was determined using a linear regression process. The slope of the straight line corresponds to the solubility of cosurfactant in the continuous phase and the intercept corresponds to the number of cosurfactant molecules adsorbed at the interface during microemulsion formation. Using equations 3.6 and 3.7, the mole fraction X_i of cosurfactant at the interface and the mole fraction X_c of cosurfactant in the continuous phase was then determined.

$$X_i = \frac{n_i}{n_i + n_s} \tag{3.6}$$

$$X_b = \frac{n_b}{n_b + n_a} \tag{3.7}$$

where n_i = number of moles of cosurfactant at the interface;

n_s = number of moles of surfactant at the interface;

n_b = number of moles of cosurfactant in the continuous phase;

and n_a = number of moles of the continuous phase.

Using equation 3.8,

$$\Delta G = -RT\ln\frac{X_i}{X_c} \tag{3.8}$$

free energy values accompanying the adsorption of cosurfactant at the interface during the transformation of a primary coarse emulsion into a transparent system were determined. The same procedure was repeated at various temperatures. Plotting the change in free energy versus temperature, the entropy change (see equation 3.9) accompanying cosurfactant adsorption was calculated, viz.,

$$\left[\frac{\Delta G}{\Delta T}\right]_P = -\Delta S \tag{3.9}$$

A straight line was obtained. A linear regression program was used to calculate the slope of this line. The slope of this straight line corresponds to the entropy change accompanying cosurfactant adsorption at the interface. The change in enthalpy corresponding to the transformation of an emulsion into a microemulsion at 30°, was then calculated by using equation 3.10.

$$\Delta G = \Delta H - T\Delta S \tag{3.10}$$

The same procedure was repeated for each system in Table 3.1. Table 3.3 shows the calculated free energy, enthalpy, and entropy values corresponding to cosurfactant adsorption at the interface for each system at 30 °C.

3.3.3. Changes in Viscosity and Percent Transmittance

Relative viscosity and percent transmittance for the emulsion system prepared with 2.0 ml n-decane/ 0.5 ml nonylphenol-1.5-ethylene oxide + 0.5 ml nonylphenol-4-ethylene oxide/

and 35 ml water (system 2 in Table 3.1) were measured upon addition of the nonylphenol-10-ethylene oxide cosurfactant; see Fig. 3.2. Upon addition of 2.5 ml of cosurfactant, filaments were first observed and the viscosity increased to 40 CP (centipoise) while the system was being stirred. A maximum viscosity of 110 CP was reached when 3.10 ml of cosurfactant was added. Filaments were still observable up to 4.2 ml of nonylphenol-10-ethylene oxide. The viscosity of the system decreased with further addition of nonylphenol-10-ethylene oxide, and the system cleared at 4.85 ml. With still more nonylphenol-10-ethylene oxide added, the system remained clear (greater than 85% transmittance) but the viscosity increased again.

3.3.4. Phase Volume Changes During Microemulsion Formation

Figure 3.3 shows the change in phase volume for 15 individual systems prepared with 2.0 ml n-octane/ 0.5 ml nonylphenol-1.5- ethylene oxide + 0.5 ml nonylphenol-4-ethylene oxide/ 30 ml water and varying amounts of octylphenol-9-ethylene oxide (system 1 in Table 3.1). Initially, the systems start out as two phases, both the upper and lower phases being clear. By adding octylphenol-9-ethylene oxide, the upper phase started to become milky and increase in volume. When 1 ml of cosurfactant was added, a one-phase opaque system was obtained. Upon adding still more surfactant, a two-phase system reappeared as the upper phase started to decrease in volume and the lower phase region began to clear. The particle size of the lower phase region was determined. In this lower phase region it was found that the particle size decreased as the concentration of octylphenol-9-ethylene oxide was increased. After 2 ml of cosurfactant was added to the system, a one-phase transparent system was obtained.

3.4. DISCUSSION

Rosano (8) has shown that the formation of transparent systems is affected by many factors, including the type and composition of the surfactant and cosurfactant, the dispersed phase volume, and the structure of the oil. For a system prepared with 2.0×10^{-3} mole

stearic acid and 2.0 ml of oil, 16 ml of 0.375 N KOH, Rosano reported that out of 52 alcohols, only five produced transparent O/W systems (transmittance > 79%). These results illustrate that only specific component combinations can produce microemulsions. As seen in Table 3.2, for emulsions prepared with various long-chain sodium sulfates, water, and oil, only specific combinations will produce transparent systems when titrated with a long-chain dimethylamine oxide as a cosurfactant.

For the six systems investigated (Table 3.3), it can be seen that the free energy values are all negative, indicating that the transformation of an emulsion into a microemulson is a spontaneous process. However, the driving forces for these processes are small and may explain why the method of preparation can sometimes affect their formation. The correct order of preparation probably lowers energy activation barriers and initiates their formation. Experimentally, the first consideration in the preparation of these transparent systems seems to be (a) that enough primary surfactant be present to cover the interfacial area, and (b) that the primary emulsion has to be as finely dispersed as possible. The method of preparation used has to produce the best kinetic conditions favorable to disperse the dispersed phase into a microemulsion (9).

Microemulsion formation involves: (1) a large increase in the interfacial area (e.g., a droplet of radius 120 nm will disperse into 1728 microdroplets of radius 10 nm-a 12-fold increase in the interfacial area); (2) the formation of a mixed surfactant/cosurfactant film at the oil/water interface, which is responsible for a very low transitory interfacial tension; and (3) an increase in the disorder (or flexibility) of the interfacial film. It is reasonable to assume that these three effects represent positive contributions to the entropy values. For the systems investigated, the entropy values were found to be postive with one exception (system 3). The negative value of microemulsion formation for system 3 may be explained by the formation of hydrogen bonds between the surfactant and cosurfactant in these transparent systems. The formation of hydrogen bonds would represent a decrease in the orientational entropy of the system. The measured entropy changes for microemulsion formation

depend on the interplay between these different positive and negative contributions to the entropy change of formation.

Under dynamic conditions, during the transformation of an initial coarse emulsion into a microemulsion, changes in the system's viscosity often are a basic characteristic prior to microemulsion formation. This effect is observed, in particular, for systems prepared with both nonionic surfactants and cosurfactants. Figure 3.2 illustrates the change in viscosity and percent transmittance for a system prepared according to system 3 and titrated to clarity with nonylphenol-10-ethylene oxide. Initially, a low-viscosity coarse emulsion is formed. Upon adding cosurfactant, the viscosity increases and reaches a maximum at 3.2 ml (10). Within this region the system remains milky and filament structures are observed througout. By adding more cosurfactant, the viscosity decreases to a minimum value at 4.8 ml. At this point the system spontaneously clears (95% transmittance). It is interesting to note that once the system becomes transparent, further addition of cosurfactant does not decrease the transmittance. Rosano et al. (14) have shown that for O/W microemulsions prepared with stearic acid, n-hexadecane, 0.375 N KOH, and 4-methylcyclohexanol, the transmittance decreases once the capacity for the cosurfactant in the aqueous phase and at the interface is exceeded. Since both sites are saturated, the excess cosurfactant penetrates the interfacial film and dissolves in the oil phase. For O/W systems this means an increase in droplet size and a concomitant decrease in transmittance. For nonionic systems (systems 1, 2, and 3), once maximum transparency is reached, excess cosurfactant increases the system's bulk viscosity, probably due to further cosurfactant adsorption on the droplet surfaces, and/or formation of micelles in the bulk.

Emulsions made of 1.95% sodium dodecylsulfate, 3.75% 1-butanol, 46.3% toluene, and varying weight percentages of a stock 48% sodium chloride solution were prepared (11). Below 4.7% sodium chloride, a two-phase system was formed with an upper clear oil phase and a lower milky aqueous phase, displaying oil-in-water emulsion characteristics Above 6.4% sodium chloride, a water-in-oil emulsion dispersion started to form, indicated

by the milky upper oil phase and clear lower aqueous phase. In the region between 4.7 and 6.4% sodium chloride, a three-phase system with a clear upper oil phase, a clear lower aqueous phase, and a middle surfactant phase was obtained. Within the three-phase region, filament structures were observed if the system was shaken gently. The formation of the filament structures seemed to be due to the ultralow values of γ_i within this region. When the overall change in the interfacial tension of upper and lower phases was plotted against sodium chloride concentration, the value of the interfacial tension was a minimum within the three-phase region (12,13). It seemed that achieving low values in interfacial tension was a necessary step in microemulsion formation. Once the value was sufficiently low (< 10^{-3} dyne/cm), spontaneous dispersion occurred with little or no mechanical work required. It also is worth mentioning that phase separation rates also varied as a function of salt concentration. Fastest separation was reported for the system in which the middle phase contained equal volumes oil and water. It has been suggested by Robbins (14) that spontaneous microemulsification will occur in the middle of the three-phase region and that the middle phase will have to be transparent or translucent.

During the preparation of microemulsions under dynamic conditions (titration method), two questions should be addressed: (1) What is the role of the cosurfactant in forming microemulsions? (2) are these systems undergoing phase volume changes as the concentration of cosurfactant is increased? Recent spectroscopic evidence (15) indicates that the role of the cosurfactant is to reduce the rigidity of the interfacial film, allowing the transition from a well-organized phase toward an isotropic microemulsion. Figure 3.3 illustrates the phase volume behavior for system 2 as the concentration of cosurfactant (in this case, octylphenol-10-ethylene oxide) is increased. Upon the addition of octylphenol-10-ethylene oxide, the upper phase starts to become milky and increase in volume. Once a total of 1 ml has been added, a one-phase system is obtained. Within this region the system is milky and birefringent, and filament structures are prevalent. As the cosurfactant concentration is further increased, the upper phase volume starts to to decrease simultaneously as the lower

phase begins to clear. When just the right amount of cosurfactant has been added, a one-phase transparent system is obtained. It seems that the transformation of an emulsion prepared with both nonionic surfactants and cosurfactants into a microemulsion follows a phase-inversion process. As the cosurfactant concentration was increased, the particle size in the lower phase was found to decrease. Upon the addition of cosurfactant to an initial coarse emulsion, the droplets start to elongate and reach a maximum in particle size (formation of filamentlike structures). As the cosurfactant concentration is further increased, these structures start to break into smaller fragments until finally microdroplets are formed (22,23). This effect was observed with systems 1 and 3 (see Table 3.1).

Shinoda (18) has proposed a general schematic illustration of the change of solution behavior with the hydrophilic-lipophilic balance (HLB) in an oil/ water/ and surfactant system (see Figure 3.4). For a system prepared with equal volumes of oil and water plus a lipophilic surfactant (or surfactant mixture), at equilibrium a two-phase system is obtained with a clear lower aqueous phase and a milky upper oil phase. When the system becomes more hydrophilic a three-phase system is formed, with upper and lower phases clear and a middle surfactant phase. Further increasing the hydrophilicity, again a two-phase system is formed, with a milky lower aqueous phase and clear upper oil phase. The same basic trend in solution behavior is observed for nonionic surfactants if the temperature is increased resulting in a decrease in the hydrophilic-lipophilic balance (HLB) value (19). However for ionic surfactants, the HLB cannot be affected dramatically by a change in temperature. For ionic surfactants, if, instead of increasing the temperature, the salt concentration is increased (decreasing the HLB), the solution behavior will also show the transition from a two-phase to three-phase to two-phase system (11,13).

This schematic diagram can be related to Figure 3.3. In the initial preparation of our O/W emulsion systems, only 1 to 2.3 ml of oil was used with a larger volume of water. Therefore, half of the diagram in Figure 3.4 should be considered (represented by the dotted line). For a primary emulsion prepared with a small O/W volume ratio and a lypophilic

surfactant (or surfactant mixture), the HLB value of the system will increase upon titrating the system with a hydrophilic cosurfactant. The upper phase increases, until a one-phase system is formed (filament structures are observed). Upon further increasing the HLB of the system, a one-phase transparent O/W dispersion is obtained. Therefore, it is concluded that microemulsions of the O/W type correspond to the lower right side of Figure 3.4, whereas microemulsions of the W/O type correspond to the upper left region. Kahlwett et al. (20) have studied the phase behavior of ternary systems (water-oil-nonionic surfactant) and quaternary systems (water-oil-nonionic surfactant-electrolyte). In the case of ternary systems the temperature was varied, while for quaternary systems the salt concentration was varied. Their results verify that maximum mutual solubility between oils and surfactants may be explained in terms of "simple" phase behavior with respect to the existence of tri-critical points in ternary systems.

Using Fourier transform proton and carbon-13 pulsed-gradient spin-echo (PGSE) NMR techniques, Lindman et al. (21) have investigated seven microemulsion systems by determining the multicomponent self-diffusion coefficient for systems prepared with oil/water and surfactant and a cosurfactant of either short- or long-chain alcohols. They reported that for the ionic surfactant/short-chain alcohol/hydrocarbon/water type of system, (1) no distinct separation into hydrophobic and hydrophilic domains was observed, (2) these systems show no extended aggregates, and (3) the internal interfaces were determined to be flexible and highly disorganized, an idea already suggested by di Meglio et al (22). Microemulsions formed with nonionic surfactants of the polyethyleneoxide type, hydrocarbon, and water are probably similar in structure to those formed with short-chain alcohols. Microemulsions prepared with long-chain alcohols are somewhat different in structure and form distinct droplets of water in a hydrophobic medium. In a review article, de Gennes and Taupin (23) have also concluded that a flexible interface is an absolute requirement for maintaining some microemulsion type systems, an idea already advanced by Schulman (24). However, in some cases a bicontinuous structure may also occur. Chatenay et al. (16) have

found that for polyphasic systems away from the three-phase domain, the interaction between droplets is hard-spherelike; whereas in the middle of the three-phase region, the structure is bicontinuous, as evidenced from conductivity measurements. These studies therefore indicate that not all interfaces fall into the same classical picture of well-organized oil or water droplets with distinct boundaries. What is seen is that internal interfaces have either a quite limited spatial extension or are very dynamic and flexible in nature and break up and re-form at a very high rate, or both.

Other structural models have been proposed to describe the structure and formation of microemulsions: Taupin and co-workers (25) have presented a model of hard oil and water globules with a relatively sharp transition between them; Scriven (26) one of a complex, periodic, three-dimensional network of both oil and water continuity; and Talmon and Prager (27) one of hard, randomly arranged polyhedra; whereas Friberg et al. (28) proposed a random structure with varying curvatures. Robbins (29) has shown that for a W/O microemulsion system, the activity of the water in the droplet core must be reduced for the water to flow into the droplets. This effect was readily verified by water vapor pressure measurements. Based on vapor pressure analysis of O/W microemulsions, two distinct regions of transparency exist (30). For small volumes of oil, encapsulated noninteracting droplets are formed; whereas a dynamic equilibrium between the breaking and re-formation of droplet interfaces has been proposed for larger volumes of oil. Similar behavior was also suggested by Weatherford (31) for W/O systems.

3.5. CONCLUSION

Transparent ternary, quaternary, and polyphasic systems have been called microemulsions. Previously, there has been some disagreement on whether these systems are thermodynamically stable or not. Limiting ourselves to the six quaternary systems (oil/water/surfactant/ cosurfactant) investigated in this study, it has been concluded that microemulsions are thermodynamically stable (29). However, the order of preparation plays a major role in their formation. It is also assumed that once the right method of preparation

is found, the energy activation barriers these systems must overcome during their formation are significantly lowered; the free energy values corresponding to the adsorption of cosurfactant at the interface are small negative numbers, indicating that the process of transforming an emulsion into a microemulsion is spontaneous, although the driving force is small; microemulsions of the O/W type correspond to the lower right region of the phase diagram shown in Figure 4; and the word microemulsion as proposed by Schulman (24) may be an unfortunate term to describe these transparent systems. The word microemulsion, as opposed to macroemulsion, should designate only transparent emulsions. In the case of W/O microemulsions, Hoar and Schulman (32) in 1943 called these systems oleopathic hydromicellar solutions and hydropathic oleomicellar solutions for W/O microemulsions. In view of our results, these terms are more appropriate to describe our systems.

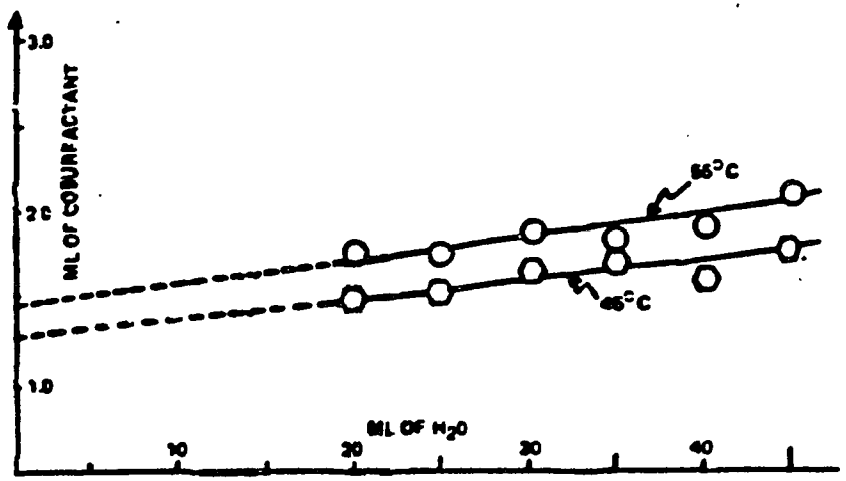

FIG. 1 2 ml n-hexadecane/0.5 ml nonylphenol-1.5-EO + 0.5 ml nonylphenol-4-EO/s variable volume of water, titrated to clarity with octylphenol-9-EO at 45°C and 55°C.

FIGURE 3.1

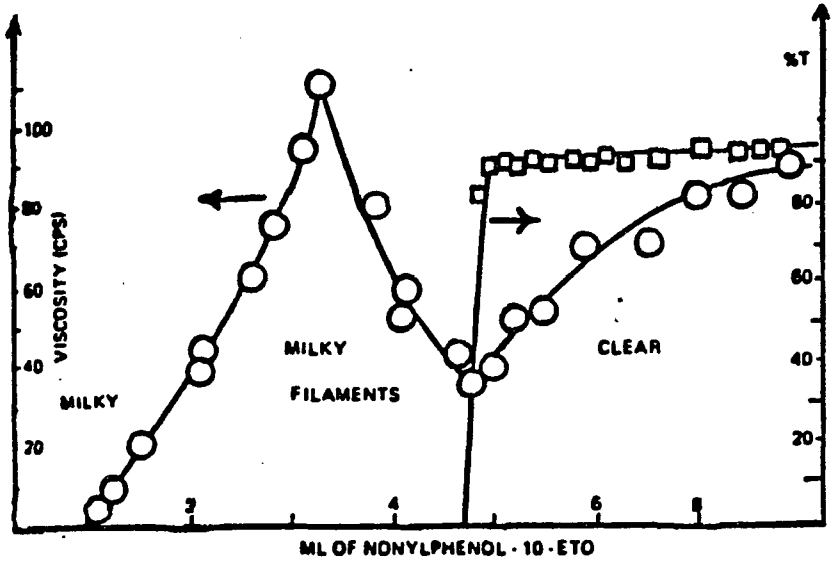

FIG. 2 Change in viscosity and percent transmittance for 2 ml n-decane/0.5 ml nonylphenol-1.5-EO + 0.5 ml nonylphenol-4-EO/ 35 ml water and titrated with nonylphenol-10-EO at 30°C.

FIGURE 3.2

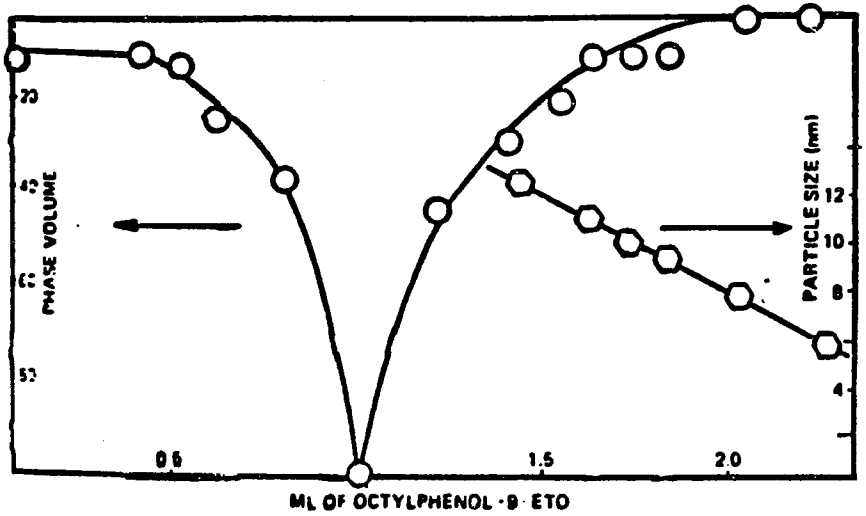

FIG. 3 Phase volume change and particle size determination for 2 ml n-octane/0.5 ml nonylphenol-1.5-EO + 0.5 ml nonylphenol-4-EO/30 ml water and titrated with nonylphenol-10-EO at 22°C.

FIGURE 3.3

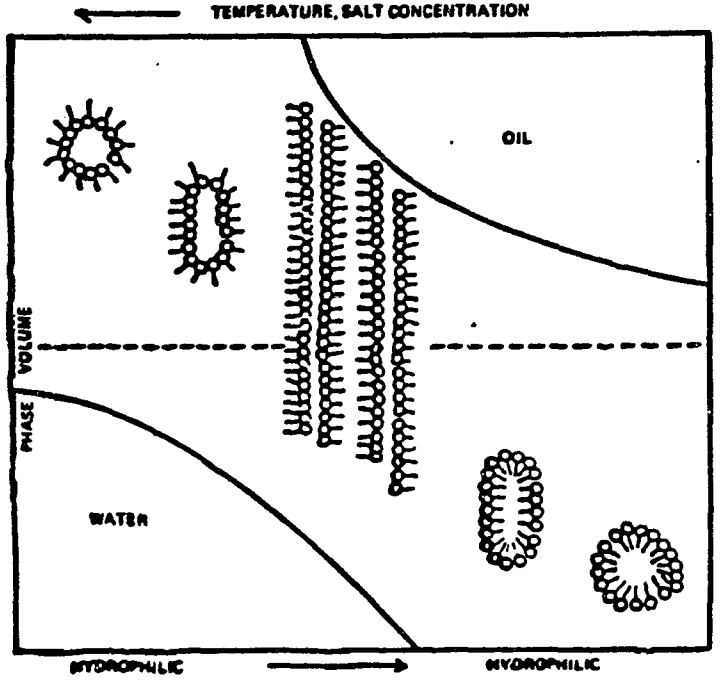

FIG. 4 Schematic illustration of the change in solution behavior of surfactant with hydrophilic-lypophilic (HLB) in a water, oil, surfactant system. (Reproduced from Ref. 34, Fig. 2.)

FIGURE 3.4

TABLE 3.1: Microemulsion Systems Investigated				
SYSTEM	CONTINUOUS PHASE	DISPERSED PHASE	SURFACTANT	COSURFACTANT
1	Water	2 ml n-Octane	0.5 ml NP-1.5-EO + 0.5 ml NP-4-EO	OP-9-EO
2	Water	2 ml n-Decane	0.5 ml NP-1.5-EO + 0.5 ml NP-4-EO	NP-10-EO
3	Water	2ml n-Hexadecane	0.5 ml NP-1.5-EO + 0.5 ml NP-4-EO	NP-9-EO
4	Toluene	2 ml Water	1.98×10^{-3} mol SDS	1-Pentanol
5	0.375 N KOH Saline	2.3 ml n-Hexadecane	2.3×10^{-3} mol Stearic Acid	1-Pentanol
6	5% NaCl Saline	1 ml n-Decane	1 gm. SDS	DDAO

Where NP-1.5-EO, NP-4-EO, SDS, OP-9-EO, and NP-9-EO correspond to nonylphenol-1.5-ethylene oxide, nonylphenol-4-ethylene oxide, sodium dodecyl sulfate, octylphenol-9-ethylene oxide, and nonylphenol-9-ethylene oxide respectively.

Table 3.2: Specificity Involved in Microemulsion Formation

Sodium Cetyl Sulfate

LDAO	n-Oct.	n-Dec.	n-Dodec.	n-Tetradec.	n-Hexadec.
HDAO	NC	NC	NC	NC	NC
TDAO	5.5 (99%)*	NC	NC	NC	NC
DDAO	3.0 (88%)	NC	NC	NC	NC

Sodium Myristyl Sulfate

LDAO	n-Oct.	n-Dec.	n-Dodec.	n-Tetradec.	n-Hexadec.
HDAO	NC	NC	NC	NC	NC
TDAO	6.6 (100%)	6.9 (95%)	7.8 (92%)	7.3 (96%)	NC
DDAO	3.6 (96%)	5.4 (97%)	NC	NC	NC

Sodium Lauryl Sulfate

LDAO	n-Oct.	n-Dec.	n-Dodec.	n-Tetradec.	n-Hexadec.
HDAO	9.0 (100%)	NC	NC	NC	NC
TDAO	3.3 (90%)*	2.1 (98%)	3.0 (90%)	4.0 (88%)	NC
DDAO	1.8 (99%)	3.3 (100%)	NC	NC	NC

TABLE 3.3: Thermodynamics of Microemulsion Formation			
SYSTEM	ΔG	ΔH	ΔS
	(kJ/mole)	(kJ/mole)	(kJ/K mole)
1	-17.4	-6.8	$3.5x10^{-2}$
2	-18.1	-6.0	$4.0x10^{-2}$
3	-19.6	-25.0	$-1.8x10^{-2}$
4	-6.4	18.7	$8.2x10^{-2}$
5	-14.8	8.7	$7.8x10^{-2}$
6	-13.9	11.3	$8.3x10^{-2}$

References.

1. Tadros, Th. F., in "*Structure/Performance Relationships in Surfactants,*" Rosen, M. J., editor, **253rd** ACS Symposium Series, ACS, Washington, D.C., 1984, p. 154.
2. Rosano, H. L., Lan, T., Weiss, A., Whittam, J. H., and Gerbacia, W. E., *J. Phys. Chem.*, **85,** 468, (1981).
3. Bowcott, J.E., and Schulman, J.H., *Z. Electro-Chem.*, **59,** (4), 283, (1955).
4. 4. Schulman, J.H., and Montague, J.H., *Ann. N.Y. Acad. Sci.*, **92,** 366, (1961).
5. Gerbacia, W.E., and Rosano, H.L., *J. Colloid Interface Sci.*, **44,** 242, (1973).
6. Gerbacia, W.E., Rosano, H.L., and Whittam, J.H., *J. Colloid Interface Sci.*, Kerker, M., editor, Academic Press, New York, 1976, **Vol. II,** pp. 245-256.
7. Rosano, H.L., Lan, T., Weiss, A., Gerbacia, W.E.F., and Whittam, J.H., *J. Colloid Interface Sci.*, **72a,** (2), 1979.
8. Rosano, H. L., *J. Soc. Cosmet. Chem.*, **25,** 609, (1974).
9. Rosano, H. L., *U. S. Patent* 4,146,499, (Mar. 27, 1979).
10. Rosano, H. L., Weiss, A., and Gerbacia, W. E., in " *Proceedings the VIIth International Congress on Surface Active Substances,*" Moscow, September 12-16, 1976, **Vol. 1,** p. 453.
11. Rosano, H. L., Jon, D., and Whittam, J. H., *J. Am. Oil Chem. Soc.*, **59,** (8), 360, (1982).
12. Bellocq, A. M., Bourbon, D., and Lemmcean, B., *to be published.*
13. Healy, R. N., Reed, R. L., and Stenmark, D. G., *SPE J.*, **16,** 147, (1976).
14. Robbins, M., *private communication.*
14. Di Meglio, J. M., Dvolaitzky, M., and Taupin, C., *to be published.*
16. Chatenay, D., Guering, P., Urback, W., Cazabat, A. M., Langevin, P., Meuiner, J., Leger, L., and Lindman, B., *to be published.*

17.Di Meglio, J. M., Paz, L., Dvoalaitzky, M., and Taupin, C., *J. Phys. Chem.*, **88,** 6036, (1984).

18.Shinoda, K., *Progr. Colloid Polymer Sci.*, **68,** 1, (1983).

19.Shinoda, K., Kunieda, H., Arai, T., and Saijo, H., *J. Phys. Chem.*, **88,** 5126, (1984).

20.Kahlweit, M., Lessner, E., and Strey, R., *J. Phys. Chem.*, **87,** 5032, (1983)

21.Lindman, B., Stilbs, P., and Moseley, M., *J. Colloid Interface Sci.*, **83,569, (1981)**

22.Di Meglio, J. M., Dvolaitzky, M., Ober, R., and Taupin, C., *J. Phys. Lett.*, **44,** L229, (1983).

23.De Gennes, P. G., and Taupin, C., *J. Chem. Phys.*, **86,** 2294, (1982).

24.Stoekenius, W., Schulman, J.H., and Prince, L.M., *Kolloid Z.*, **169,** 170, (1960).

25.Lagues, M., Ober, R., and Taupin, C., *J. Phys. Lett.*, **39,** 487, (1978).

26.Scriven, L. E., in "*Micellization, Solubilization, and Microemulsions*," Mittal, K. L., editor, Plenum Press, New York, 1977, **Vol. 2,** p. 877.

27.Talmon, Y., and Prager, S., *J. Chem. Phys.*, **69,** 517, (1978).

28.Friberg, S., Lapezynska, I., and Gillberg, G., *J. Colloid and Interface Sci.*, **56,** 19, (1976).

29.Robbins, M. L., *Preprints, 48th National Colloid Symposium, 1974, p. 174.*

30.Cavallo, J. L., and Rosano, H. L., *J. Phys. Chem.*, **90,** 6817, (1986).

31.Weatherford, W. D., *J. Dispersion Sci. Technol.*, **6,** 467, (1985).

31.Hoar, T.P., and Schulman, J.H., *Nature*, **152,** 102, (1943).

The MEASUREMENT of MICRODROPLET PARTICLE SIZE in OIL-in-WATER MICROEMULSION SYSTEMS USING D.C. POLAROGRAPHY

4.1. Introduction

Microemulsions are transparent dispersions of oil and water stabilized by surfactant molecules. In most cases, microemulsions should be considered thermodynamically stable systems (1-5) that solubilize large volume fractions of both oil and water (6). These homogeneous solutions are isotropic and have low viscosity. Microemulsion systems are characterized by flexible interfacial structures (6). This conclusion is based on e.p.r. spectroscopic measurements of these systems (7-10).

Most microemulsion systems can be described by a structure consisting of dispersed microdroplets (6,11). The microdroplets in these systems consist of an inner core of dispersed phase (either oil or water) surrounded by an outer mixed surfactant layer. In general, there are two main types of droplet structure in microemulsion systems: oil-in-water, where oil microdroplets are dispersed in an aqueous continuous phase; and water-in-oil, where water microdroplets are dispersed in an oil continuous phase. In some cases, microemulsion systems are best described by bicontinuous and not droplet structures (12).

Different methods have been used to determine the size of the dispersed microdroplets in droplet structure microemulsion systems. In this publication D.C. polarography was used to measure the microdroplet diffusion coefficient in ten different oil-in-water microemulsion systems (see Table 4.1). The measurement of microdroplet diffusion coefficients in oil-in-

water microemulsion systems by the D.C. polarographic technique has been documented by Mackay et al. (13-16). This technique depends on tagging the microdroplet with an oil soluble electroactive reducible probe capable of being reduced at the cathode. HDCP (1-hexadecyl-4-cyanopyridininium) ion was used as the oil soluble electroactive in the D.C. polarographic measurements performed in this publication. Microdroplet diffusion coefficients between 2.50 x 10^{-7} to 4.08 x 10^{-7} were measured by using HDCP ion as the oil soluble electroactive probe for the ten oil-in-water microemulsion systems investigated. From these D.C. polarographic measurements, microdroplet radii in the range of 60.0 to 97.9 Å were calculated by using the Stokes-Einstein equation. Polarographic measurement of microdroplet diffusion coefficients provides a valuable technique whereby the gauging of the hydrodynamic radii of the dispersed microdroplets in these oil-in-water microemulsion systems can be deduced.

4.2. EXPERIMENTAL.

4.2.1. Materials.

Sodium dodecyl sulfate, n-dodecane, 1-pentanol, cyclohexane, and toluene were purchased from Aldrich Chemical Company. Potassium chloride, and 4-methylcyclohexanol were purchased from Fischer Scientific Company. Cadmium chloride was purchased from Mallinckrodt, Inc. We would like to thank Henkel, Inc., for supplying sodium hexadecyl sulfate. 1-hexadecyl-4-cyanopyridinium iodide was synthesized following the suggested method of Mackay (17-18). This synthesis involves refluxing a 1:1 stoichiometric mixture of 4-cyanopyridine and 1-hexadecyl iodide in acetone for four hours, collecting the precipitate, and recrystallizing the product in ethanol and ethanol/ethyl acetate mixtures.

4.2.2. Preparation of Microemulsion Systems.

All microemulsion systems were prepared by the titration method (19-20). An initial coarse emulsion was prepared by mixing water, straight chain sodium alkyl sulfate (either SDS or SCS), electroactive probe, and the corresponding oil. Two different electroactive probes (cadmium chloride or 1-hexadecyl-4-cyanopyridinium iodide) were employed in this study. When cadmium chloride was employed as the electroactive probe, a stock solution of 0.01M cadmium chloride was diluted with water so as to vary the cadmium chloride concentration without changing the total aqueous volume of the initial coarse emulsion. When 1-hexadecyl-4-cyanopyridinium iodide was employed as the electroactive probe, it was added directly to the initial coarse emulsion. The initial coarse emulsion was then stirred at 30 ^{o}C and the required amount of cosurfactant needed to titrate the system was then added dropwise. The type and quantity of water, oil, surfactant (straight chain sodium alkyl sulfate), and cosurfactant needed to prepare the twelve different microemulsion systems are illustrated in Table 4.1. The quantity of electroactive probe was varied in each microemulsion system studied. Systems 2,4,6,8, and 10 were prepared by adding the appropriate aliquot of water to the corresponding 1,3,5,7 and 9 system.

4.2.3. Procedure for D. C. Polarography.

D.C. polarographic measurements were performed using a Tacussel Electronique type PRG5 and a Bioanalytical Systems Model CV-27 voltammograph. The polarograms were plotted on a Houston Instruments Model 200XY Recorder. The working, counter, and reference electrodes were dropping mercury, platinum, and calomel respectively. Solutions for polarographic analysis must be deoxygenated to remove the oxygen polarographic wave. This is accomplished by bubbling with nitrogen for at least ten minutes. Oxygen redissolu-

tion is then prevented by allowing nitrogen gas to flow over the solution after completion of the deoxygenation process, whenever the deoxygenation process needed to be interrupted because of excessive foaming, and during the time required for measurements. This prevented oxygen redissolution in the system. The polarographic measurements were performed at approximately 23 °C (room temperature). A solution of 10^{-3} M cadmium chloride /10^{-1} M potassium chloride solution was used as the calibration standard. The literature value of 6.9 x 10^{-6} cm^2 sec^{-1} was used for the cadmium diffusion coefficient (21) for the calibration. The experimental apparatus is illustrated in Figure 4.1.

4.2.4. Procedure for Photon Correlation Spectroscopy.

Light from a 20 mW He-Ne ion laser at 633.8 nm was focused on the sample in a glass cuvette maintained at a constant temperature of 18 °C by a water circulator. A Brookhaven Instruments model B1-2030SN goniometer allows detection of scattered light at variable angles to the incident light. Our measurements were detected at 90° to the incident light using a Brookhaven Instruments model B1-2DS1 photomultiplier tube. The photomultiplier tube operated at a D.C. voltage of 370 Volts. A Brookhaven Instruments model B1-2030SN autocorrelator was used to accumulate the data. From the autocorrelator, the data was fed to a computer which then used a Brookhaven Instruments B1-30 software program to analyze the data. Particle size analysis of the data was then outputted to a printer.

4.3. RESULTS.

4.3.1. D.C. Polarography Results.

Typical polarograms are illustrated in Figures 4.2 and 4.3. Figure 4.2 illustrates a typical cadmium (II) ion polarogram and Figure 4.3 illustrates a typical 1-hexadecyl-4-cyanopyridinium ion polarogram. The cadmium ion (22,23) is characterized by a half-wave

potential of -0.66V in water and 1-hexadecyl-4-cyanopyridinium iodide (24) is characterized by two half-wave potentials of -0.64V and -1.32V in water (values with respect to the saturated calomel electrode). For each individual system, polarograms were taken at varying electroactive probe concentration. For each polarogram the diffusion current was then determined. Recall the classical equation of D.C. polarography, the Ilkovic equation (see equation 4.1):

$$i = 607\, n\, C\, m^{\frac{2}{3}}\, t^{\frac{1}{6}}\sqrt{D} \qquad (4.1)$$

where i = the diffusion current in microamperes,

n = the number of electrons consumed in the reduction of the substance or ion responsible for the wave,

D = diffusion coefficient of that substance in cm^2s,

C = concentration of that substance in mol/cm^3

m = rate of flow of mercury through the column in mg/s,

and t = time elapsing between the fall of the mercury drops in s.

In the absence of migration and residual current, this equation tells us that the diffusion current is directly proportional to the concentration of the electroactive species being reduced.

For the ten microemulsion systems studied in Table 4.1, graphs of the diffusion current versus the electroactive probe concentration gave straight lines that passed through the origin. From the slope of this graph, we were able to determine the molar diffusion current (see equation 4.2 and 4.3). The probe to swollen micelle ratio was kept below unity for each oil-in-water microemulsion system investigated by D.C. polarography.

$$\tilde{i} = \frac{i}{C} \qquad (4.2)$$

$$\tilde{i} = 607\, n\, m^{\frac{2}{3}}\, t^{\frac{1}{6}}\sqrt{D} \qquad (4.3)$$

The normalized diffusion current for each of the ten systems was then determined by using the two different electroactive probes. We then calculated the diffusion coefficient from the normalized diffusion current for each corresponding system. An easily derived equation (see equation 4.4) facilitates this calculation.

$$i_2 = i_1 \sqrt{\frac{D_2}{D_1}} \tag{4.4}$$

where i_1 = measured normalized cadmium diffusion current in water,

i_2 = measured normalized diffusion current (using oil soluble electroactive probe),

D_1 = cadmium diffusion coefficient (literature value),

and D_2 = calculated diffusion coefficient.

Aqueous cadmium ion is equilibrated between the aqueous and the microdroplet surface and therefore cannot be used to measure the microdroplet diffusion coefficient for the oil-in-water systems investigated. Microdroplet diffusion coefficients were measured by the oil soluble electroactive probe 1-hexadecyl-4-cyanopyridinium ion and not cadmium ion. By using the Stokes-Einstein equation (see equation 4.5), the hydrodynamic radius of the swollen micelle was then calculated from the measured microdroplet diffusion coefficient for each of the twelve systems investigated.

$$D = \frac{k\,T}{6\,\pi\,\eta\,R} \tag{4.5}$$

where k = Boltzman's constant,

T = temperature,

R = the hydrodynamic radius,

and η = the viscosity of the continuous phase.

The viscosity of water was employed in this calculation. The calculated cadmium chloride

diffusion coefficient, 1-hexadecyl-4-cyanopyridinium iodide diffusion coefficient, and hydrodynamic radius for each of the twelve microemulsion systems investigated is tabulated in Table 4.2.

4.3.2. Photon Correlation Spectroscopy Results.

Particle size of microemulsion droplets have also been measured by PCS (Photon Correlation Spectroscopy). These results are listed in Table 4.3. Particle size determinations via P.C.S. versus D.C. polarography are listed in this table. The agreement between the two independent techniques to measure particle size is good. However, particle size determinations via P.C.S. were not always possible for the oil-in-water microemulsion investigated by D.C. polarography.

4.4. DISCUSSION

Schulman was the first one to suggest that microemulsions may be described as one-phase disperse systems with spherical droplets in the size range of 80 to 800 Å (25). This conclusion was based on the fact that these isotropic and homogeneous systems were optically transparent and showed a Tyndall effect. According to Schulman these transparent systems are of two general types: oil-in-water, where oil microdroplets are dispersed in an aqueous continuous phase; and water-in-oil, where water microdroplets are dispersed in an oil continuous phase. It was postulated by Schulman that the dispersed phase was present in spherical water or oil droplets stabilized by an interfacial mixed monolayer of the soap and alcohol molecules. Using high resolution electron spectroscopy (26), Schulman demonstrated that these systems consist of dispersed droplets surrounded by a mixed surfactant interfacial sheath. Subsequently, other experimental techniques were used by Schulman to analyze the size and structure of microemulsion systems. Using X-ray diffraction measurements (27), Schulman also investigated the size and structure of the dispersed microdroplets in one oil-in-water and one water-in-oil microemulsion system. It was shown by Schulman

that, with soap solutions of less than 27% in the water phase, the spacings of the X-ray bands gave strong support to the concept that the structure for the oil-in-water system consisted of monodisperse oil spheres in water while the water-in-oil system consisted of monodisperse water spheres in oil. In an attempt to obtain an independent confirmation of the spherical microdroplet model suggested, these systems investigated by X-ray diffraction were also studied using light scattering measurements (28). For calculated diameters of less than 300 Å, light scattering and X-ray diffraction measurements on the particle size of these microdroplet systems were in good agreement.

A wide variety of different experimental techniques have been used to determine the size of the dispersed microdroplets in droplet structure microemulsion systems. These include low angle x-ray diffraction (27,29), light scattering (28-32), ultracentrifugation (33-34), vapor pressure depression (35), D.C. polarography (13-16), small-angle neutron scattering (26,36-39), fluorescent spectroscopy (39-41), cyclic voltammetry (42,43), and time resolved luminescent quenching (42). These different particle size measurements lead to the conclusion that the microemulsion systems investigated in these studies are best described by a structure consisting of dispersed microdroplets. Microdroplet radii between 50 to 800 Å have been found for the microemulsion systems investigated by these different experimental techniques.

In some cases, microemulsion systems should not be described by microdroplet but by bicontinuous structures. Scriven (12) was the first one to suggest that some microemulsion systems are best described by bicontinuous structures. Scriven described these bicontinuous structures as a complex, periodic, three-dimensional network of oil and water continuity. In bicontinuous systems both the oil and water domains extend over macroscopic distances. Bicontinuous structures can account for those microemulsion systems which pass continuously from an oil-in-water to a water-in-oil system as the oil to water ratio is varied. N.M.R. spectroscopic evidence has demonstrated the presence of microemulsion systems having bicontinuous structures (44,45). More recently, Langevin (46) describes bicontinuous

structures to consist of either elongated cylinders that are eventually interconnected or of distorted lamellae that have spongelike characteristics. Langevin noted that these bicontinuous structures are encountered when the spontaneous curvature of the surfactant layer is small and approaches zero. Shinoda and Lindman described these systems by fingerprint structures (47). Bicontinuous systems are best described by microemulsion systems consisting of rapidly fluctuating small aggregates.

The measurement of particle size by D.C. polarography was initiated by Novodoff and Hoyer in 1968 (22). This technique was first used to measure the particle size of anionic micelles consisting of sodium decylsulfate, sodium dodecylsulfate, and sodium tetradecylsulfate solutions. Anionic surfactant aggregates to produce micelles having a negatively charged surface (see Figure 4.4). By tagging the negatively charged surface of an anionic micelle with a positively charged cadmium (II) cation, Novodoff, Rosano, and Hoyer (22-23) were able to measure the micellar diffusion coefficient for sodium dodecylsulfate, tetradecylsulfate, and hexadecylsulfate micellar solutions. These workers demonstrated conclusively that the divalent cadmium (II) cation is strongly bound to the surface of the anionic micelle for these micellar solutions (23). Micellar radii 16.8, 32.2, and 51.0 Å were measured by this technique at 25 $^{\circ}$ for the corresponding anionic sodium decylsulfate, dodecylsulfate, and tetradecylsulfate surfactant solutions.

In the case of oil-in-water microemulsion systems, aqueous ions are only weakly bound to the microdroplet surface and can not be used to measure the microdroplet diffusion coefficient (also termed "self" diffusion coefficient) for these oil-in-water systems. Mackay et al. demonstrated that the transport properties for aqueous ions in nonionic and ionic oil-in-water microemulsions (16,50-53) is governed by movement through the aqueous phase (see equation 4.6).

$$D = D_0 (1 - \phi)^{n+1} \qquad (4.6)$$

The relationship governing the diffusion of aqueous ions in both ionic and nonionic oil-in-water microemulsion systems is referred to as the "obstruction effect." The effect of the

dispersed phase on the diffusion of the aqueous ions in these systems is to retard their movement. The greater the volume fraction of dispersed phase the larger the decrease in the diffusion of the aqueous ion. For microemulsions composed of ionic surfactant, Mackay demonstrated that this relationship is valid regardless of whether the aqueous ion is of opposite or the same relative charge as the swollen micelle surface.

Mackay et al. (14-15) demonstrated that oil soluble electroactive probes are solubilized inside the swollen micellar surface and can be used to measure the microdroplet diffusion coefficient by D.C. polarography for oil-in-water microemulsion systems. Measurement of the microdroplet diffusion coefficient allows the calculation of the microdroplet particle size for these oil-in-water microemulsion systems. These workers were able to measure the microdroplet diffusion coefficients in several different oil-in-water microemulsion systems by using 1-dodecyl-4-cyanopyridinium ion (DDCP) as the oil soluble electroactive probe. Investigating an oil-in-water microemulsion system consisting of sodium cetyl sulfate/ 1-pentanol/ water/ and heavy mineral oil by D.C. polarography with 1-dodecyl-4-cyanopyridinium (DDCP) ion as the oil soluble electroactive probe, Mackay et al. (14) measured the microdroplet diffusion coefficient and were able to calculate microdroplet radii of 45 Å for this oil-in-water system. This value of 45 Å obtained by D.C. polarography compared favorably with a value of 50 Å from low angle x-ray scattering (27).

In a subsequent publication Mackay et al. (14) investigated this oil-in-water system further by both D.C. polarography and QLS (quasi-light scattering). Polarography and QLS measurements were performed at constant emulsifier composition (40% SCS/ 60% 1-pentanol emulsifier) but at increasing water content. Using DDCP as the oil soluble electroactive probe in these D.C. polarography measurements, microdroplet radii were found to increase in size with increasing water content for this oil-in-water system. Microdroplet radii between 117 to 332 Å were found by D.C. polarography as the water content increased from 60 to 73 weight percent in this system. The value of 117 Å found by D.C. polarography for this oil-in-water at a 60% weight percent water compared favorably with a

value of 100 Å found by low angle x-ray scattering (27). In this publication QLS was also used to determine measure diffusion coefficients in this oil-in-water system. These workers found that the values of the diffusion coefficients as measured by QLS did not correspond to those measured by D.C. polarography. These workers concluded that whereas the D.C. polarographic data measure microdroplet diffusion coefficient the QLS data measure a collective diffusion coefficient in oil-in-water micoemulsion systems. QLS experiments were also performed with or without electroactive probe present in the system. The QLS data demonstrated that there is was no difference in the measured diffusion coefficient whether or not electroactive probe was present in the system, indicating that at the concentrations used that electroactive probe had no effect on the microstructure of the system. This paper demonstrated conclusively that oil soluble electroactive probes can be used to measure microdroplet particle size by the D.C. polarographic technique in oil-in-water microemulsion systems and that at the concentrations used that these electroactive probes do not perturb the size or structure of these microemulsion systems. A subsequent publication by these workers (15) investigated the size of the microdroplets in this oil-in-water system by D.C. polarography as a function of temperature. At constant composition the size of the microdroplet radii was found to decrease as the temperature increased for this oil-in-water system.

Recently, cyclic voltammetry has been used by Mackay et al. to determine microdroplet particle size in ten different oil-in-water microemulsion systems. Using ferrocene as the oil soluble electroactive probe, microdroplet radii between 68.8 to 463.5 Å were found by Mackay et al. for the oil-in-water microemulsion systems investigated by cyclic voltammetry. Previously, Qutubuddin et al. (41) measured the microdroplet diffusion coefficients in an oil-in-water microemulsion system consisting of n-octane/ CTAB (cetylammonium bromide)/ n-butanol/ NaBr/ and H_2O by using cyclic voltammetry and rotating disk voltammatry. These workers used ferrocene as the oil soluble electroactive probe to measure the microdroplet diffusion coefficient in this oil-in-water system. Qutubuddin et al. stated in

this paper that the properties of a suitable electroactive probe for the measurement of microdroplet diffusion coefficients in oil-in-water microemulsion systems are: (i) diffusion controlled electrochemical charge transfer; (ii) hydrophobic nature; (iii) acceptable (or noninterfering) half-wave potential; (iv) negligible or no adsorption on an electrode surface; and (v) no effect of the addition of the probe on the properties of the microemulsion. Qutubuddin et al. workers demonstrated conclusively that ferrocene fulfills these requirements and is a suitable electrochemical probe that can be used in cyclic voltammetry to measure microdroplet diffusion coefficients and to calculate microdroplet particle size in oil-in-water microemulsion systems. From these electrochemical measurements these workers calculated the hydrodynamic radii for the microdroplets in this oil-in-water system to be in the range between 50 to 150 Å. These workers found that the size of the microdroplets increases as the volume fraction of oil (where n-octane is the dispersed phase) increases while the amount of surfactant and cosurfactant is held constant. More recently, cyclic voltammatry has also been used by Mackay et al. (40) in oil-in-water microemusion systems to determine the microdroplet particle size as a function of dispersed phase. These workers also found that the size of the microdroplets increases as the volume fraction of dispersed phase is increased at constant emulsifier concentration. A wide variety of other experimental techniques demonstrates that the particle size increases in droplet structure microemulsion systems as the volume fraction of dispersed phase is increased.

In this paper we measured the microdroplet diffusion coefficient by D.C. polarography and were able to calculate the microdroplet particle size in ten different oil-in-water microemulsion systems. The oil soluble electroactive reducible probe used in our D.C. measurements was HDCP (1-hexadecyl-4-cyanopyridinium) ion. Microdroplet particle size was calculated from the measured HDCP ion diffusion coefficient by using the Stokes-Einstein equation (see equation 4.5). For each oil-in-water microemulsion system investigated in this paper (see Table 4.2) by D.C. polarography both cadmium (II) and HDCP ion diffusion coefficients were measured. Examination of the D.C. polarographic results in

Table 4.3 leads to the conclusion that the measured cadmium (II) ion diffusion coefficient is larger than the corresponding HDCP ion diffusion coefficient in each oil-in-water microemulsion system investigated. However, the cadmium(II) diffusion coefficient is smaller than the corresponding diffusion coefficient expected for a completely free aqueous ion in solution. Our cadmium (II) diffusion coefficient results support Mackay's conclusion that the movement of aqueous ions in oil-in-water microemulsion occurs in the aqueous continuous phase and is governed by the "obstruction effect." The D.C. polarographic measurements of the oil soluble electroactive probe and the corresponding calculated microdroplet particle sizes in Table 4.2 lead us to conclude that the oil-in-water microemulsion systems investigated in this paper consist of dispersed oil microdroplets surrounded by a continuous aqueous phase. Microdroplet radii between 60.0 to 97.9 Å were found for the oil-in-water systems investigated by D.C. polarography in this paper (see Table 4.3). These results demonstrate that the oil-in-water microemulsion systems investigated in this publication by D.C. polarography should be described by a microdroplet structures and not bicontinuous structures.

Photon Correlation Spectroscopy (PCS) experiments were conducted as a corroborating measure of the microdroplet particle size for each oil-in-water microemulsion system investigated by D.C. polarography in this paper. Using the PCS technique, attempts to measure the particle size of the microemulsion droplets were not always successful (compare Table 4.3 to 4.2). This technique depends on monitoring the time dependence of the fluctuations in the scattered light intensity. The experimental procedure involves the generation of an autocorrelation function from the data. An autocorrelation function may be described as an exponentially decaying curve of the scattered light intensity versus time. However, the scattered light intensity is proportional to the sixth power of the radius of the scattering particles. The size of microemulsion droplets is typically below 200 Å and smaller microdroplets are less likely to scatter light than larger particles. Unless the droplet concentration for a microemulsion is very large, it is not always possible to generate a

meaningful autocorrelation function. This was a problem for most of the oil-in-water systems investigated by D.C. polarography in this publication. We were also limited by how concentrated we could make our systems. Therefore, we were not always able to measure the particle size of our microemulsion systems using PCS. We were always able to measure the particle size using D.C. polarography. This demonstrates emphatically the advantage of using this technique. D.C. polarography also provides a faster and more economical way of determining the particle size. When a good autocorrelation was generated by PCS the calculated microdroplet size was in good agreement with the microdroplet particle size calculated from D.C. polarography. This fact demonstrates that D.C. polarography provides a reliable method to measure the microdroplet particle size in oil-in-water microemulsion systems. This technique depends on the use of an oil soluble electroactive probe.

In a previous publication Rosano et al. (54) used Differential Scanning Calorimetry (DSC) and titration experiments to investigate an oil-in-water microemulsion system (SDS/n-hexadecane/H_2O/& 1-pentanol). The DCS thermograms of this system were performed by varying the volume of dispersed phase (n-hexadecane) while the amount of aqueous phase and surfactant was held constant (see DSC figure). The DSC experiments demonstrate that this oil-in-water microemulsion system is characterized by three thermal peaks occurring at -9.65, -2.04, and +18.33 °C. These thermal peaks correspond to the thermal melting of the interface, aqueous phase, and dispersed phase (n-hexadecane), respectively. DSC thermograms of this microemulsion system indicate that as the amount of dispersed phase (n-hexadecane) was increased, the thermogram peak attributed to the interfacial sheath remained constant. In contrast, the thermogram peak attributed to n-hexadecane increases in size as the volume of dispersed phase (n-hexadecane) increases. This data supports the conclusion that the structure of these oil-in-water systems may be described by swollen microdroplets encapsulated by an interfacial sheath of constant interfacial stoichiometry. The interfacial stoichiometry of the microdroplets in this system was determined from data obtained from titration experiments. This procedure depends on the

use of material balance equations and demonstrates that the microdroplet interface is composed of all of the surfactant and part of the oil and cosurfactant in these oil-in-water microemulsion systems. This result may also help to explain why a minimum volume of oil is necessary to prepare some oil-in-water microemulsion systems. This minimum volume of oil is incorporated into the interfacial sheath and is necessary to satisfy the required stoichiometry of the microdroplet interface. Additional oil above the minimum volume may then be incorporated in the inner core of the dispersed microdroplets in these droplet structure oil-in-water systems.

From the investigation of sedimentation rates of microemulsion systems by ultracentrifugation (55), it was found that a fixed amount of primary surfactant will cover only a constant interfacial area. Other experimental techniques also support the conclusion that a fixed amount of primary surfactant will cover only a constant interfacial area. This result suggests that a certain minimum amount of primary surfactant is needed in order to disperse a given volume V of dispersed phase into microdroplets of radius r in these droplet structure microemulsion systems (see equation 4.7).

$$n = \frac{3V}{R\sigma} \tag{4.7}$$

where n = the minimum amount of primary surfactant needed in order to disperse a given volume V of dispersed phase,

V = given volume of dispersed phase,

R = radius of the monodisperse microdroplets,

and σ = the cross sectional area per surfactant molecule.

The minimum amount of primary surfactant is needed to cover the large increase in the microdroplet oil/water interfacial area in these disperse systems. Within this constraint of constant interfacial area, a change in the volume of the dispersed phase will cause the droplets to swell or shrink with a corresponding decrease or increase in the number of droplets. A wide variety of different experimental techniques has been used to investigate

microdroplet particle size as a function of dispersed phase in microemulsion systems prepared with a fixed amount of primary surfactant. These different techniques lead to the conclusion that the microdroplet particle size increases as the dispersed phase volume increases in these droplet structure microemulsion systems prepared with a fixed amount of primary surfactant.

Examination of the microdroplet particle size (see Table 4.2) of the oil-in-water microemulsion systems investigated by D.C. polarography in this publication, demonstrates that the measured particle size increases as the volume of dispersed phase increases for a given microemulsion system. For example, System 3 and 1 (see Table 4.1) are prepared with the same amount of primary surfactant (2.0 g SHS) and continuous phase (40 ml water) but a different amount of dispersed phase (1.0 ml of n-dodecane for System 3 and 2.0 ml of n-dodecane for System 1). As the volume of dispersed phase increases from 1.0 ml of n-dodecane for System 3 to 2.0 ml of docecane for System 1 the corresponding microdroplet particle size increases from 74.7 Å for System 3 to 85.6 Å for System 1. A similar conclusion can be drawn by comparing System 7 with System 9. As the volume of dispersed phase increases from 1.0 ml of cyclohexane for System 9 to 2.0 ml of cyclohexane for System 7 the corresponding microdroplet particle size increases from 60.0 Å for System 9 to 69.3 Å for Sample 7. Other experimental evidence supports the conclusion that the size of the microdroplets increases as the volume of dispersed phase increases for microemulsion systems prepared at constant amounts of both primary surfactant and continuous phase.

With all these experimental facts, it may be suggested that microemulsion systems having a microdroplet structure can be considered as dispersed spheres encapsulated by an interfacial sheath of constant interfacial composition. The microdroplet model can be described as an inner core composed of dispersed phase surrounded by an interfacial sheath where all of the surfactant and part of the cosurfactant and oil form the interfacial shell. The interfacial sheath may be compared to a liquid crystal structure shell. De Gennes and

Taupin (6) described microemulsion formation as the melting of the liquid crystal shell into a soft and flexible interface. At low dispersed volume fraction, microemulsion systems are essentially monodispersed. Initial increase in dispersed phase will increase the droplet size up to the percolation threshold, ϕ_c. Below the percolation threshold the microdroplets behave as isolated and noninteracting particles. Further increase in volume of the dispersed phase will result in percolation. Above the percolation threshold the microdroplets begin to interact. The microdroplets are polydisperse in the regime where percolation occurs.

5. Conclusions

1. Oil soluble electroactive probes are needed in order to measure by D.C. polarography the microdroplet diffusion coefficient (also termed the "self" diffusion coefficient) in oil-in-water microemulsion systems. When an oil soluble electroactive probe is used to measure the microdroplet diffusion coefficient the hydrodynamic radius of the microdroplets in these oil-in-water micfroemulsion systems can be calculated by using the Stokes-Einstein equation.

2. HDCP ion was used as an oil soluble electroactive probe to measure the microdroplet diffusion coefficient by D.C. polarography in ten different oil-in-water microemulsion systems. Microdroplet radii between 60.0 to 97.9 Å were found for the oil-in-water microemulsion systems investigated by D.C. polarography in this publication.

3. The size of the microdroplets increases when the volume of dispersed phase increases for a microemulsion system prepared at constant amount of both primary surfactant and continuous phase.

4. The typical structure of most microemulsion systems can be described by dispersed microdroplets surrounded by continuous phase. There are two general types of microdroplet microemulsion systems: oil-in-water, where oil microdroplets are dispersed in an aqueous continuous phase; and water-in-oil, where water microdroplets are dispersed in an oil continuous phase. The model for the microdropiet can be described as an inner core consisting

of dispersed phase that is surrounded by an outer interfacial shell where all of the surfactant and part of the cosurfactant and dispersed phase form the interfacial sheath. The microdroplet interfacial sheath has a definite or constant stochiometry in these systems. In some cases, microemulsion systems should not be described by microdroplet but by bicontinuous structures.

FIGURE 4.1

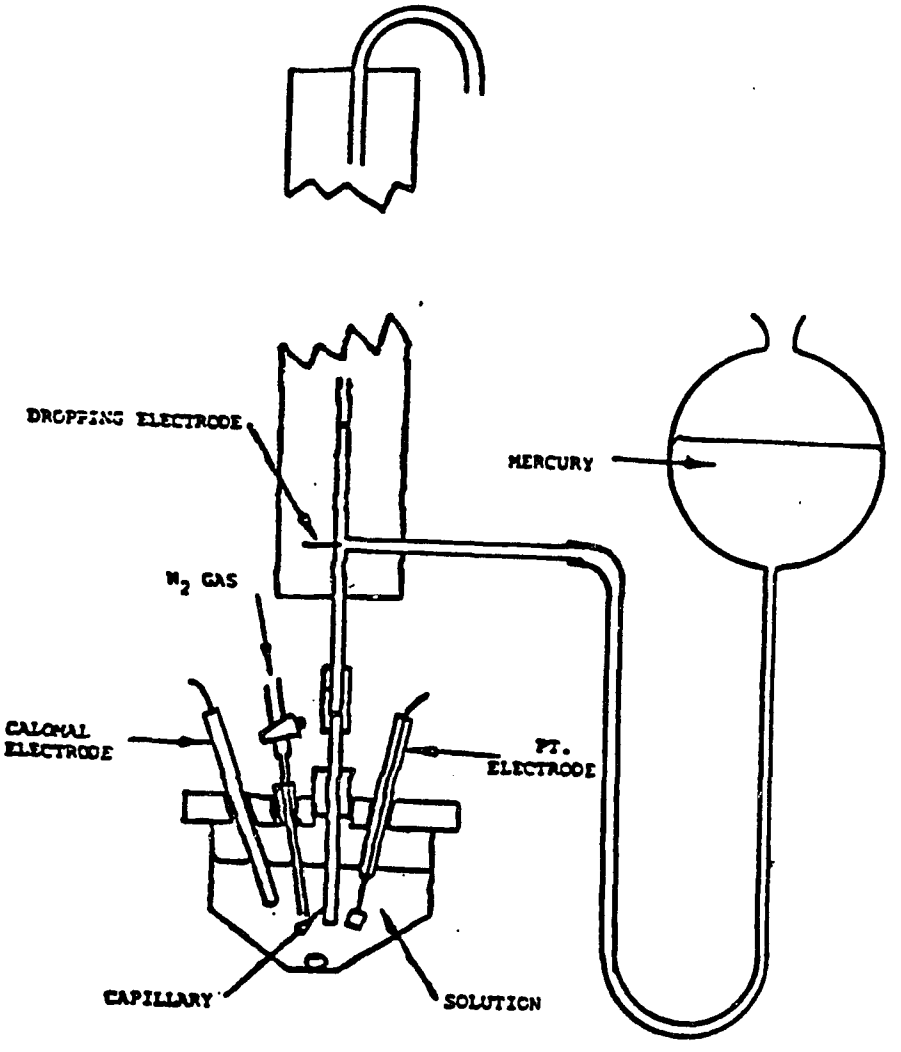

EXPERIMENTAL APPARATUS

1. Houston Instruments Model 200XY Recorder was used to record the data.
2. Bioanalytical Systems Model CV-27 Voltammagraph was used to control voltage across the two electrodes.
3. The working, counter, and reference electrodes were mercury, platinum, and calomel respectively.

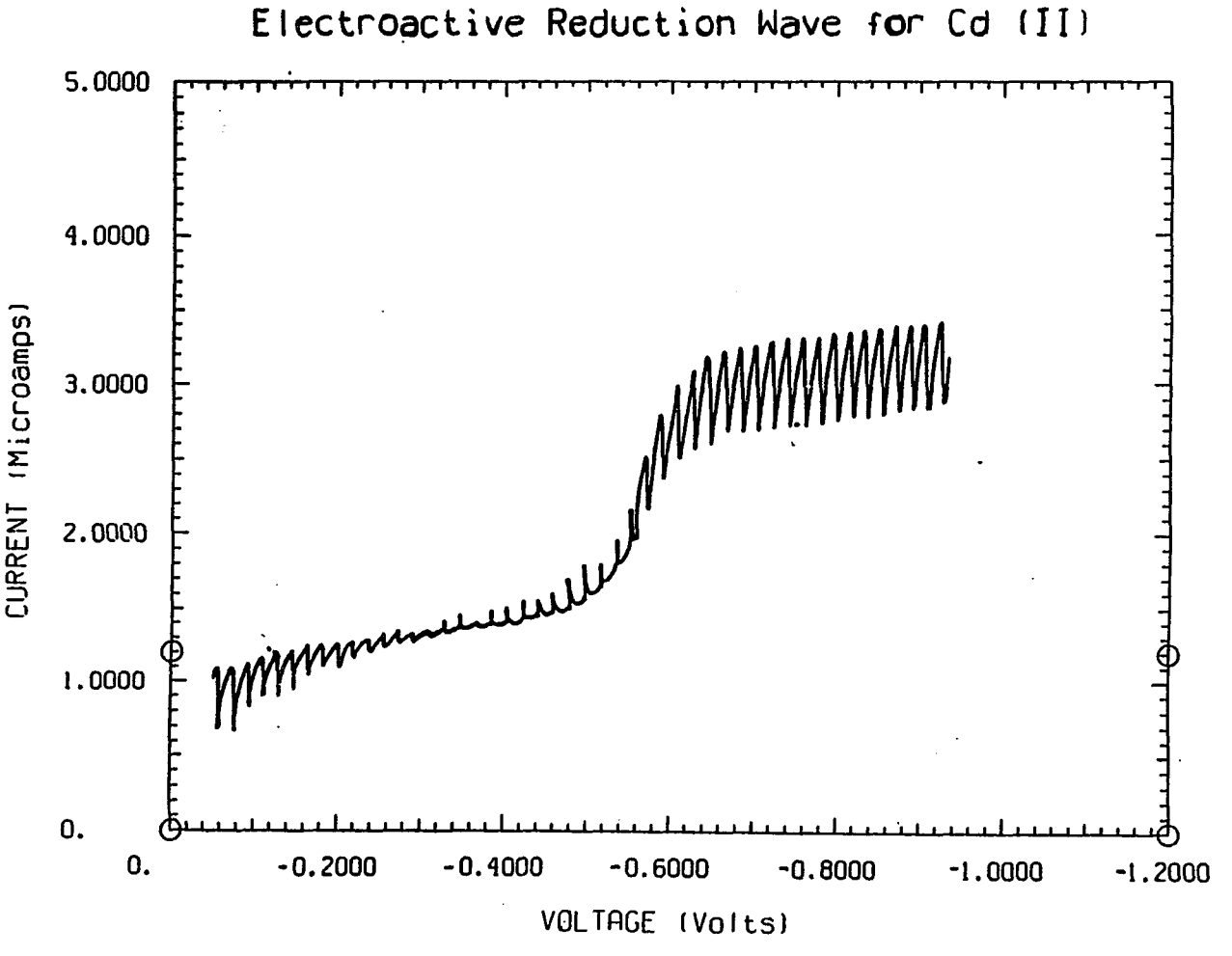
Electroactive Reduction Wave for Cd (II)
5.0000
4.0000
3.0000
2.0000
1.0000
0.
CURRENT (Microamps)
0.
-0.2000
-0.4000
-0.6000
-0.8000
-1.0000
-1.2000
VOLTAGE (Volts)

FIGURE 4.2

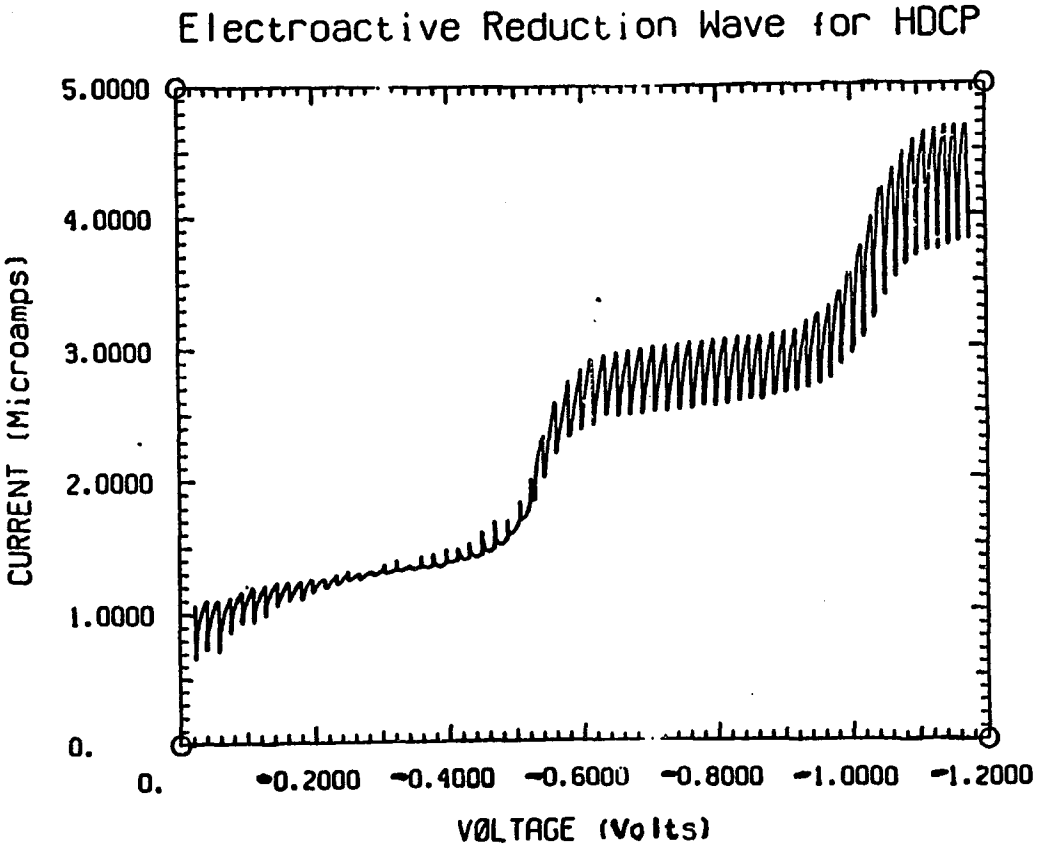
Electroactive Reduction Wave for HDCP
5.0000
4.0000
3.0000
2.0000
1.0000
0.
CURRENT (Microamps)
0.
-0.2000
-0.4000
-0.6000
-0.8000
-1.0000
-1.2000
VOLTAGE (Volts)

FIGURE 4.3

FIGURE 4.4

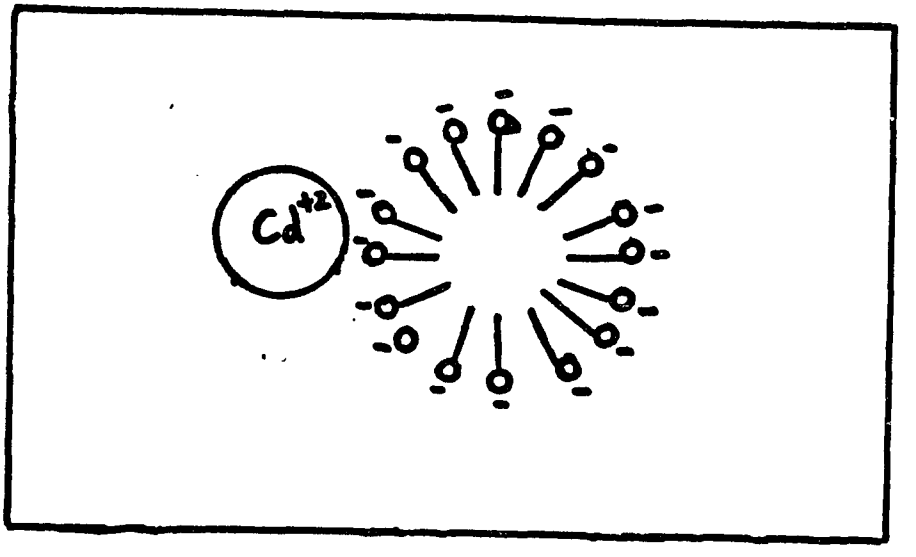

Using Cd^{+2} ions as the electroactive probe, Nivoduff, Hoyer, and Rosano used D.C. polarography to measure the micellar diffusion coefficient of ANIONIC MICELLAR SOLUTIONS.[4] Anionic surfactant forms micelles which have a very large negative surface potential, therefore positively charged Cd^{+2} ions are strongly bound electrostatically to the negatively charged surface of the anionic micelle. Therfore, Cd^{+2} ions stick and diffuse with the anionic micelle and can be used to measure the micellar diffusion coefficient. The Stokes-Einstein equation can be used to measure the micelle particle size if the micellar diffusion coefficient is known.

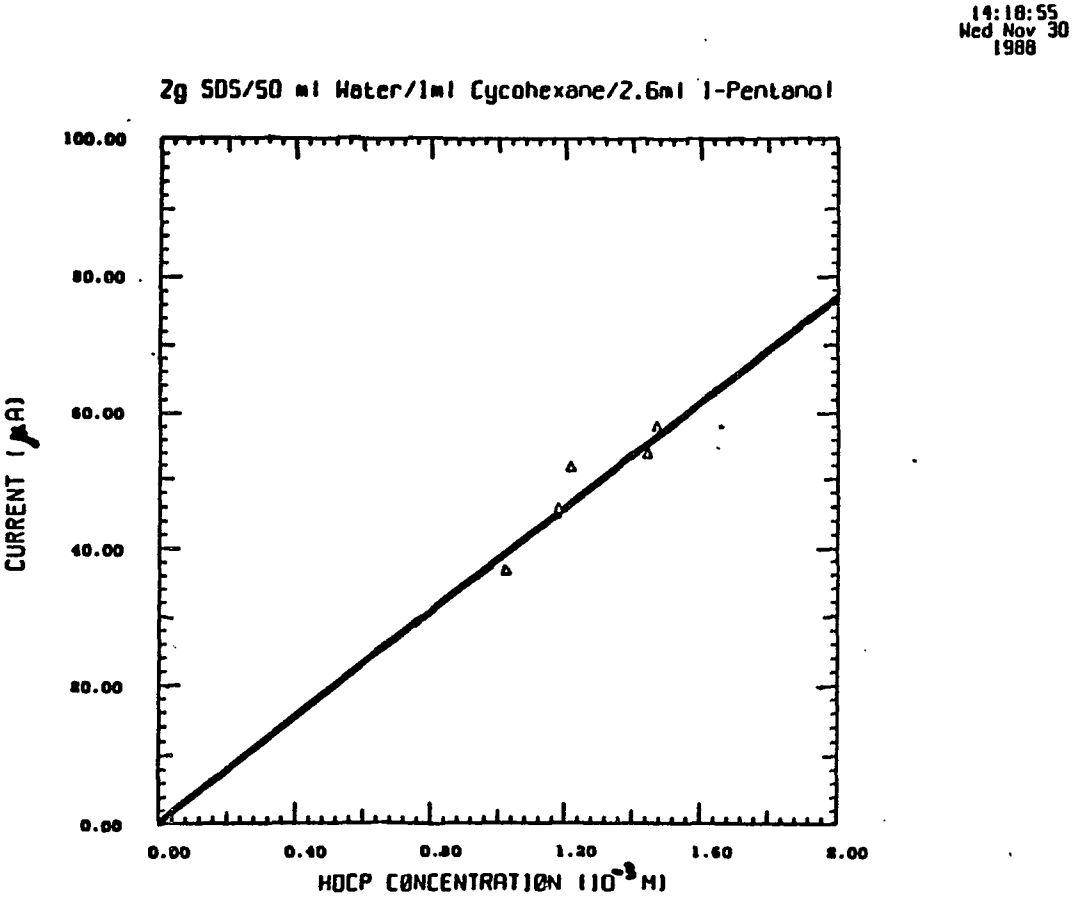
14:18:55
Wed Nov 30
1988
2g SDS/50 ml Water/1ml Cyclohexane/2.6ml 1-Pentanol
100.00
80.00
60.00
40.00
20.00
0.00
CURRENT (μA)
0.00
0.40
0.80
1.20
1.60
2.00
HDCP CONCENTRATION (10^{-3} M)

FIGURE 4.5

Table 4.1: Composition of Microemulsion Systems

System	Surfactant	Cosurfactant	Dispersed	Continuous
1	2.0g SHS	4.0ml 1-pentanol	2.0mln-dodecane	40ml water
2	2.0g SHS	4.0ml 1-pentanol	2.0mln-dodecane	63.8ml water
3	2.0g SHS	3.2ml 1-pentanol	1.0mln-dodecane	40ml water
4	2.0g SHS	3.2ml 1-pentanol	1.0mln-dodecane	62.9ml water
5	2.0g SDS	1.8ml 4MCH	1.0ml toluene	60ml water
6	2.0g SDS	1.8ml 4MCH	1.0ml toluene	92.2ml water
7	2.0g SDS	2.7ml 1-pentanol	2.0mlCH	50ml water
8	2.0g SDS	2.7ml 1-pentanol	2.0mlCH	78.0ml water
9	2.0g SDS	2.6ml 1-pentanol	1.0miCH	50ml water
10	2.0g SDS	2.6ml 1-pentanol	1.0mlCH	77.5ml water

Table 4.2: Microemulsion Polarographic Results			
System	Cd.Diff.Coeff.	HDCP Diff.Coeff.	Hydr.Radius
1	7.47×10^{-7}	2.86×10^{-7}	85.6
2	1.18×10^{-6}	3.14×10^{-7}	77.8
3	1.26×10^{-6}	3.27×10^{-7}	74.7
4	2.56×10^{-7}	3.33×10^{-7}	73.4
5	3.58×10^{-7}	2.50×10^{-7}	97.9
6	6.46×10^{-7}	2.51×10^{-7}	97.7
7	5.02×10^{-7}	3.53×10^{-7}	69.3
8	6.33×10^{-7}	4.00×10^{-7}	61.1
9	8.28×10^{-7}	4.06×10^{-7}	60.3
10	9.12×10^{-7}	4.08×10^{-7}	60.0

Table 4.3: Comparison of Particle Size Measurements		
System	P.C.S.	D.C.Polarography
1	89.2	85.6
2	86.1	77.8

References

1. Rosano, H.L., and Lyons, G.B., *J. Phys. Chem.*, **89,** 363, (1985).

2. Rosano, H.L., Cavallo. J.L., and Lyons, G.B.; Presented at the 5th International Conference on Colloid and Surface Science, Potsdam, New York, June 25th-28th, 1985.

3. Rosano, H.L., Cavallo, J.L., and Lyons, G.B., in "*Microemulsion Systems,*" **Proceedings of the 59th Colloid and Surface Science Symposium and 5th International Congress on Colloid and Surface Science,** Marcel Dekker, New York, (1987), Chapt. 16, pp. 265-279.

4. Shinoda, K., Friberg, S., *Adv. Coll. Inter. Sci.*, **4,** 281, (1978).

5. Reed, R.L., Nealy, R.W., in "*Improved Oil Recovery by Surfactant and Polymer Flooding,*" Academic Press, New York, 1977.

6. De Gennes, P.G., Taupin, C., *J. Phys. Chem.*, **86,** 2294, (1982).

7. Di Meglio, J.M., Dvolaitsky, M., Leger, L., Ober, R., Paz, L., Taupin, C., Presented at the 5th International Congress on Surface and Colloid Science, Potsdam, New York, June 25-28, 1985,; ibid., in "*Microemulsion Systems,*" **Proceedings of the 59th International Congress on Surface and Colloid Science,** Marcel Dekker, New York, 1987.

8. Di Meglio, J.M., Dvolaitsky, M., Taupin, C., *J. Phys. Chem.*, **88,** 6036, (1983).

9. Di Meglio, J.M., Dvolaitsky, M., Ober, R., Taupin, C., *J. Phys. Lettres,* **44,** L-229, (1983).

10. Di Meglio, J.M., Dvolaitsky, M., Taupin, C., to be published, **J. Phys. Chem.**

11. "*Microemulsions,*" L.M. Prince, Ed., Academic Press, New York, 1977.

12. Scriven, L.E., in "*Micellization, Solubilzation, and Microemulsion,*" **Vol. 2,** K.L. Mittal, Ed., Plenum Press, New York, 1977, pg. 877.

13. Mackay, R.A., Dixit, N., Agarwal, R., and Seiders, P., *J. Dispersion Sci. Technol.*, **4,** 397, (1983).

14.Mackay, R.A., in "*Microemulsions,*" I.D. Robb, Ed., Plenum Press, New York, 1982, pp. 207-219.

15.Mackay, R.A., Dixit, N.S., Hermansky, C., and Kertes, A.S., *Colloids and Surfaces,* **2,** 27, (1986).

16.Mackay, R.A., *Advances in Colloid Interface Sci.,* **15,** 131, (1981).

17.Zana, R., Mackay, R.A., *to be published in J. Coll. Inter. Sci.*

18.R.A. Mackay, *private communication.*

19.Rosano, H.L., *U.S. Patent No. 4,* 146, 499, March 27, 1979.

20.Rosano, H.L., *J. Cosmetic Chem.,* **25,** 609, (1974).

21.Macero, D.J., Ruffs, C.L., *J. Electroanal.,* **7,** 328, (1964).

22.Hoyer, H., Novodoff, J., *J. Coll. Inter. Sci.,* **26,** 490, (1968).

23.Novodoff, J., Rosano, H.L., Hoyer, H., *J. Coll. Inter. Sci.,* **38,** 426, (1972).

24.Meites, L., in "*Polarographic Techniques,*" Interscience Puublishing, 2nd Edition, New York, (1963).

25.Hoar, T.P., Schulman, J.H., *Nature (London),* **152,** 102, (1943).

26.Stoekenius, W., Schulman, J.H., and Prince, L.M., *Kolloid Z.,* **169,** 170, (1960).

27.Schulman, J.H., and Riley, D.P., *J. Colloid Sci.,* **3,** 383, (1948).

28.Schulman, J.H., and Friend, J.A., *J. Colloid Sci.,* **4,** 497, (1949).

29.Kim, M.W., Dozier, W.D., and Klein, R., *J. Chem. Phys.,* **84,** 5919, (1986).

30.Huang, J.S., and Kim, M.W., *Phys. Review Letters,* **47,** 1462, (1981).

31.Fourche, G., Belloco, A.M., Brunetti, S., *J. Colloid Interface Sci.,* **88,** 302, (1982).

32.Cazabat, A.M., and Langevin, D., *J. Chem. Phys.,* **4,** 3148, (1981).

33.Bowcott, J.E.L., and Schulman, J.H., *Z. Electrochem.,* **59,** 283, (1955).

34.Dvolaitsky, M., Guyot, M., Lagues, M., Le Pesant, J.P., Ober, R., Sauterey, C., and Taupin, C., *J. Chem. Phys.,* **69,** 3279, (1978).

35.Cavallo, J.L., and Rosano, H.L., *J. Phys. Chem.*, **90,** 6817, (1986).

36.Huang, J.S., Safran, S.A., Kim, M.W., Grest, G.S., Kotlarchyk, M., and Quirke, N., *Phys. Rev. Letters*, **53,** 592, (1984).

37.Ober, R., and Taupin, C., *J. Phys. Chem.*, **84,** 2418, (1980).

38.Kotlarchyk, M., Chen, S.H., Huang, J.S., and Kim, M.W., *Physical Review A*, **29,** 2054, (1984).

39.Zana, R., Lang, J., *Colloids and Surfaces*, **48,** 153, (1990).

40.Lianos, P., Lang, J., Strzielle, C., Zana, R., *J. Phys. Chem.*, **86,** 1019, (1982).

41.Almgren, M., Greieser, F., Thomas, J.K., *J. Am. Chem. Soc.*, **102,** 3188, (1980).

42.Cannon, P.L., Jr., Garlick, S.M., Christeson, S.D., Wong, N.M., Novelli, A.C., Longo, F.R., Mackay, R.A., *to be published.*

43.Chokshi, K., Qutubuddin, S., Hassam, A., *J. Coll. Inter. Sci.*, **129,** 315, (1989).

44.Lindman, B., Stilbs, P., in "*Microemulsion Systems*," **Proceedings of the 59th Colloid and Surface Science Symposium and 5th International Congress on Colloid and Surface Science,** Marcel Dekker, New York, 1987, Chapt. 7, pp. 129-144.

45.Lindman, B., Stilbs, P., Moseley, M.E., *J. Coll. Inter. Sci.*, **83,** 569, (1981).

46.Langevin, D., *Adv. Coll. Inter. Sci.*, **34,** 583, (1991).

47.Shinoda, K., Lindman, B., *Langmuir*, **3,** 135, (1987).

50.Mackay, R.A., Dixit, N., and Agarwal, R., "*Inorganic Reactions in Organized Media*," **ACS Symposium Series No. 177,** S.H. Holt, Ed., 1982, pp. 179-198.

51.Mackay, R.A., Hermansky, C., and Agarwal, R., *Colloid and Surfaces*, **2,** 27, (1986).

52.Mackay, R.A., and Agarwal, R., *J. Colloid Interface Sci.*, **65,** 225, (1978).

53.Mackay, R.A., and Agarwal, R., *J. Colloid Interface Sci.*, **65,** 225, (1978).

54.Rosano, H.L., Nixon, A.L., and Cavallo, J.L., *J. Phys. Chem.*, **93,** 4536, (1989); also, to be published in "*The Proceedings of the 2nd World Surfactants Congress*," *ASPA, Paris,*

France, March 24th-28th, 1988.

55.Rosano, H.L., Lan, T., Weiss, A., Gerbacia, W.E.E., and Whittam, J.H., *J. Colloid Interface Sci.*, **72,** 233, (1979).

CHAPTER 5:

INTERFACIAL STOICHIOMETRY and VAPOR PRESSURE MEASUREMENTS in OIL-IN-WATER MICROEMULSION SYSTEMS

5.1. Introduction

Microemulsions have attracted considerable interest since their introduction by Schulman (1). These systems were described by Schulman as one phase optically transparent dispersions of oil, water, and surfactant. Schulman noted that the spontaneous formation of these transparent dispersions depended on the addition of a cosurfactant to the system. These transparent one phase dispersions have low viscosity and solubilize large volume fractions of both oil and water. In most cases, microemulsions may be considered to be thermodynamically stable systems (2-4).

In most cases, microemulsion structure can be described as consisting of dispersed microdroplets of either oil-in-water or water-in-oil. The microdroplets in these systems consist of an inner core of dispersed phase (either oil or water) surrounded by an interfacial layer of constant stoichiometry. In this publication the microdroplet interfacial stoichiometry was determined for seven different oil-in-water systems by titration experiments (see Table 5.1). In some cases, microemulsion systems should not be described by microdroplet but by bicontinuous structures (5-7).

As discussed in Chapter 4 of this dissertation, different methods have been employed to determine the size of the dispersed droplets for these transparent one-phase systems (8-33). Microdroplet radii between 45 to 800 Å have been measured by these different experimental techniques. In this publication two different oil-in-water sytems were investigated

by vapor pressure as a function of increasing oil volume (see Table 5.2). Microdroplet radii were determined from these vapor pressure measurements. As determined from these vapor pressure measurements, the size of the microdroplets in these two oil-in-water systems was found in the size range of between 53.6 to 120.8 Å. Microdroplet radii were found to increase as the volume fraction of dispersed phase increased for both of the oil-in-water microemulsion systems prepared at constant amount of primary surfactant and investigated by vapor pressure in this publication.

5.2. Experimental

5.2.1. Chemicals

N-octane, n-decane, n-dodecane, n-tetradecane, and n-hexadecane were spectroscopic grade (99%+, gold label Aldrich Chemical Co., Milwaukee, Wis.). Sodium dodecyl sulfate (Eastman Kodak Co., Rochester, N.Y.) was electrophoresis grade (99%+). Sodium chloride and sodium hydroxide were reagent grade. Dodecyldimethylamine oxide (Onyx Chemical Co., Jersey City, N.J.) was 30% active. All chemicals were used as received. Freshly distilled water was used in all preparations, and all glassware was first thoroughly cleaned with a fresh sulfuric acid/ potassium dichromate solution.

5.2.2. The Measurement of the Interfacial Stoichiometry of Some Microemulsion Systems

The interfacial stoichiometry of several different microemulsion systems (see Table 5.1) was determined by a novel technique. The first step in this novel technique involves preparing optically transparent micellar solutions by mixing aqueous phase and surfactant in water-jacketed beakers maintained at 30°C. A constant amount of saline and surfactant is used in this process (see Table 5.1). Using a magnetic stirrer, continuous stirring is used throughout this procedure so as to ensure a homogenous solution. Oil phase is then added dropwise. For small aliquots of oil the system remains transparent as a swollen micellar solution is formed. Beyond a certain initial amount of oil (interfacial oil volume) the

system becomes opaque. For each system investigated in Table 5.1, the corresponding initial volume of oil (referred to as the interfacial oil volume) needed to make the transparent micellar solution opaque was determined (see Table 5.3).

The point method (34) for preparation of microemulsion systems is used. Having determined the interfacial oil volume needed to make each corresponding oil-in-water system opaque (see Table 5.3), the next step involves titrating the optically opaque system (or emulsion) to clarity with cosurfactant. The minimum volume of cosurfactant needed to titrate the system to clarity (transmittance greater than 90% at 520 nm) versus the volume of oil used was then recorded. Additional oil is then added to the system. This causes the system to become optically opaque again. Additional cosurfactant is then added dropwise until the system becomes transparent. Again the minimum volume of cosurfactant needed to titrate the system to clarity versus the oil volume is recorded. This procedure (adding more oil and then titrating) is repeated so as to generate numerous data points. By plotting these data points (the minimum volume of cosurfactant needed to titrate the system to clarity versus the corresponding oil volume used), a straight line graph is obtained. A linear regression formula is used to fit these data points to the line. From the linear regression formula the slope, the intercept, and the correlation of this straight line is obtained. These results are illustrated in Table 5.3 for each oil-in-water system investigated. For each system investigated in Table 5.1, the titration curve is illustrated in the corresponding figures (see Figure 5.1 for System 1 to Figure 5.7 for System 7). Each figure illustrates the oil volume versus the minimum volume of cosurfactant needed to titrate the corresponding system to clarity. For example, Figure 5.1 demonstrates this for System 1 from Table 5.1.

5.2.3. Preparation of Samples to be used in Vapor Pressure Analysis

Two different transparent oil-in-water systems were investigated by vapor pressure analysis (see Table 5.2). These transparent systems were prepared by the titration technique (34). A variable volume of oil (dispersed phase) was used in the preparation of samples needed for vapor pressure measurements. Initial coarse emulsions were prepared by mixing

saline (25 ml of 5% NaCl + 0.01N NaOH; pH=11.2)/ SDS/ and a variable volume of oil (either n-octane for System 8 or n-decane for System 9) in a water-jacketed beaker maintained at 30°C by a thermostated water bath (see Table 5.2). The initial coarse emulsion is optically opaque. The system was then titrated to clarity using a cosurfactant (dodecyldimethylamine oxide) delivered from a microburet. Continuous stirring was maintained throughout the titration process to ensure homogenous stirring. Percent transmittance was measured as the system started to clear with a Spectronic 20 spectrometer (Bausch and Lomb Co., Rochester, N.Y.) at 520 nm. The minimum volume of cosurfactant needed to titrate each sample to clarity (transmittance greater than 90%) was used to prepare each sample. The titration curve (minimum volume of cosurfactant versus oil volume) needed to prepare the samples is illustrated by Figure 5.8 for System 8 and by Figure 5.9 for System 9. The different samples of varying oil volume were then stored in sealed glass tubes so as to be subsequently used in vapor pressure measurements.

5.2.4. Vapor Pressure Measurements

Vapor pressure versus the boiling point of the samples of varying oil volume were then determined. The vapor pressure of each sample was determined with an isoteniscope. The experimental apparatus is illustrated in Figure 5.10. The sample was placed in the isoteniscope and submerged in a hot water bath. The system was allowed to boil for 10 minutes to evacuate any residual air present. The bath was then slowly cooled until an equilibrium between the liquid and vapor was obtained in the isoteniscope. The pressure within the system along with the temperature of the water bath was then recorded. The pressure was then further reduced and the temperature of the water bath was reduced until equilibrium between the liquid and vapor in the isoteniscope was reestablished. The new equilibrium vapor pressure and boiling point was then recorded. This procedure was repeated to generate numerous data points of equilibrium vapor pressure versus equilibrium boiling point for each sample. Vapor pressure versus boiling point was measured in the temperature range 25-60°C. From the experimental data, the log of the vapor pressure

versus the inverse of the boiling point temperature was calculated. By using the Clausius-Clapeyron equation (see equation 5.1), the vapor pressure and the heat of vaporization as a function of oil volume (dispersed phase) was determined for each oil-in-water microemulsion system investigated.

$$\ln \frac{p}{p_0} = -\frac{\Delta H_{vap}}{R}\left[\frac{1}{T} - \frac{1}{T_0}\right] \qquad (5.1)$$

where p = vapor pressure at temperature T;

p_o = vapor pressure at temperature T_o;

R = ideal gas constant;

ΔH_{vap} = the heat of vaporization of the oil-in-water microemulsion system.

5.3. Results

5.3.1. Titration Results (Interfacial Stoichiometry Measurements)

The model for the microdroplet in these oil-in-water systems may be described as an oil core surrounded by an interfacial shell where all of the surfactant and part of the cosurfactant and oil form the interfacial sheath. The stoichiometry of the interfacial shell is determined from the titration results for each system investigated. The primary surfactant is located in the interfacial sheath of the microdroplets. Therefore, the number of moles of surfactant in the interfacial shell of the microdroplets is calculated from the initial composition of each system (see Table 5.1).

For a given volume of dispersed phase, the minimum volume of cosurfactant needed to titrate each system investigated to clarity was plotted. Graphs of the minimum volume of cosurfactant versus the volume of oil give straight lines. The lowest point on this straight line was dependent on the addition of a certain minimum amount of oil to each oil-in-water system. A linear regression formula was used to fit the data points to the straight line for each system investigated. The slope, intercept, interfacial oil volume, and correlation of the straight line for each oil-in-water system investigated (see Table 5.1) are tabu-

lated in Table 5.3. The lowest point on the straight line in each of these graphs corresponds to the interfacial oil volume. For each system investigated in Table 5.3, the titration curves are illustrated in the corresponding figures (see Figure 5.1 for for System 1 to Figure 5.7 for System 7).

In our results, the oil volume corresponding to the lowest point (i.e., point with smallest oil and corresponding cosurfactant volume) on this straight line graph represents the oil volume required at the microdroplet interface. Any additional volume of oil above the oil volume corresponding to the initial point on this straight line is incorporated in the interior of the microdroplet and is not associated with the microdroplet interface. We calculate the number of moles of oil required at the microdroplet interface from the oil volume corresponding to the initial point on this straight line graph. We can also calculate the number of moles of cosurfactant at the microdroplet interface by using the cosurfactant volume corresponding to the initial point on this straight line graph. At this cosurfactant volume the interior region (oil pseudophase) of the microdroplet does not exist. The cosurfactant volume corresponding to the initial point represents cosurfactant in both the continuous phase and at the microdroplet interface. Since the intercept of this straight line (cosurfactant volume at zero oil volume) corresponds to volume of cosurfactant in the continuous phase, we can calculate the cosurfactant volume at the microdroplet interface by subtracting the cosurfactant volume at the initial point of this straight line from the cosurfactant volume at the intercept of this straight line. Knowing the interfacial cosurfactant volume we calculate the number of moles of cosurfactant at the microdroplet interface. Therefore we can calculate the number of moles of surfactant, cosurfactant, and oil in the microdroplet interfacial sheath for each oil-in-water microemulsion system investigated by this titration procedure. We repeat this procedure for each system studied in Table 5.1. The calculated number of moles of cosurfactant, surfactant, and oil at the microdroplet interface for each oil-in-water system studied is summarized in Table 5.4. Interfacial stochiometries were then calculated for each system studied (see Table 5.5).

5.3.2. Vapor Pressure Measurements

The vapor pressure for each transparent oil-in-water system was determined from equation 5.2 by plotting ln p vs. 1/T. A linear regression formula was used to fit the experimental data points to a straight line. In all cases straight lines were obtained with excellent correlation. This procedure was repeated as a function of oil volume (n-octane for System 8 or n-decane for System 9). The slope, intercept, and correlation as a function of oil volume (dispersed phase) are tabulated in Table 5.6 for microemulsion system 8 and in Table 5.7 for microemulsion system 11. From the slope of this straight line the heat of vaporization (see Table 5.6 and 5.7), ΔH_{vap}, was determined as a function of oil volume (dispersed phase).

The heat of vaporization as a function of n-octane (dispersed phase) volume is illustrated by Figure 5.11 for System 8. A maximum (62.8 kJ/mol) occurs in the low dispersed volume (n-octane) region of this curve and is observed at 0.98 ml of n-octane. The heat of vaporization is a large number in the low dispersed volume (n-octane) of this curve (ΔH_{vap} > 57 kJ/mol for volumes of n-octane below 1.55 ml). This indicates that the dispersed microdroplets in System 8 are more strongly bound in the low dispersed volume region of this curve. The large ΔH_{vap} (heat of vaporization) demonstrates that the dispersed microdroplets are characterized by a relatively rigid interfacial structure in the low dispersed volume region of this curve. Above 0.98 ml of n-octane (dispersed phase), the measured heat of vaporization decreases as the volume of dispersed phase increases. The heat of vaporization is a smaller number in the high dispersed volume region of this curve (ΔH_{vap} < 50 kJ/mol for n-octane volumes greater than 3.33 ml). This indicates that the dispersed microdroplets are less strongly bound in System 8 for dispersed volumes (n-octane) greater than 3.33 ml. The relatively small ΔH_{vap} (heat of vaporization) demonstrates that the dispersed microdroplets are characterized by a flexible interfacial structure in the high dispersed volume (n-octane) region of this curve. It is interesting to note that a certain critical volume (0.98 ml) of n-octane (dispersed phase) is needed in System 8 before ΔH_{vap}

decreases with increasing dispersed volume. Beyond this critical n-octane volume, the decreasing ΔH_{vap} demonstrates that the interfacial flexibility increases with increasing n-octane volume (dispersed phase).

The heat of vaporization as a function of n-decane volume (dispersed phase) is illustrated by Figure 5.12 for System 9. A maximum occurs in the low dispersed volume region (n-decane) of the curve in Figure 5.12 (ΔH_{vap} = 53.28 kJ/mol at 0.24 ml of n-decane). The shape of this curve is very similar in shape to the curve seen for System 8 in Figure 5.11. Both of these oil-in-water microemulsion systems are characterized by a large heat of vaporization in the low dispersed volume region compared to a small heat of vaporization in the high dispersed volume region. Comparison of Figure 5.11 for System 8 and Figure 5.12 for System 9 supports this conclusion. When System 9 is prepared with less than 0.24 ml of n-decane the ΔH_{vap} is greater than 48 kJ/mol. When System 9 is prepared with more than 0.82 ml of n-decane the ΔH_{vap} is less than 46 kJ/mol. These results demonstrate that the dispersed microdroplets are more strongly bound in the low dispersed volume region compared to being less strongly bound in the high dispersed volume region. However, this effect is much less pronounced for System 9 compared to System 8. The fact that the heat of vaporization decreases beyond some critical volume of dispersed phase suggests that the interface between the dispersed microdroplets and the continuous phase becomes a less rigid and increasingly flexible structure as the volume of dispersed phase (n-octane or n-decane) increases. This critical volume of dispersed phase corresponds to a much smaller volume than the maximum amount of oil (dispersed phase) that can be solubilized for each oil-in-water system (n-octane for System 8 and n-decane for System 9).

The vapor pressure vs. oil volume was determined between 20-60°C for the two oil-in-water systems investigated. Examination of Figure 5.13 for System 8 demonstrates an initial vapor pressure lowering in the low dispersed volume region. When System 8 is prepared at 30°C with 0.54 ml of n-octane the vapor pressure decreases to a value of 22.92 mm Hg compared to a value of 28.27 mm Hg for the 5% NaCl + 0.01N NaOH (pH = 12.2)

saline solution which is used in the preparation of the oil-in-water microemulsion system. Above 3.00 ml of dispersed phase for System 8 there is no longer a vapor pressure lowering. When System 8 is prepared with 4.76 ml of n-octane the vapor pressure increases to a maximum value of 52.09 mm Hg at 30°C. Examination of Figure 5.14 for System 9 also demonstrates a lowering in vapor pressure at low dispersed (n-decane) volume. When System 9 is prepared at 30°C with 0.18 ml of n-decane (dispersed phase) the vapor pressure decreases to a value of 21.30 mm Hg compared to a value of 28.27 mm Hg for saline. Above 0.24 ml of n-decane the vapor pressure increases as the volume of dispersed phase (n-decane) increases. Above 0.82 ml of dispersed phase (n-decane) there is no longer a vapor pressure lowering in System 9. When System 9 is prepared with 1.01 ml of n-decane the vapor pressure increases to a maximum value of 29.81 mm Hg at 30°C.

The vapor pressure results shown in Figure 5.13 for System 8 and in Figure 5.14 for System 9 demonstrate that two distinct vapor pressure regions are present in both of these oil-in-water systems. The vapor pressure behavior in each system is different in the low dispersed volume region relative to the high dispersed volume region. The low dispersed volume region in each of these systems is characterized by a vapor pressure lowering. This behavior is similar to high molecular weight polymer solutions or regular colloidal dispersions whereby the vapor pressure of the solution is less than that of the continuous phase. The high dispersed volume region for each of these oil-in-water systems is characterized by a dramatic vapor pressure increase compared to the low dispersed volume region. The vapor pressure is larger than that of the continuous phase in the high dispersed volume region for each of these oil-in-water systems.

Assuming that the vapor pressure lowering region in System 8 and 9 is composed of monodispersed noninteracting droplets, the Van't Hoff equation (see equation 5.2) was used to calculate the average molecular weight (MW) of each microdroplet.

$$MW = \frac{RTC}{\pi} \tag{5.2}$$

where R = ideal gas constant;

T = the temperature in Kelvin;

C = the solution concentration in g/l;

and π = p_0 -p, i.e., the vapor pressure difference between the solution containing no oil and microemulsions containing various volumes of hydrocarbon (dispersed phase).

Microdroplet MW values were determined for n-octane oil volumes from 0.54 to 1.75 ml of n-octane in System 8. From our experimental results, for volumes of n-octane larger than 1.75 ml, the dramatic increase in value of the MW indicates that the droplets start to percolate. Microdroplet MW values were determined in System 9 for n-decane oil volumes from 0.18 to 0.60 ml of n-decane. From our experimental results, for n-decane volumes greater than 0.50 ml of n-decane, the dramatic increase in value of the MW indicates that the droplets start to percolate. Microdroplet MW as a function of oil volume (n-octane for System 8 and n-decane for System 9) are tabulated in Table 5.8 for System 8 and in Table 5.9 for System 9.

$$\frac{MW}{SW} = \frac{4\pi r^2}{\sigma} \tag{5.3}$$

where MW = average gram molecular weight per microdroplet;

σ = average cross sectional area per surfactant molecule;

C = the solution concentration in g/l;

and SW = the surfactant weight. between the solution containing no oil and microemulsions containing various volumes of hydrocarbon (dispersed phase).

Microdroplet radii as a function of oil volume were calculated for System 8 (see Table 5.11) and System 9 (see Table 5.12) assuming that $\sigma = 30$ Å^2.

5.4. Discussion

The hydrocarbon oils used to prepare oil-in-water systems 1 to 5 (see Table 5.1) represent an homologous series. A constant amount of aqueous phase and primary surfactant (SDS) was used for each of the five oil-in-water systems investigated. Each system oil-in-water investigated is composed of 2g SDS/40 ml 5% NaCl + 0.01N NaOH (pH = 11.2)/ a variable volume of a long-chain n-alkane/ and 1-pentanol. The composition of each of these oil-in-water systems differs only in the hydrocarbon oil (a long-chain alkane) used. Each corresponding figure (see Figure 5.1 to 5.5) for these systems represents the oil volume versus minimum volume of cosurfactant (1-pentanol) needed to titrate each oil-in-water system to clarity. N-octane, n-decane, n-dodecane, n-tetradecane, and n-hexadecane are the corresponding hydrocarbon oils investigated in the homologous series. Examination of Figure 5.1 to 5.5 shows that n-decane represents the hydrocarbon oil in the homologous series for which the largest oil volume is solubilized. For example, oil-in-water System 2 can solubilize a maximum of 2.70 ml of n-decane compared to a maximum solubilization of 2.00 ml of n-octane for System 1, 2.00 ml of n-dodecane for System 3, 1.70 ml of n-tetradecane for System 4, and 1.60 ml of n-hexadecane for System 5. The maximum volume of oil that can be solubilized for each corresponding system in this homologous series is summarized in Table 5.10. Above n-decane in this homologous series we see a progressive decrease in the maximum amount of oil that can be solubilized as we increase the chainlength of the solubilized oil. We can conclude from these results that n-decane offers the best chainmatching combination with SDS surfactant in the n-octane to n-hexadecane homologous series.

As discussed in Chapter 4 of this dissertation, Rosano et al. (35) concluded from DSC, titration, and ultracentrifugation measurements (35-36) that the amount and composition of the interfacial layer surrounding the dispersed phase microdroplets is constant in microemulsion systems. This result may also help to explain why a minimum amount of oil is necessary in order to prepare certain oil-in-water microemulsion systems. This

minimum volume of oil (dispersed phase) is incorporated into the interfacial sheath and is necessary to satisfy the required stoichiometry of the interface. Additional oil above the minimum volume may then be incorporated in the inner core of the dispersed microdroplets in these oil-in-water systems. In this publication the interfacial stochiometry of several different oil-in-water systems (see Table 5.1 and 5.4) was determined by titration experiments. The microdroplets model for these oil-in-water systems can be described as an inner oil core surrounded by an interfacial shell of constant composition where all of the surfactant and part of the cosurfactant and oil form the interfacial shell.

Within this constraint of a constant interfacial area for microemulsion systems prepared with a fixed amount of primary surfactant, a change in volume of the dispersed phase will cause the droplets to swell or shrink with a concomitant decrease or increase in the size of the microdroplets accordingly (see eq. 5.4).

$$n = \frac{3V}{r\sigma} \tag{5.4}$$

where n = the minimum amount of primary surfactant needed in order to disperse a given volume V of dispersed phase,

V = given volume of dispersed phase,

R = radius of the monodisperse microdroplets,

and σ = the cross sectional area per surfactant molecule.

In this publication vapor pressure measurements were used to measure microdroplet particle size as a function of dispersed phase (oil) for two different oil-in-water systems (see Table 5.2). Each of the two oil-in-water systems investigated by vapor pressure was prepared with a constant amount of primary surfactant. Microdroplet radii versus volume of dispersed phase (n-octane for System 8 and n-decane for System 9) are illustrated in Table 5.11 for System 8 and in Table 5.12 for System 9. These vapor pressure measurements demonstrate that microdroplet particle size increases as the volume of dispersed phase

increases for each oil-in-water investigated at a fixed amount of primary surfactant. For example, a microdroplet radius of 53.6 Å is measured when System 9 is prepared with 0.18 ml of n-decane compared to microdroplet radii of 72.1 Å for 0.40 ml of n-decane and 120.8 Å for 0.60 ml of n-decane (see Table 5.12 for System 9). In System 8 a microdroplet radius of 55.4 Å is measured for 0.77 ml of n-octane compared to microdroplet radii of 106.4 Å for 1.18 ml of n-octane and 141.4 Å for 1.55 ml of n-octane (see Table 5.11 for System 8).

Two different regimes of phase behavior have been found to exist in droplet structure microemulsion systems. One regime of phase behavior occurs below a certain critical volume fraction of dispersed phase and the other regime occurs at or above this critical volume fraction of dispersed phase. A phenomenon called percolation may or may not be occurring in these microemulsion systems. Below a certain critical volume of dispersed phase the microdroplets behave as isolated, noninteracting particles in microemulsion systems. Percolation occurs when there is interaction between the dispersed phase droplets and begins to occur beyond some critical dispersed phase volume. Percolation may be described as a dynamic process where transient merging and reformulaion of the microdroplets in these systems occurs. Percolation behavior has been documented by vapor pressure measurements (28,37) in oil-in-water microemulsion systems and by electrical conductivity (38-39) and P.C.S. measurements (40-44) in water-in-oil microemulsion systems.

In a previous publication vapor pressure measurements (28) were used by Rosano et al. to investigate an oil-in-water microemulsion system (n-octane/ sodium cetyl sulfate (SCS)/5% NaCl + 0.01N NaOH (pH 11.2)/ and dodecyldimethylamine oxide (DDAO)). The microemulsion system was prepared with a constant amount of primary surfactant while the volume of dispersed phase was varied. The system was prepared as a function of dispersed phase (n-octane) by titrating to clarity with the cosurfactant DDAO. Vapor pressure measurements as a function of increasing volume of dispersed phase (n-octane) were investigated. Based on these vapor pressure measurements, two different regimes of phase

behavior can be observed for this oil-in-water microemulsion system. At low volume fractions of dispersed phase, the microdroplets contain only a small volume of oil which is tightly encapsulated by the microdroplet interfacial sheath. This prevents hydrocarbon from being present in the vapor phase above the microemulsion system and a lowering in vapor pressure is recorded. In the low dispersed phase (n-octane) volume fraction regime, the heat of vaporization was found to be a relatively large number (>48 kJ/mol). This shows that the oil-in-water microdroplets are structurally stable and that oil is tightly bound by the microdroplet interfacial sheath. The microdroplets behave as isolated, noninteracting particles in the low dispersed volume fraction region. However, in the high volume fraction region for hydrocarbon, the microemulsion system starts to behave differently, i.e., the radius of the droplets increases to a certain critical droplet size as more n-octane is present in the dispersed phase. At some critical droplet size interaction between droplets begins. Microdroplet interaction results in the merging and coalescence of neighboring microdroplets. Coexistence of closed and open microemulsion droplets is a product of coalescence and this results in an increase in vapor pressure as hydrocarbon is free to enter the vapor phase from open microdroplets. Facile merging between neighboring microdroplets suggests that oil is weakly bound by the interfacial sheath and this is reflected by the lower heat of vaporization and increased vapor pressure in the high dispersed volume fraction region relative to the low dispersed volume fraction region.

In this publication vapor pressure measurements for two different oil-in-water microemulsion systems (see Table 5.2) were investigated. The oil-in-water microemulsion systems investigated in this publication were prepared at a constant amount of primary surfactant while the volume of dispersed phase (oil) was varied (see Table 5.2). Two distinct regions of vapor pressure behavior are also found for the two oil-in-water systems investigated in this publication. Vapor pressure measurements for System 8 (see Figure 5.13) demonstrate that a vapor pressure lowering occurs when System 8 is prepared with less than 2.48 ml of dispersed phase. If System 8 is prepared with more than 3.33 ml of dispersed

phase the vapor pressure increases dramatically. Vapor pressure measurements for System 9 (see Figure 5.14) demonstrate that a vapor pressure lowering occurs when System 9 is prepared with less than 0.60 ml of dispersed phase. If System 9 is prepared with more than 0.82 ml of dispersed phase the vapor pressure increases. The vapor pressure measurements for the two oil-in-water systems investigated in this publication support the conclusion that a change in phase behavior occurs with increasing volume of dispersed phase. At low volume fraction of dispersed phase each oil-in-water system investigated is characterized by a vapor pressure lowering and a relatively large heat of vaporization. This demonstrates that in the low dispersed volume fraction region that the initial increment of dispersed phase (oil) is tightly encapsulated by the interfacial sheath of the microdroplets and that there is a strong association between the hydrocarbon tails of the surfactant and the hydrocarbon dispersed phase. At high volume fraction of dispersed phase for the two oil-in-water systems investigated a dramatic increase in vapor pressure and a smaller heat of vaporization occurs relative to the low volume fraction region of dispersed phase. This demonstrates that the dispersed phase (oil) is weakly bound by the microdroplet interfacial sheath in the high dispersed volume fraction region. Microdroplet interaction in this region results in the merging and reformulation of microdroplets. The weakly bound oil is more accessible to the vapor phase and this accounts for the increase in vapor pressure in the high dispersed volume fraction region.

In the case of water-in-oil microemulsion systems, when the dispersed phase (aqueous phase) volume increases, it was reported (38-39) that the electrical conductance of the system remained initially very low and at or above a certain critical volume of aqueous phase, the electrical conductivity of the microemulsion increased. If the volume fraction of the water is less than the "percolation threshold," Φ_c, of water, the oil phase is continuous and all the water is surrounded by the oil. Since the water is isolated and oil is poorly or non-conducting, the conductivity is very low. A charge on a water microdroplet can propagate either by hopping to a neighboring microdroplet or via the diffusion of the charged droplet.

Therefore, the electrical conductivity is small but finite in this region. For a microemulsion system of aqueous volume fraction above the percolation threshold, Φ_c, some of the water droplets start to form connected sets of globules resulting in a large increase in the electrical conductivity of the system. Safran (45-47) suggested that spherical microemulsions undergo a nonconducting to conducting transition at a relatively small (approximately 10%) volume fraction of dispersed phase. Monte Carlo simulation was also used to explain how clustering due to attractive interactions plays an important role in dramatically lowering the percolation threshold of microemulsion systems. This attractive interaction is extremely short-ranged, i.e., in the order of 3 Å. The essential point is that beyond a certain critical volume of dispersed phase, the droplets start to interact and form transitory larger globules.

The heat of vaporization as a function of oil volume measured in these vapor pressure experiments is a reflection of the microdroplet interfacial rigidity. Larger ΔH_{vap} reflect increased rigidity while smaller ΔH_{vap} reflect decreased rigidity. The presence of maxima in the heat of vaporization versus oil volume curves demonstrates that a change in behavior occurs for the microdroplet interfacial rigidity in these oil-in-water systems. A maximum in the heat of vaporization (ΔH_{vap} = 62.8 kJ/mol) versus dispersed phase volume curve occurs when System 8 (see Figure 5.11) is prepared with 0.98 ml of dispersed phase. Likewise, a maximum in the heat of vaporization (ΔH_{vap} = 53.3 kJ/mol) versus dispersed phase occurs when System 9 (see Figure 5.12) is prepared with 0.24 ml of dispersed phase. Below these maxima the interfacial rigidity increases with increasing oil volume. The large heat of vaporization that occurs for small amounts of oil demonstrates that a strong association between oil and surfactant occurs and that the micellar aggregates behave more like rigid macromolecules in this region. Each oil-in-water system may be described as a swollen micellar solution for very small amounts of oil. Swollen micellar solutions differ from microemulsion systems in that they solubilize relatively small volumes of dispersed phase and are characterized by rigid relatively interfacial structures. Above the maxima in the curves for each of these oil-in-water systems the interfacial rigidity decreases with increas-

ing oil volume. Above these maxima each oil-in-water system begins to acquire characteristics corresponding to a flexible microemulsion interface. The smaller heat of vaporization demonstrates that the microdroplet interface may be described as a soft and flexible structure in this region. These vapor pressure results suggests that oil plays a major role in decreasing the interfacial rigidity (or increasing the interfacial flexibility) in these oil-in-water systems. We conclude that an initial increment of oil is needed to satisfy the interfacial requirements before additional oil begins to decrease the interfacial rigidity in each oil-in-water system investigated by vapor pressure.

The corresponding titration curve for each oil-in-water system is illustrated in Figures 5.1 to 5.7. Each of these oil-in-water systems solubilizes a small amount of oil when only primary surfactant is used to prepare each oil-in-water system. The addition of cosurfactant to these oil/ water/ and surfactant systems allows the solubilization of far larger volumes of oil. The role of cosurfactant in the formation of microemulsion systems has been discussed by other workers. As an early pioneer in the field of microemulsion formation Schulman (48) described the role of cosurfactant is to increase the disorder of the interfacial film in these disperse systems. Rosano et al. (49) described the role of cosurfactant as a dynamic lowering of interfacial tension that occurs during transport of the cosurfactant across the interfacial film. He concluded that after resolution of the microdroplets in the sytem that the interfacial tension returns to a small but finite value.

Di Meglio et al. (50-52) has determined the rigidity constant K for lamellar and micellar phases close to the isotropic microemulsion region by the spin-labelling technique. This technique consists of studying the electronic paramagnetic resonance of a nitroxide radical probe. If a nitroxide radical probe is labelled upon the alkyl chain of 0.1% of surfactant molecules, the local curvature of the interfacial film may then be determined. With only one per thousand surfactant molecules labelled, no appreciable perturbation of the interfacial film is introduced. Near the vicinity of the microemulsion region, Di Meglio demonstrated that by increasing the swelling (oil/ water) ratio or the cosurfactant concentration that the

amplitudes of the undulations increase leading to a concomitant decrease in the rigidity of the interfacial film. Di Meglio concluded that the role of both oil and cosurfactant is to lower the rigidity of the interfacial film during the resolution of the lamellar system into a transparent, isotropic microemulsion. These results support our conclusion drawn from vapor pressure measurements that a large decrease in interfacial rigidity occurs as the volume of dispersed phase increases in these systems.

The decrease in interfacial rigidity that occurs with increased dispersed volume has been documented by other experimental work (53-55). Using P.C.S. (Photon Correlation Spectroscopy) Zulauf and Eicke (53) studied the droplet particle size of inverted micellar solutions of AOT/ and water and water-in-oil microemulsions consisting of water/ AOT/ and isooctane. These workers report the inverse c.m.c. (critical micelle concentration) for AOT in isooctane to be 5×10^{-4}M. Without added water, a Stokes radius of 15 Å was found for inverted micelles of AOT in isooctane. This value (Stokes radius = 15 Å) was independent of the AOT concentration in the range of 8×10^{-3} to 2×10^{-1}M for this inverse micellar solution. In this concentration range no change in the Stokes radius (15 Å) could be detected when the temperature was varied between -20 and +95 °C for inverted micellar solutions of AOT in isooctane (no water added). When this water-in-oil system was prepared with a $[H_2O]/[AOT]$ molar ratio below ten the size of the Stokes radii did not vary with temperature between 0-50 °C and a constant Stokes radius was found for a given $[H_2O]/[AOT]$ molar ratio. The Stokes radii in this water-in-oil system increased as the $[H_2O]/[AOT]$ molar ratio increased. Above a $[H_2O]/[AOT]$ molar ratio of ten, the Stokes radii depended strongly on temperature and did start to show some concentration dependence.

From these particle size results by Zulauf and Eicke it can be concluded that two different regimes of phase behavior occur in this water-in-oil system. Below a $[H_2O]/[AOT]$ molar ratio of ten for the system studied, the inverted micellar aggregates behave like rigid macromolecules in the temperature range 0-50 °C. This is demonstrated by the fact that the

size of inverted micellar radii do not change with increasing temperature for a given $[H_2O]/[AOT]$ molar ratio. This apparent rigdity can be interpreted by assuming that the water is highly structured in the aggregates by hydrogen bonds stabilized by strong dipole moments of the head groups of the surfactant molecules. This behavior is consistent with an inverse swollen micellar solution. The inverse swollen micellar solution is characterized by a small volume of solubilized dispersed phase (water) and a relatively rigid microdroplet interface compared to the water-in-oil microemulsion region. The data also supports the conclusion drawn from D.S.C., titration, and vapor pressure measurements that the initial volume of dispersed phase is tightly bound by the microdroplet interfacial sheath. When the $[H_2O]/[AOT]$ molar ratio is greater than ten, water can be considered as a pseudo phase, and a well defined monolayer separates the bulk water in the core from the continuous isooctane phase. In contrast to the micellar solution, the behavior of the microemulsion is determined by the surface free energy of the surfactant film and is extremely sensitve to external parameters such as temperature, pressure, and the mutual solubilty of the coexisting phases. This is demonstrated by the temperature dependence of the Stokes radii for $[H_2O]/[AOT]$ molar ratios greater than ten. This behavior is typical of a microemulsion system. Unlike the highly rigid structure of a micellar solution, the microemulsion interface is a very flexible structure. The Zulauf and Eicke particle size results demonstrate that there is a clear distinction between swollen micellar solutions and microemulsions. These particle size results demonstrate that microemulsions systems are characterized by flexible interfacial structures and solubilize large volumes of dispersed phase relative to swollen micellar solutions which are characterized by rigid interfacial structures and solubilize only small volumes of dispersed phase. Zulauf and Eicke concluded that the onset of phenomena characteristic of water-in-oil microemulsions occurs when water becomes a major constituent in the colloidal system and the interface becomes soft and flexible.

Other experimental evidence supports the conclusion that two different regimes of phase behavior occur in water-in-oil disperse systems. Investigating several different

water-in-oil systems consisting of Aerosol OT/ water/ and various hydrocarbons, N.M.R. spectroscopic experiments were obtained by Eicke (54). At low water volume fraction (when the $[H_2O]/[AOT]$ molar ratio is below ten), proton N.M.R. spectroscopic measurements of these water-in-oil systems show that an upfield shift is observed in the water proton resonance compared to bulk water. This indicates the disruption of the bulk liquid-like water structure at the interface and the formation of relatively rigid association structures through strong hydrogen bonding with the polar groups of Aerosol OT. This water type is referred to as "trapped" water. Solubilized water is strongly bound to the microdroplet interface for low $[H_2O]/[AOT]$ molar ratios. This demonstrates that the initial increment of water (dispersed phase) is strongly bound to the microdroplet interface. Above a $[H_2O]/[AOT]$ molar ratio the solubilized water in the water-in-oil system begins to behave differently. When the $[H_2O]/[AOT]$ molar ratio is between the 10-20 range, solubilized water is partly free within the aggregates. For this $[H_2O]/[AOT]$ molar ratio range, the water molecules experience a rapid exchange between strongly and less bound water. Because of this rapid exchange, the chemical shift is somewhat intermediate between strongly and less bound water. With still larger amounts of solubilized water (when $[H_2O]/[AOT]$ molar ratio greater than 20), water molecules adopt the character of apparently free water and the chemical shift of the water proton resonance is equal to the chemical shift expected for bulk water. These results also demonstrate that a certain minimum amount of dispersed phase is necessary to form the flexible interface characteristic of microemulsion systems. Above this certain minimum amount of dispersed phase, these N.M.R. results suggest that the interfacial rigidity decreases as the volume of dispersed phase increases for these water-in-oil systems.

Additional N.M.R. spectroscopic experiments demonstrate the difference between highly structured and rigid interfaces of swollen micellar solutions compared to the flexible interfaces found in microemulsion systems. High resolution N.M.R. spectra are impossible in emulsion systems or other regularly organized systems. This is due to the rigid interfa-

cial structure found in these type of systems. Using high resolution N.M.R., N.M.R. proton relaxation times, viscosity, and electron microscopy experiments, Bellocq et al. (55) studied the structural properties of a microemulsion system consisting of water/ toluene/ SDS/ and n-butanol. High resolution N.M.R. spectra recorded in the single-phase microemulsion system are well resolved. This indicates that the molecules constituting this system have not entered rigid structures. These results suggest that for this microemulsion system the interface also has a fluid structure.

Furthermore, Bellocq et al. demonstrated that there is fast exchange between hydroxyl protons of n-butanol and water protons. This can be established in part from the fact a single OH line is observed, and also from the triplet seen for the $(CH_2)_\alpha$ protons of n-butanol. The fact that no coupling can be observed between the $(CH_2)_\alpha$ protons and the hydroxylic protons clearly establishes exchange. This demonstrates that the interfacial film is permeable to cosurfactant (n-butanol). Cosurfactant is rapidly exchanged between the aqueous phase, the hydrocarbon phase, and the interface. These workers concluded from their experimental results that the role of the cosurfactant in microemulsion stabilty is to increase both the fluidity and permeabilty of the interfacial structure.

Bellocq et al. (55) also showed that for the $(CH_2)_9$ proton resonances generated by the SDS molecule, a line broadening occurs when the ratio of toluene increases in the microemulsion system. This can be interpreted as an effect of the toluene anisotropy on the chain of the surfactant. Anisotropy leads to differentiation between the chemical shifts of the SDS CH_2 groups. This demonstrates the fact that toluene enters the interfacial film. Schulman (48,56-59) and other workers have discussed the importance of film penetration by hydrocarbon in the mixed interfacial film to explain the formation of microemulsion systems. Schulman concluded that film penetration is responsible for the metastable negative interfacial tension occurring in these systems. Schulman concluded that hydrocarbon penetration results in the formation of a liquid or disordered interface in microemulsion systems compared to the more ordered (or rigid) interface of more organized systems (lamellar, rod

structures, etc.). A large increase in entropy favors the formation of these disordered systems.

Emphasizing the role played by the interfacial flexibility of the oil/water interface, the mechanism of microemulsion formation has been explained by De Gennes and Taupin (2). De Gennes and Taupin invoked the concept of the flexibility of the interfacial film to explain why some oil, water, and surfactant systems form periodic arrays of surfactant while other systems form isotropic microemulsions. De Gennes and Taupin noted that the oil/water interface, saturated by surfactant, will have a nearly vanishing interfacial tension in microemulsions. Therefore, they concluded that one essential parameter was the elastic constant K describing the curvature elasticity of the fluid interface. When K is above some critical value K_c the interfaces tend to build up periodic arrays resulting in organized phases. When K is below K_c the interface becomes extremely wrinkled and the resulting gain in entropy is larger than the loss of energy due to departure from a periodic array. This case K below K_c would correspond to microemulsion formation. The major effect of cosurfactant addition in this model is to increase the flexibility of the oil/water interface. Therefore, cosurfactant addition can favor microemulsion formation. More recently, Langevin (6) has also discussed the range of surfactant bending elasticities for systems in which microemulsions can be formed. Langevin pointed out that when the elasticity is too large, ordered phases are obtained and a microemulsion cannot form; when the elasticity is too small, the surfactant film cannot form and the medium is a structureless molecular mixture. According to Langevin, oil, water, and surfactant mixtures that have very small curvature elasticities (approaching zero) form microemulsion systems that have bicontinuous structures.

5.5. Conclusions

1. The swollen microdroplets in droplet structure microemulsion systems consist of dipersed phase (either oil or water) spheres encapsulated by an interfacial sheath of constant

stochiometry. The microdroplet model for these microemulsion systems may be considered as an inner core of dispersed phase surrounded by an interfacial shell where all of the surfactant and part of the dispersed phase and cosurfactant form the interfacial sheath.

2. Two distinct regions of phase behavior occur in microemulsion systems. One regime occurs at low dispersed volume fraction and the other region occurs at high dispersed volume fraction. Below a certain critical volume fraction of dispersed phase the dispersed microdroplets behave as isolated, noninteracting particles. Below this critical volume fraction the dispersed phase is tightly bound by the microdroplet interfacial sheath. At or above a certain critical volume fraction of dispersed phase the microdroplets in oil-in-water and water-in-oil microemulsion systems begin to interact. In the high dispersed volume fraction region the dispersed phase is weakly bound by the microdroplet interfacial sheath. Interaction between neighboring microdroplets is referred to as percolation in these microemulsion systems.

3. The initial increment of dispersed phase is tightly bound to microdroplet interfacial sheath in these dispersions.

4. Microemulsification depends on the formation of a flexible interface relative to the correspondingly rigid interface of regular organized phases (i.e., lamellar, micellar, hexagonal, etc.). At very small volumes of dispersed phase the interface in oil/ water/ surfactant/ and cosurfactant dispersions is relatively rigid due to a strong intermolecular association between surfactant and dispersed phase. In order to solubilize a large proportion of dispersed phase a flexible interface must be formed. Experimental evidence indicates that both dispersed phase and cosurfactant play a major role in the formation of a flexible interface in oil-in-water microemulsion systems. An increase in interfacial flexibility occurs as the cosurfactant concentration and the dispersed phase increases in microemulsion systems. The onset of phenomena characteristic of microemulsion systems occurs when the dispersed phase becomes a major constituent in the system and the interface becomes soft and flexible. Microemulsions differ from micellar solutions in that microemulsions have a flexible

interface and can solubilize a large volume fraction of dispersed phase relative to micellar solutions which have relatively rigid interfacial structures and can solubilize only a very small volume fraction of dispersed phase.

5. An increase in microdroplet particle size increases as the volume of dispersed phase increases for microemulsion systems prepared with a fixed amount of primary surfactant.

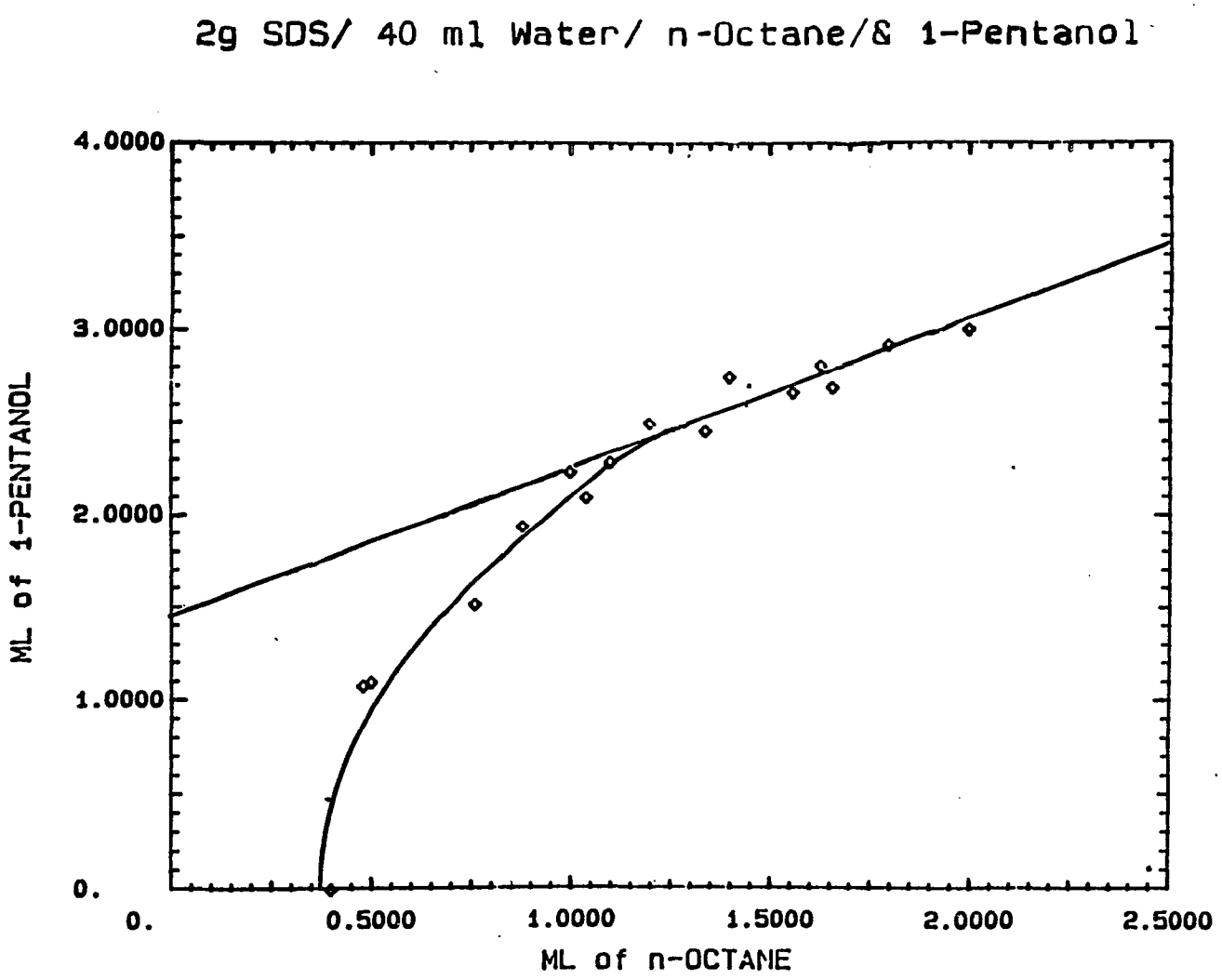
2g SDS/ 40 ml Water/ n-Octane/& 1-Pentanol
4.0000
3.0000
2.0000
1.0000
0.
ML of 1-PENTANOL
0.
0.5000
1.0000
1.5000
2.0000
2.5000
ML of n-OCTANE

FIGURE 5.1

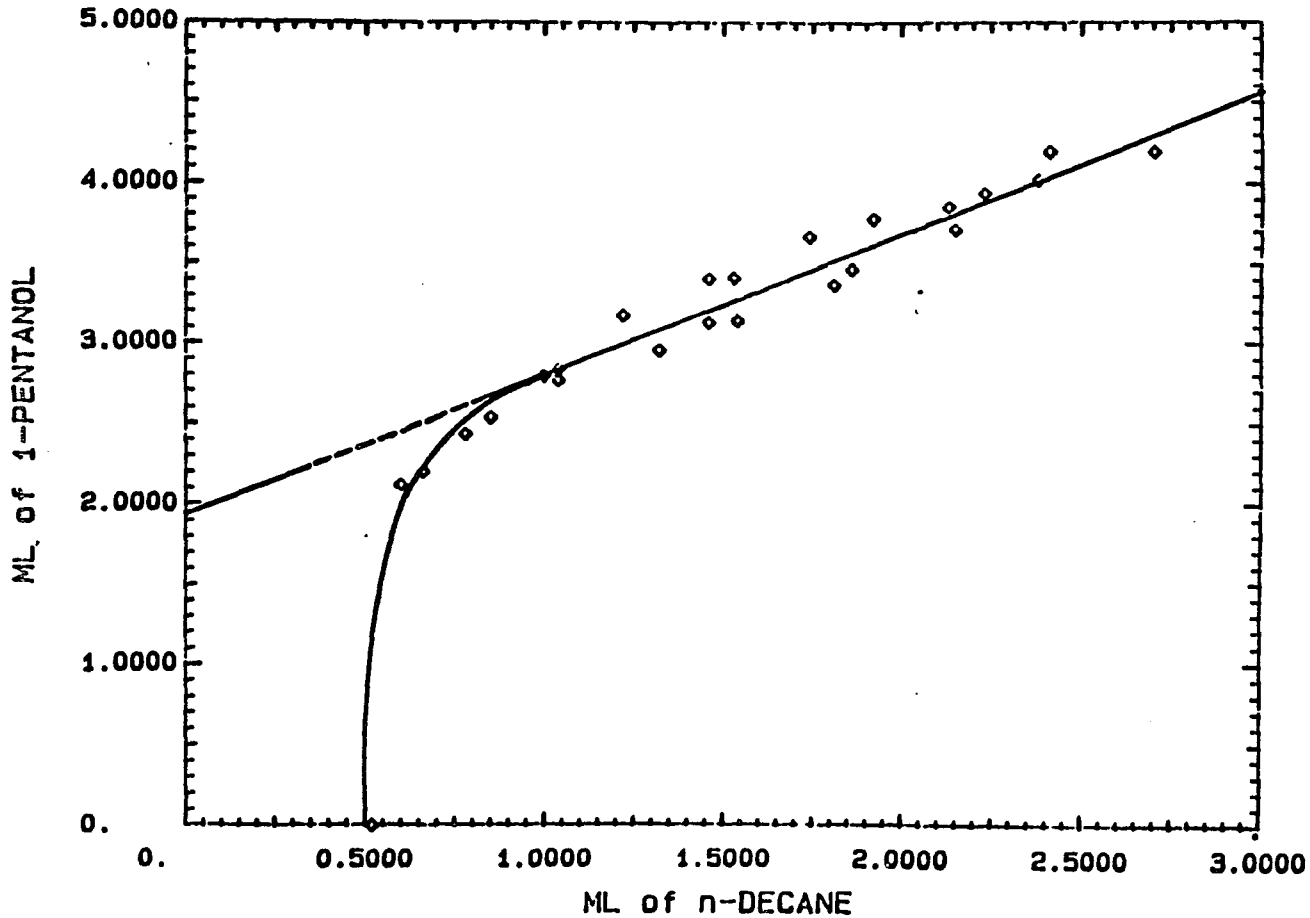
2g SDS/40 ml Water/n-Decane/& 1-Pentanol
ML of 1-PENTANOL
5.0000
4.0000
3.0000
2.0000
1.0000
0.
0.
0.5000
1.0000
1.5000
2.0000
2.5000
3.0000
ML of n-DECANE

FIGURE 5.2

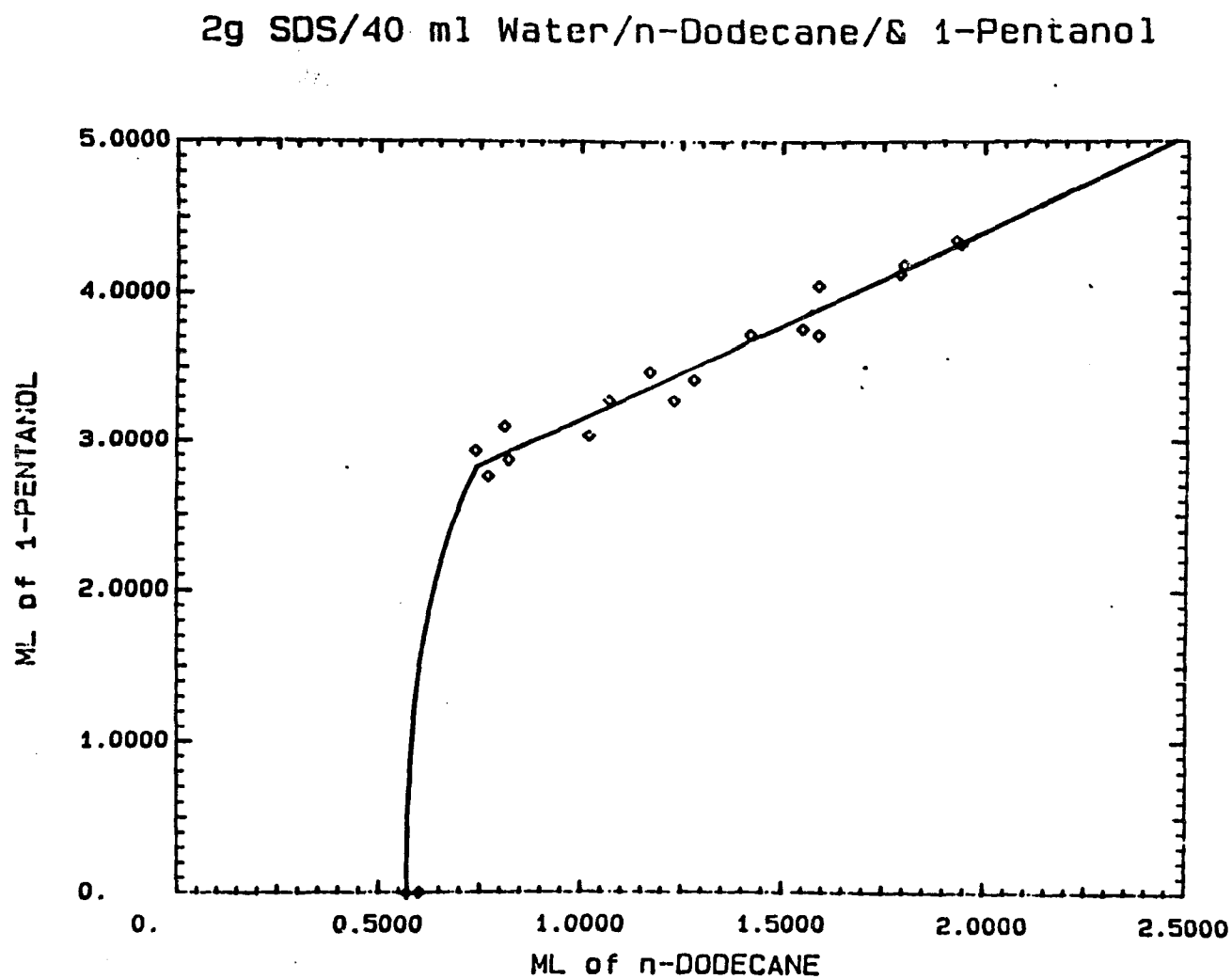
2g SDS/40 ml Water/n-Dodecane/& 1-Pentanol
5.0000
4.0000
3.0000
2.0000
1.0000
0.
ML of 1-PENTANOL
0.
0.5000
1.0000
1.5000
2.0000
2.5000
ML of n-DODECANE

FIGURE 5.3

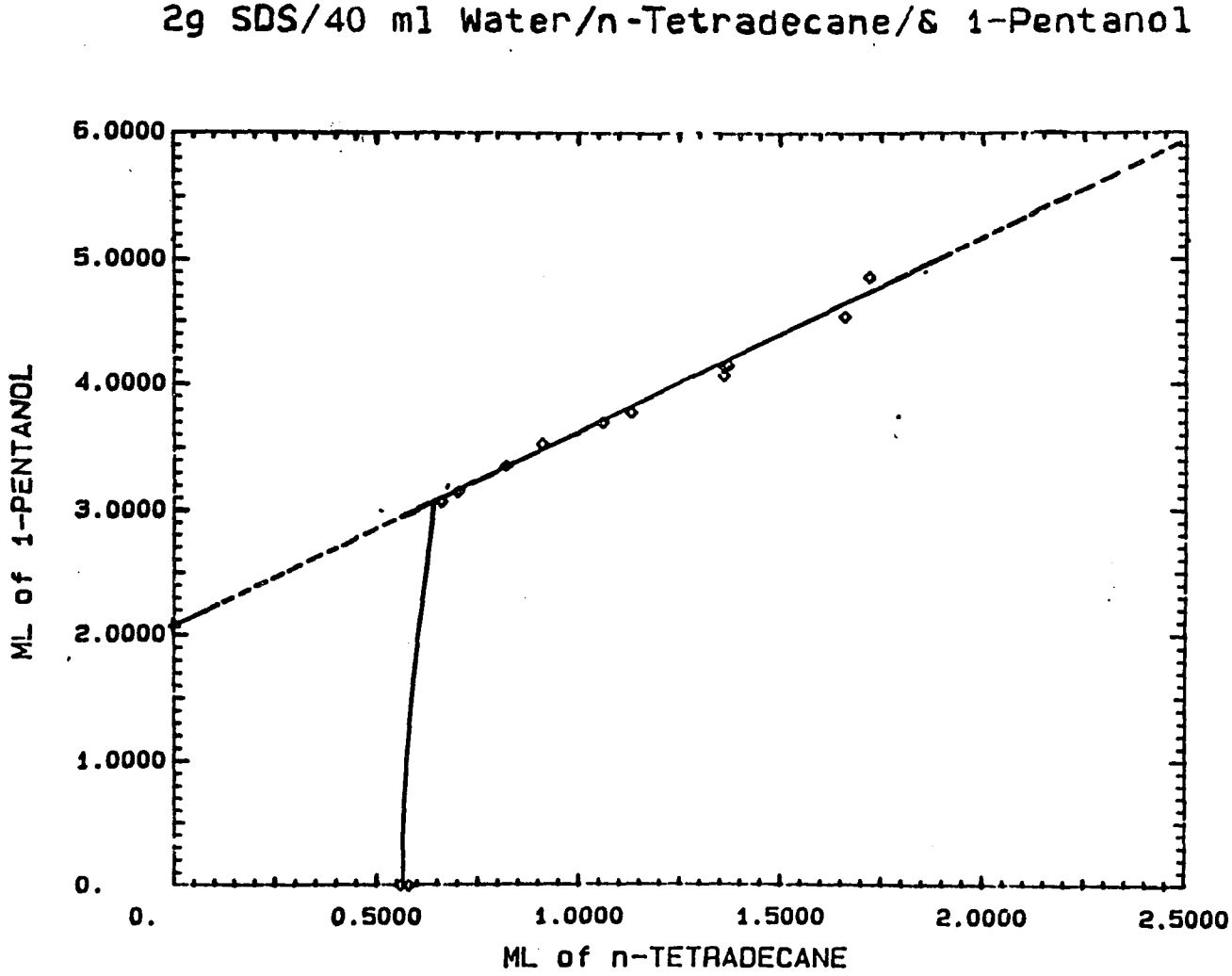
2g SDS/40 ml Water/n-Tetradecane/& 1-Pentanol
6.0000
5.0000
4.0000
3.0000
2.0000
1.0000
0.
ML of 1-PENTANOL
0.
0.5000
1.0000
1.5000
2.0000
2.5000
ML of n-TETRADECANE

FIGURE 5.4

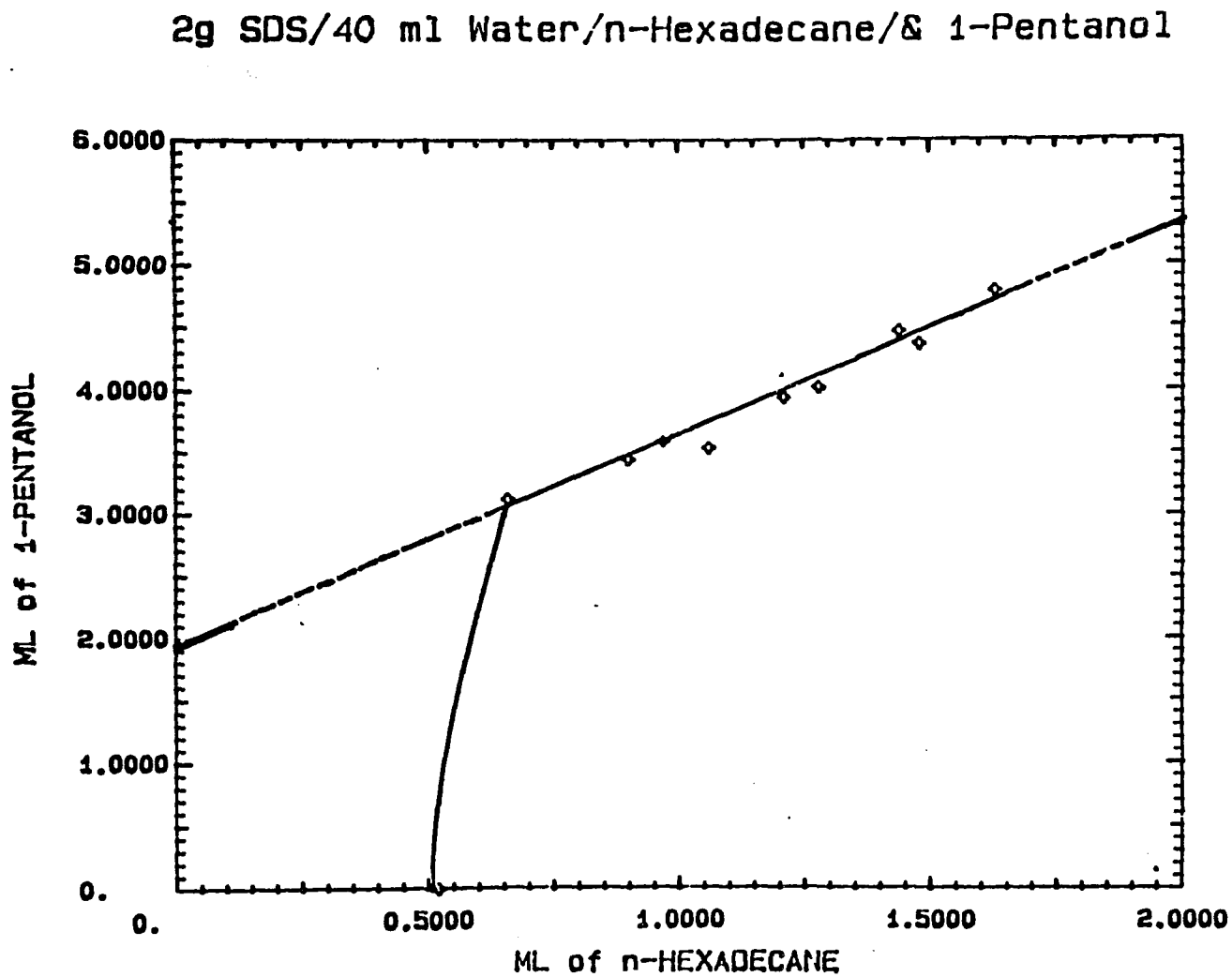
2g SDS/40 ml Water/n-Hexadecane/& 1-Pentanol
6.0000
5.0000
4.0000
3.0000
2.0000
1.0000
0.
ML of 1-PENTANOL
0.
0.5000
1.0000
1.5000
2.0000
ML of n-HEXADECANE

FIGURE 5.5

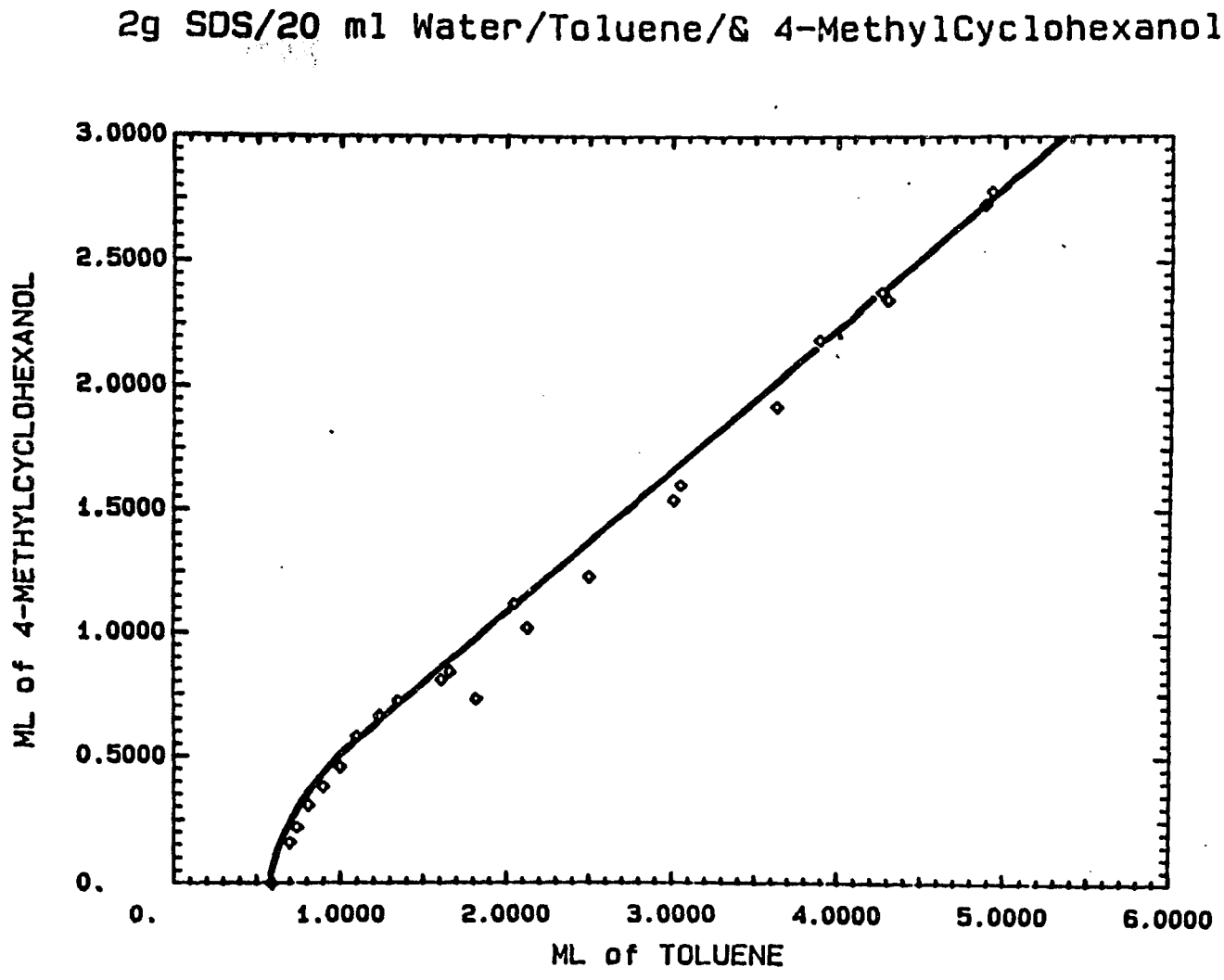
2g SDS/20 ml Water/Toluene/& 4-MethylCyclohexanol
ML of 4-METHYLCYCLOHEXANOL
3.0000
2.5000
2.0000
1.5000
1.0000
0.5000
0.
0.
1.0000
2.0000
3.0000
4.0000
5.0000
6.0000
ML of TOLUENE

FIGURE 5.6

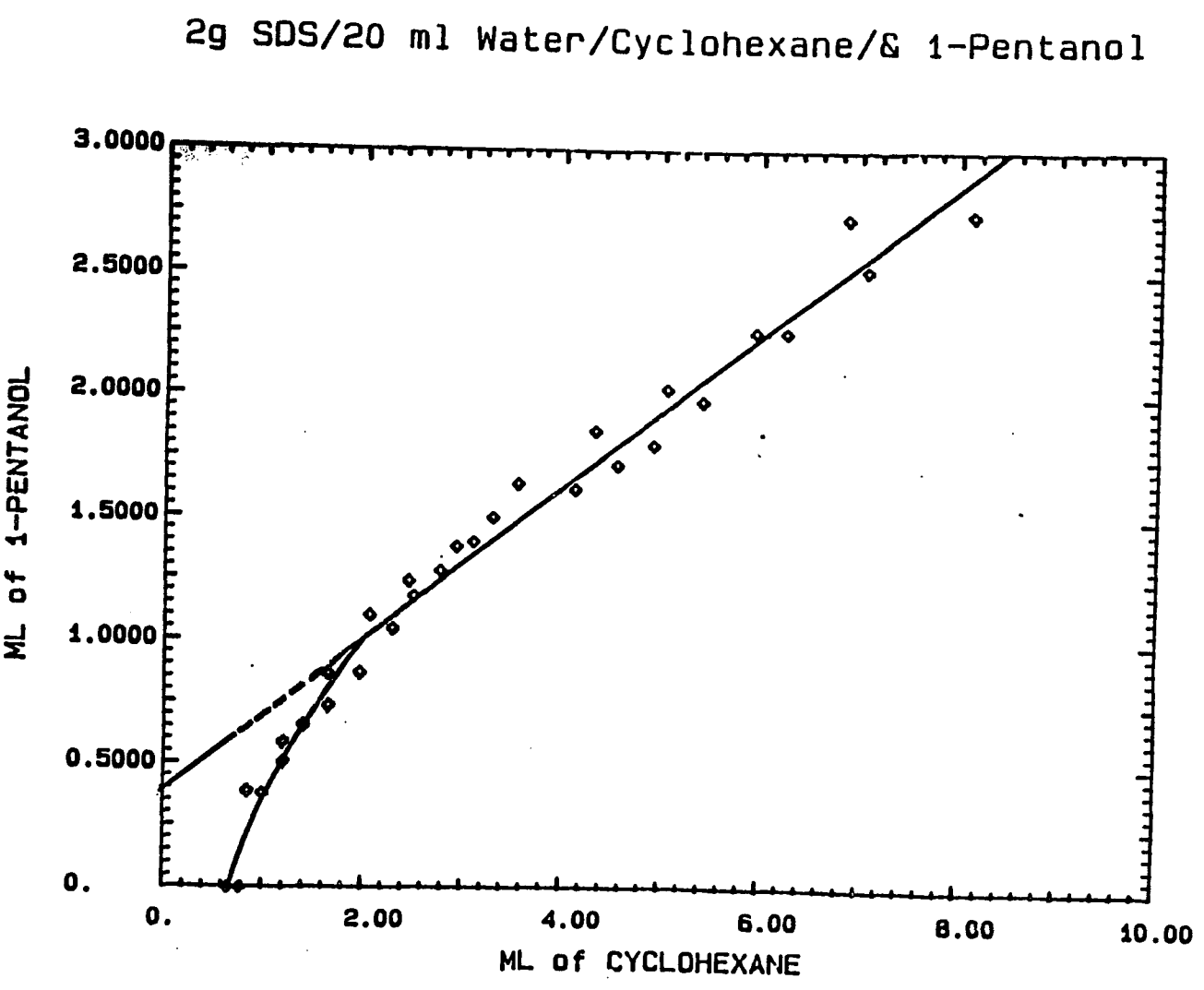
2g SDS/20 ml Water/Cyclohexane/& 1-Pentanol
3.0000
2.5000
2.0000
1.5000
1.0000
0.5000
0.
ML of 1-PENTANOL
0.
2.00
4.00
6.00
8.00
10.00
ML of CYCLOHEXANE

FIGURE 5.7

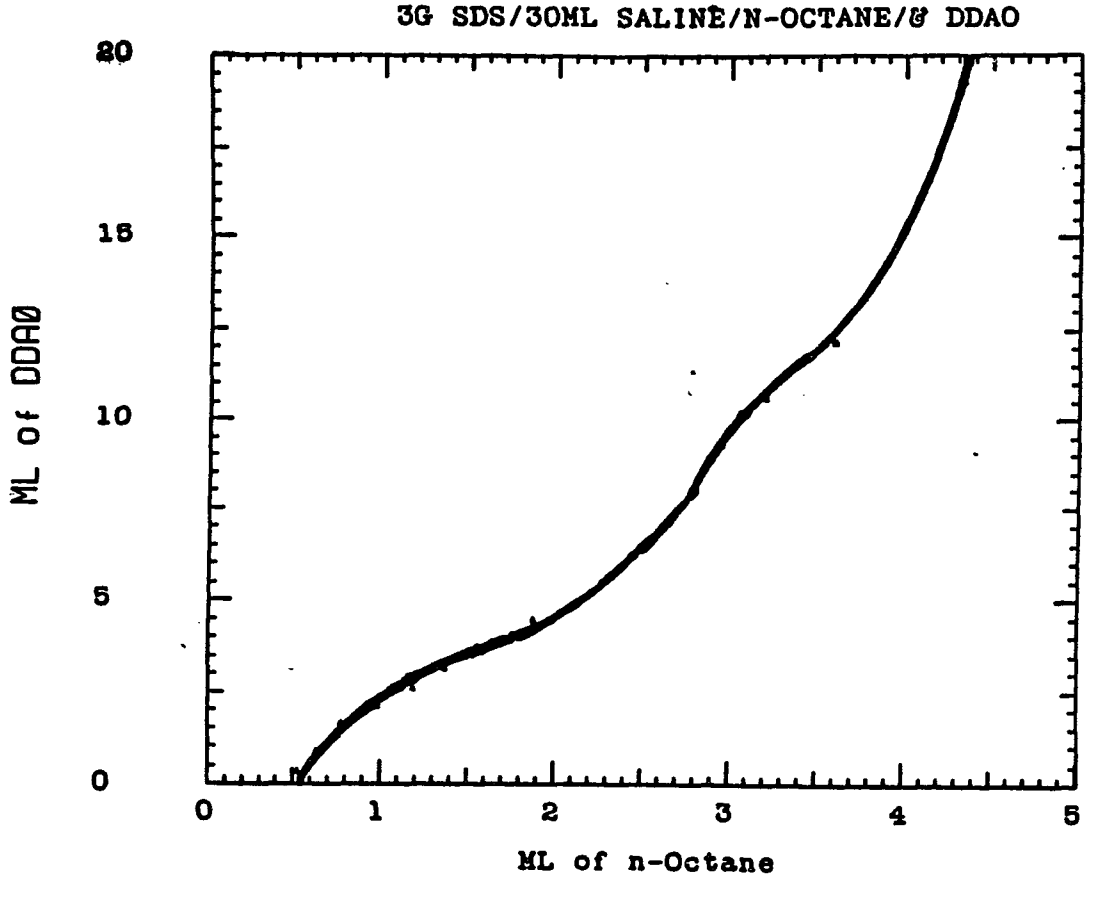
3G SDS/30ML SALINE/N-OCTANE/@ DDAO
ML of DDA0
20
15
10
5
0
0
1
2
3
4
5
ML of n-Octane

FIGURE 5.8

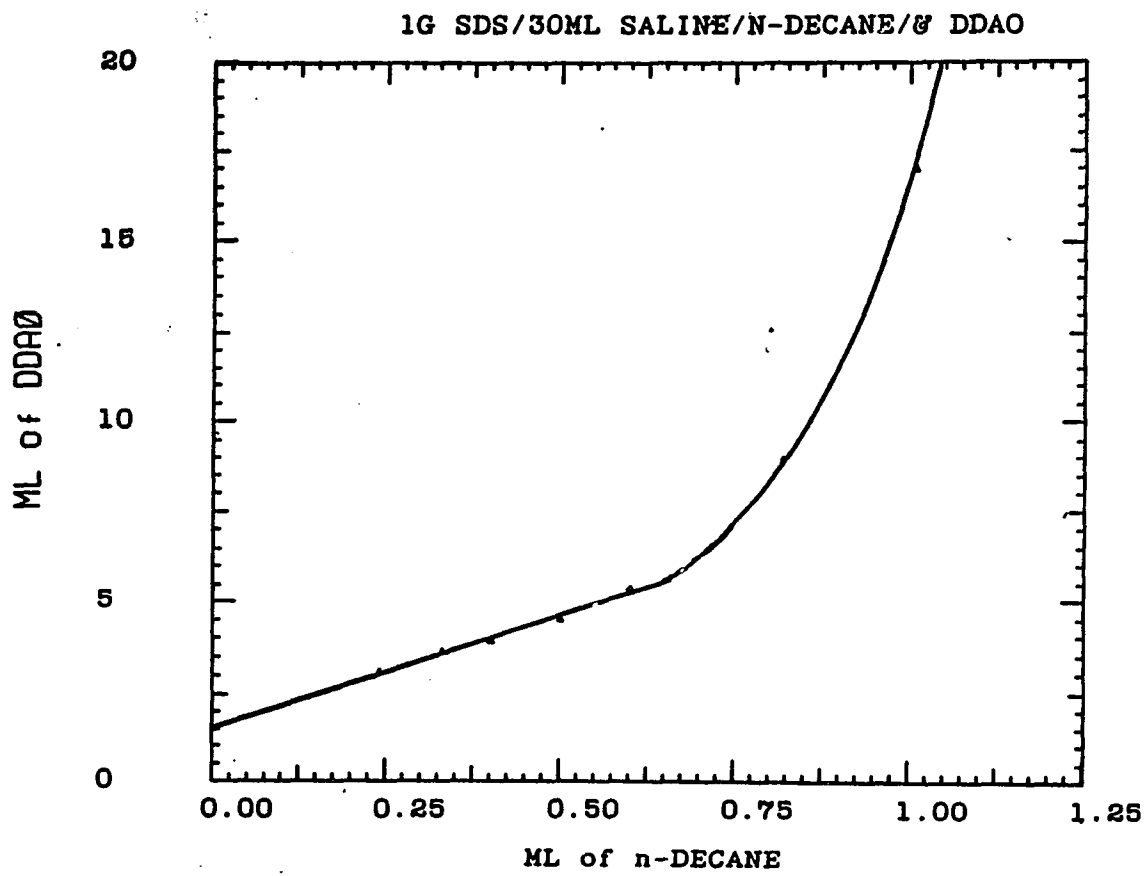
1G SDS/30ML SALINE/N-DECANE/@ DDAO
ML of DDAØ
20
15
10
5
0
0.00
0.25
0.50
0.75
1.00
1.25
ML of n-DECANE

FIGURE 5.9

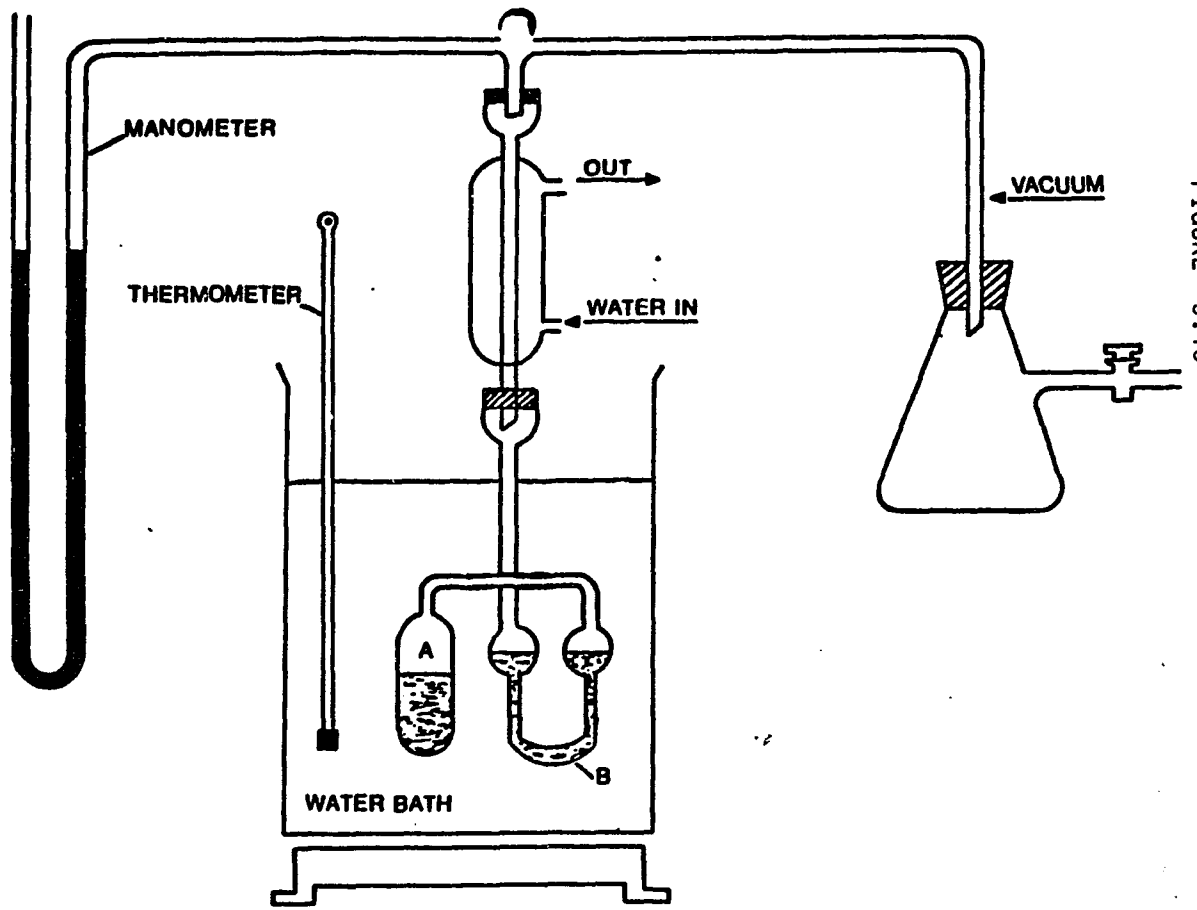

FIGURE 5.10

FIGURE 5.11

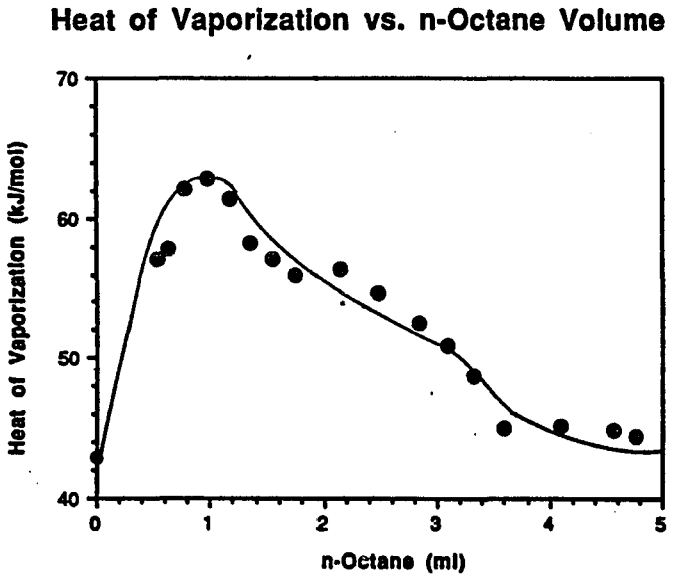
Heat of Vaporization vs. n-Octane Volume
Heat of Vaporization (kJ/mol)
70
60
50
40
0
1
2
3
4
5
n-Octane (ml)

FIGURE 5.12

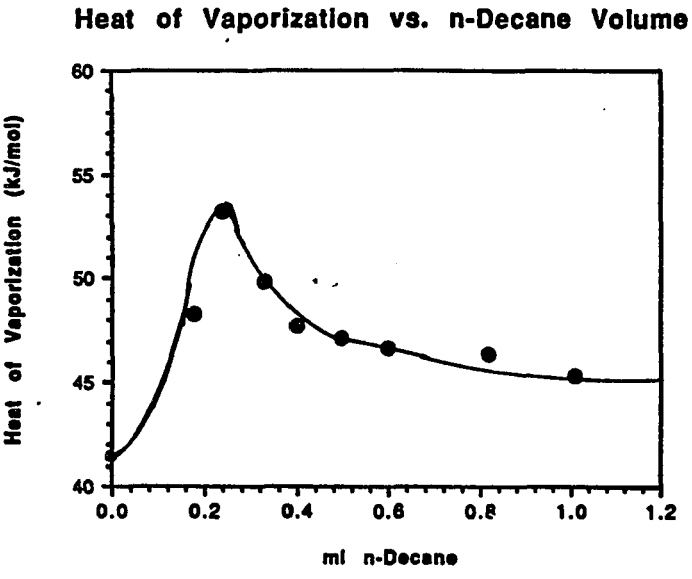
Heat of Vaporization vs. n-Decane Volume
Heat of Vaporization (kJ/mol)
60
55
50
45
40
0.0
0.2
0.4
0.6
0.8
1.0
1.2
ml n-Decane

FIGURE 5.13

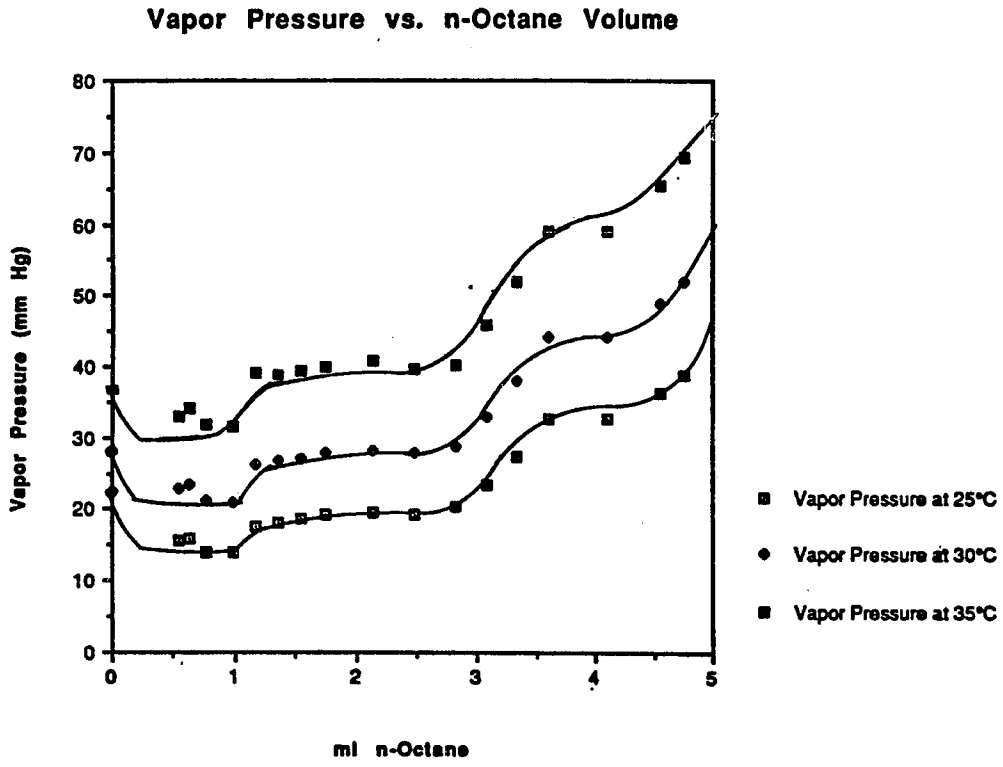
Vapor Pressure vs. n-Octane Volume
Vapor Pressure (mm Hg)
80
70
60
50
40
30
20
10
0
0
1
2
3
4
5
ml n-Octane
Vapor Pressure at 25°C
Vapor Pressure at 30°C
Vapor Pressure at 35°C

FIGURE 5.14

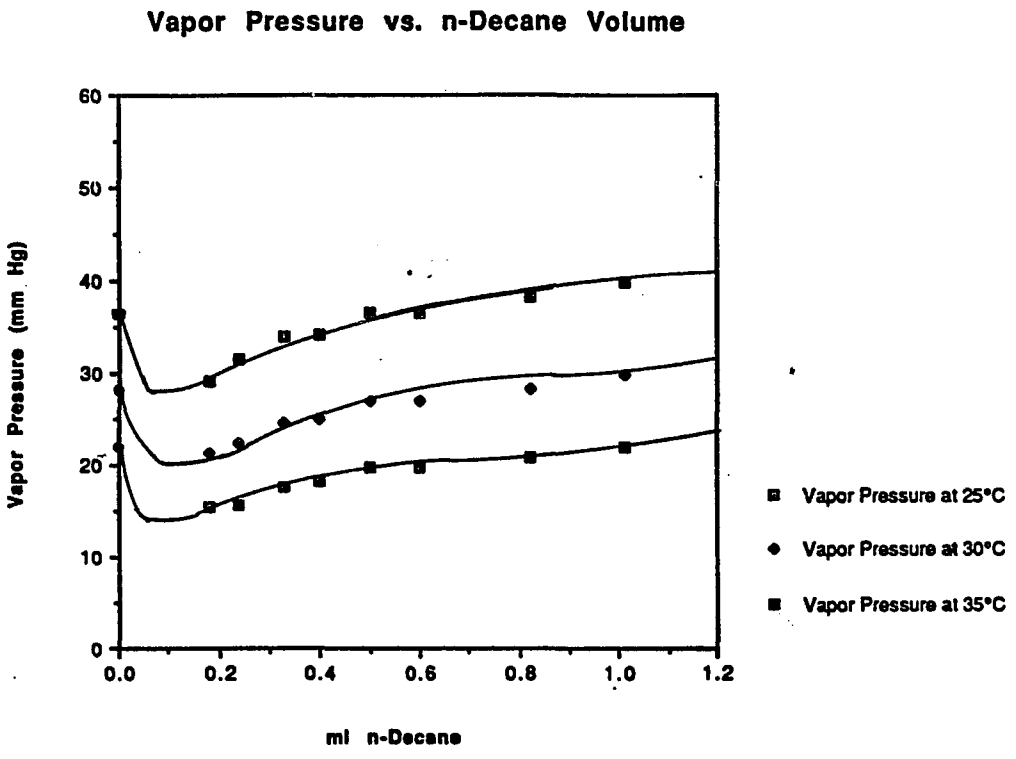
Vapor Pressure vs. n-Decane Volume
Vapor Pressure (mm Hg)
60
50
40
30
20
10
0
0.0
0.2
0.4
0.6
0.8
1.0
1.2
ml n-Decane
Vapor Pressure at 25°C
Vapor Pressure at 30°C
Vapor Pressure at 35°C

Table 5.1: Interfacial Stochiometry Measurements

System	Oil Phase	Water Phase	Surfactant	Cosurfactant
1	n-Octane	40 ml Water	2g SDS	1-Pentanol
2	n-Decane	40 ml Water	2g SDS	1-Pentanol
3	n-Dodecane	40 ml Water	2g SDS	1-Pentanol
4	n-Tetradecane	40 ml Water	2g SDS	1-Pentanol
5	n-Hexadecane	40 ml Water	2g SDS	1-Pentanol
6	Toluene	20 ml Water	2g SDS	4MCH
7	Cyclohexane	20 ml Water	2g SDS	1-Pentanol

Table 5.2: Vapor Pressure Measurements

System	Oil Phase	Water Phase	Surfactant	Cosurfactant
8	n-Octane	25ml Saline	3g SDS	DDAO
9	n-Decane	25ml Saline	1g SDS	DDAO

Table 5.3: Titration Results

System	Intrf.OilVolume	Slope	Intercept	Correlation
1	1.1	0.807	1.443	0.9342
2	0.90	0.881	1.942	0.9624
3	0.70	1.245	1.904	0.9787
4	0.61	1.535	2.070	1.0000
5	0.90	1.692	1.958	0.9943
6	0.60	0.577	-0.113	0.9973
7	0.78	0.299	0.447	0.9839

Table 5.4: Interfacial Compositions

System	Moles of Oil	Moles of Cosurfactant	Moles of SDS
1	6.95×10^{-3}	6.99×10^{-3}	6.94×10^{-3}
2	4.62×10^{-3}	7.29×10^{-3}	6.94×10^{-3}
3	3.08×10^{-3}	8.02×10^{-3}	6.94×10^{-3}
4	2.35×10^{-3}	9.20×10^{-3}	6.94×10^{-3}
5	2.05×10^{-3}	1.07×10^{-2}	6.94×10^{-3}
6	9.41×10^{-3}	3.99×10^{-3}	6.94×10^{-3}
7	1.85×10^{-2}	5.11×10^{-3}	6.94×10^{-3}

Table 5.5: Interfacial Stochiometries

System	Molecules of Oil	Molecules of Cosurfactant	Molecules of SDS
1	1	1	1
2	2	3	3
3	2	5	5
4	1	4	3
5	3	16	10
6	9	4	7
7	10	3	4

Table 5.6: System 8 Vapor Pressure Measurements				
ml n-Octane	ml DDAO	Slope	Intercept	Heat of Vap.(kJ/mol)
0.54	0.34	-2.979×10^{3}	10.187	57.01
0.63	0.87	-3.020×10^{3}	10.332	57.80
0.77	1.64	-3.248×10^{3}	11.043	62.16
0.98	2.11	-3.281×10^{3}	11.146	62.80
1.18	2.57	-3.207×10^{3}	11.000	61.38
1.36	3.16	-3.041×10^{3}	10.459	58.19
1.55	3.74	-2.983×10^{3}	10.275	57.09
1.75	4.06	-2.925×10^{3}	10.094	55.99
2.14	5.37	-2.942×10^{3}	10.157	56.30
2.48	6.38	-2.852×10^{3}	9.854	54.59
2.83	7.49	-2.741×10^{3}	9.501	52.46
3.08	8.85	-2.663×10^{3}	9.303	50.97
3.33	11.15	-2.547×10^{3}	8.981	48.75
3.60	12.20	-2.349×10^{3}	8.393	44.96
4.10	17.90	-2.359×10^{3}	8.427	45.14
4.56	24.00	-2.349×10^{3}	8.439	44.95
4.76	27.60	-2.321×10^{3}	8.373	44.41

Table 5.7: System 9 Vapor Pressure Measurements				
ml n-Decane	ml DDAO	Slope	Intercept	Heat of Vap. (kJ/mol)
0.18	1.85	-2.523×10^3	8.651	48.28
0.24	3.10	-2.783×10^3	9.529	53.28
0.33	3.63	-2.605×10^3	8.984	49.86
0.40	3.90	-2.492×10^3	8.619	47.72
0.50	4.50	-2.463×10^3	8.556	47.16
0.60	5.40	-2.437×10^3	8.471	46.66
0.82	8.99	-2.422×10^3	8.442	46.38
1.01	16.99	-2.368×10^3	8.285	45.31

Table 5.8: Microdroplet MW vs. n-Octane Vol.			
ml n-Octane	ml DDAO	Π/c	MW
0.54	0.34	6.57×10^{-2}	3.80×10^{5}
0.63	0.87	6.12×10^{-2}	4.06×10^{5}
0.77	1.64	9.09×10^{-2}	2.74×10^{5}
0.98	2.11	9.67×10^{-2}	2.57×10^{5}
1.18	2.57	2.60×10^{-2}	9.58×10^{5}
1.36	3.16	2.10×10^{-2}	1.18×10^{6}
1.55	3.74	1.49×10^{-2}	1.67×10^{6}
1.75	4.06	5.68×10^{-3}	4.38×10^{6}

Table 5.9: Microdroplet MW vs. n-Decane Vol.

ml n-Decane	ml DDAO	Π/c	MW
0.18	1.85	9.00×10^{-2}	2.76×10^{5}
0.24	3.10	8.02×10^{-2}	3.10×10^{5}
0.33	3.63	5.05×10^{-2}	4.92×10^{5}
0.40	3.90	4.49×10^{-2}	5.54×10^{5}
0.50	4.50	1.81×10^{-2}	1.38×10^{6}
0.60	5.40	1.80×10^{-2}	1.38×10^{6}

Table 5.10: Maximum Solubilization of Oil

System	Max.Solub.ofOil	Vol.ofCosurf.Needed
1	2.00ml n-Octane	3.00ml 1-Pentanol
2	2.70ml n-Decane	4.30ml 1-Pentanol
3	2.00ml n-Dodecane	4.40ml 1-Pentanol
4	1.70ml n-Tetradecane	4.80ml 1-Pentanol
5	1.70ml n-Hexadecane	4.80ml 1-Pentanol

Table 5.11: Microdroplet Radii vs. n-Octane Volume

ml n-Octane	GMW	Radius (Å)
0.54	3.80×10^5	64.0
0.63	4.06×10^5	66.9
0.77	2.74×10^5	55.4
0.98	2.57×10^5	54.0
1.18	9.58×10^5	106.4
1.36	1.18×10^6	118.9
1.55	1.67×10^6	141.4
1.75	4.38×10^6	229.1

Table 5.12: Microdroplet Radii vs. n-Decane Volume.

ml n-Octane	GMW	Radius (Å)
0.18	2.76×10^5	53.6
0.24	3.10×10^5	57.2
0.40	4.92×10^5	72.1
0.50	5.54×10^5	76.5
0.60	1.39×10^6	120.8
0.82	1.38×10^6	120.8

References

1. Hoar, T.P., Schulman, J.H., *Nature (London)*, **152,** 102, (1943).

2. De Gennes, P.G., Taupin, C., *J. Phys. Chem.*, **82,** 2294, (1982).

3. Rosano, H.L., Lyons, G.B., *J. Phys. Chem.*, **89,** 363, (1985).

4. Rosano, H.L., Cavallo, J.L., Lyons, G.B., *Presented at the 5th International Conference on Surface and Colloid Science,* Potsdam, N.Y., June 25-28, 1975; Rosano, H.L., Cavallo, J.L., Lyons, G.B., in "*Microemulsion Systems,*" **Proceedings of the 59th Colloid and Surface Science Symposium and 5th International Congress on Colloid and Surface Science,** Marcel Dekker, New York, (1987), Chapt. 16, pp. 265-279.

5. Scriven, L.E., in "*Micellization, Solubilization, and Microemulsions,*" **Vol. 2,** K.L. Mittal, Ed., Plenum Press, New York, 1977, pg. 877.

6. Langevin, D., *Advances in Coll. Inter. Sci.*, **34,** 583, (1991).

7. Shinoda, K., Lindman, B., *Langmuir*, **3,** 135, (1987).

8. Schulman, J.H., Matalon, R., Cohen, M., *Discuss. Faraday Soc.*, **11,** 117, (1951).

9. Stoekenius, W., Schulman, J.H., Prince, L.M., *Kolloid-Z.*, **169,** 170, (1960).

10. Schulman, J.H., Riley, D.P., *J. Colloid Sci.*, **3,** 383, (1948).

11. Schulman, J.H., Friend, J.A., *J. Colloid Sci.*, **4,** 497, (1949).

12. Kim, M.W., Dozier, W.D., Klein, R., *J. Chem. Phys.*, **84,** 5919, (1986).

13. Huang, J.S., Kim, M.W., *Phys. Review Letters*, **47,** 1462, (1981).

14. Fourche, G., Belloco, A.M., Brunetti, S., *J. Colloid Interface Sci.*, **88,** 302, (1982).

15. Cazabat, A.M., Langevin, D., *J. Chem. Phys.*, **4,** 3148, (1981).

16. Bowcott, J.E.L., Schulman, J.H., *Z. Electrochem.*, **59,** 283, (1955).

17. Dvolaitsky, M., Guyot, M., Lagues, M., Le pesant, J.P., Ober, R., Sauterey, C., Taupin, C., *J. Chem. Phys.*, **9,** 3279, (1978).

18. Mackay, R.A., *Advances in Colloid Interface Sci.*, **15,** 131, (1981).

19. Mackay, R.A., Dixit, N., Agarwal, R., Seiders, P., *J. Dispersion Sci. Technol.*, **4,** 397, (1983).

20. Mackay, R.A., in "*Microemulsions*," I.D. Robb, Ed., Plenum Press, New York, 1982, pp. 207-219.

21. Mackay, R.A., Dixit, N., and Agarwal, R., in "*Inorganic Reactions in Organized Media*," **ACS Symposium Series No. 177,** S.H. Holt, Ed., 1982, pp. 179-198.

22. Mackay, R.A., Dixit, N.S., Hermansky, C., and Kertes, A.S., *to be published, J. Colloid Interface Sci.*

23. Mackay, R.A., Hermansky, C., Agarwal, R., in "*Colloid and Interface Science*," **Vol. II,** M. Kerker, Ed., Academic Press, New York, 1976, pp. 289-303.

24. Hwang, J.S., Cummins, H.Z., *J. Chem. Phys.*, **77,** 616, (1982).

25. Huang, J.S., Safran, S.A., Kim, M.W., Grest, G.S., Kotlarchyk, M., Quirke, N., *Phys. Rev. Letters*, **53,** 592, (1984).

26. Ober, R., Taupin, C., *J. Phys. Chem.*, **84,** 2418, (1980).

27. Kotlarchyk, M., Chen, S.H., Huang, J.S., Kim, M.W., *Physical Review A*, **29,** 2054, (1984).

28. Cavallo, J.L., Rosano, H.L., *J. Phys. Chem.*, **90,** 6817, (1986).

29. Lyons, G.B., Rosano, H.L., *to be published.*

30. Zana, R., Lang, J., *Colloids and Surfaces*, **48,** 153, (1990).

31. Almgren, M., Greieser, F., Thomas, J.K., *J. Am. Chem. Soc.*, **102,** 3188 ,(1980).

32. Cannon, P.L., Jr., Garlick, S.M., Christeson, S.D., Wong, N.M., Novelli, A.C., Longo, F.R., Mackay, R.A., *to be published.*

33. Chokshi, K., Qutubuddin, S., Hassam, A., *J. Coll. Inter. Sci.*, **129,** 315, (1989).

34. Rosano, H.L., *J. Cosmetic Chem.*, **25,** 609, (1974).

35. Rosano, H.L., Nixon, A.L., Cavallo, J.L., *J. Phys. Chem.*, **93,** 4536, (1989); also, to be published in **"The Proceedings of the 2nd World Surfactants Congress,"** ASPA, Paris, France, March 24th-28th, 1988.

36. Rosano, H.L., Lan, T., Weiss, A., Gerbacia, W.E.F., Whittam, J.H., *J. Coll. Inter. Sci.*, **72,** 233, (1979).

37. Weatherford, W.D., *J. Dispersion Sci. Technol.*, **6,** 467, (1985).

38. Lagues, M., Sauterey, C., *J. Phys. Chem.*, **384,** 3503, (1980).

39. Bennett, K.E., Hatfield, J.C., Macosko, C.W., Scriven, L.E., in *"Microemulsions,"* Robb, I.D., Ed., Plenum Press, pp. 65-94, (1982).

40. Van Dijk, H.A., *Phys. Rev. Lett.*, **55,** 1003, (1985).

41. Eicke, H.F., Kubick, R., Hasse, Zschokke, I., in *"Microemulsions,"* Ed. by Robb, I.D., Plenum Press, 65, (1982).

42. Cazabat, A.M., Langevin, D., Meunier, J., Pouchelon, A., *J. Phys. Lett.*, **43,** L89, (1982).

43. Kim, M.W., Huang, J.S., *Phys. Rev.*, **A34,** 719, (1986).

44. Bhattachavharaya, S., Stokes, J., Kim, M.W., Webman, I., *Phys. Rev. Lett.*, **55,** 1884, (1985).

45. Bug, A.L.R., Safran, S.A., Grest, G.S., Webman, I., *Phys. Rev. Letters*, **350,** 1930, (1983).

46. **Safran,** S.A., Turkevich, L.A., *Discuss. Faraday Soc.*, **11,** 1117, (1951).

47. **Safran,** S.A., Grest, G.S., Bug, A.L.R., Webman, I., in *"Microemulsion Systems,"* **Proceedings of the 59th Colloid and Surface Science Symposium and 5th International Congress on Colloid and Surface Science,** Rosano, H.L., and Clausse, M., Marcel Dekker, New York, (1987), Chapt. 7, pp. 129-144.

48. Schulman, J.H., *N.Y. Acad. Sci.*, **92,** 366, (1961).

49. Rosano, H.L., Jon, D., Whittam, J.H., *J. Am. Oil Chem. Soc.*, **59,** 8, 360, (1982).

50. Di Meglio, J.M., Dvolaitsky, M., Leger, L., Ober, R., Paz, L., Taupin, C., **Presented at the 5th International Congress on Surface and Colloid Science,** Potsdam, New York, June 25-28, 1985.

51.Di Meglio, J.M., Paz, L., Dvolaisky, M., Taupin, C., *J. Phys. Chem.*, **88,** 6036, (1983).

52.Di Meglio, J.M., Dvolaisky, M., Ober, R., Taupin, C., *J. Phys. Lett.*, **44,** L-229, (1983).

53.Zulauf, M., Eicke, H.F., *J. Phys. Chem.*, **83,** 480, (1982).

54. Eicke, H.F., Rehak, J., *Helv. Chim. Acta,* **59,** 2883, (1976).

55. Bellocq, *to be published.*

56. Gerbacia, W.E., Rosano, H.L., *J. Colloid Interface Sci.*, **44,** 242, (1973).

57. Bowcott, J.E., Schulman, J.H., *Z. Elektrochem.*, **59,** 4, 283, (1955).

58. Schulman, J.H., Stoeckenius, W., Prince, I.M., *J. Phys. Chem.*, **63,** 1677, (1959).

59. Goddard, E.D., Schulman, J.H., *J. Colloid Sci.*, **8,** 309, (1953). (1973).

CHAPTER 6:

SUMMARY

At the inception of this dissertation there was some question as to whether microemulsion systems were kinetically stable or thermodynamically stable systems. This conclusion was based on the fact that for some microemulsion systems the order of mixing the various components (i.e., oil, water, surfactant, and cosurfactant) plays a major role in their formation. In Chapter 2 and 3 of this dissertation the free energy, enthalpy, and entropy changes accompanying cosurfactant adsorption during microemulsion formation were determined. In all cases the free energy changes accompanying cosurfactant adsorption during microemulsion formation were found to be small negative numbers. This result demonstrated that the process was spontaneous but that the driving force for this process was small. The small negative numbers found for these free energy changes may explain why the method of preparation may affect their formation. It is assumed that once the right method of preparation is found, the kinetic energy barriers these systems must overcome during their formation are significantly lowered. In most cases microemulsion systems may be considered to be thermodynamically stable sytems.

Consistent with the optical properties of these systems (i.e., transparent and isotropic), microemulsion structure was first described by Schulman to consist of dispersed droplets in the size range of 80 to 800 Å. An early pioneer in the field of microemulsion formation, Schulman concluded that there were two different types of microemulsion systems: oil-in-water, where oil microdroplets are dispersed in an aqueous continuous phase; and water-in-oil, where water microdroplets are dispersed in an oil continuous phase. A wide variety of different experimental techniques have been used to determine the size of the microdroplets in microemulsion systems. In Chapter 4 and 5 of this dissertation the microdroplet particle size in several different oil-in-water microemulsion systems were determined by the D.C. polarographic technique and by vapor pressure measurements. Microdroplet radii in the

size range of between 60.0 to 97.9 Å were found for three different oil-in-water microemulsion systems investigated by D.C. polarography. Microdroplet radii between 53.6 to 120.8 Å were found for two different oil-in-water microemulsion systems investigated by vapor pressure measurements. Microdroplet radii were found to increase as the volume fraction of dispersed phase (oil) increased for the oil-in-water microemulsion systems prepared at constant amount of primary surfactant and investigated by D.C. polarography and vapor pressure measurements in this dissertation. Whereas Schulman described the structure of microemulsion systems to consist of dispersed microdroplets of either oil-in-water or water-in-oil, other workers have suggested that some microemulsion systems are best described by bicontinuous and not droplet structures. The experimental evidence supports the conclusion that oil-in-water microemulsion systems investigated by D.C. polarographic technique in Chapter 4 and by vapor pressure measurements in Chapter 5 of this dissertation are best described by microdroplet and not bicontinuous structures.

Based on the vapor pressure measurements in this dissertation, two different regimes of phase behavior are encountered in droplet structure microemulsion systems. One regime occurs at low volume fraction of dispersed phase while the other regime occurs at or above some critical volume fraction of dispersed phase. This conclusion has been drawn by earlier workers. Previously, this behavior has been documented by vapor pressure measurements for oil-in-water microemulsion systems and by electrical conductivity and P.C.S. measurements for water-in-oil microemulsion systems. In this dissertation two different regimes of phase behavior are found for two different oil-in-water microemulsion systems investigated by vapor pressure as a function of increasing dispersed phase (oil). At low volume fraction of dispersed phase (oil) the microdroplets in these systems do not interact. This is demonstrated by the lowering of the vapor pressure and the relatively small measured heat of vaporization in the low dispersed volume fraction regime. At or above a certain critical volume fraction of dispersed phase the microdroplets interact. This process whereby the microdroplets begin to interact above a certain critical volume of dispersed

phase is referred to as the "percolation threshold." This is demonstrated by the large increase in vapor pressure and the relatively large measured heat of vaporization in the high dispersed volume fraction regime.

BIBLIOGRAPHY

Chapter One

1. Stoeckenius, W., Schulman, J. H., and Prince, L. M., *Kolloid Z.*,**169,** 170, (1960).

2. Hoar, T. P., Schulman, J. H., *Nature,* **152,** 102 (1943)

3. Stoeckenius, W., *J. Biophys. Biochem. Cytol.*, **5,** 491, (1959).

4. Bowcott, J.E., and Schulman, J.H., *Z. Elektrochem.*, **59,** 4, 283, (1955).

5. Schulman, J.H., *N.Y. Acad. Sci.*, **92,** 366, (1961).

6. Goddard, E.D., Schulman, J.H., *J. Colloid Sci.*, **8,** 309, (1953).

7. Shulman, J.H., Stoekenius, W., and Prince, L.M., *J. Phys. Chem.*, **63,** 1677, (1959).

8. Schulman, J.H., Matalon, R., and Cohen, M., *Discussions Faraday Soc.*, **11,** 117, (1951).

9. Prince, L.M., *J. Coll. Interface,* **23,** 165, (1967).

10. Cooke, C.E., Jr., and Schulman, J.H., *Proc. 2nd Scandinavian Symp. Surface Activity,* Stockholm, November, 1964.

11. Shinoda, K., Kuneida, H., Arai, T., and Saijo, H., *J. Phys. Chem.*, **88,** 5126, (1984).

12. Saito, H., and Shinoda, K., *J. Colloid & Interface Sci.*, **32,** 647, (1970). Shinoda, K., *Progress in Colloid & Polymer Sci.*, **68,** 1, (1983).

14. Shinoda, K., and Kuneida, H., *J. Colloid & Interface Sci.*, **42,** 381, (1972).

15. Friberg, S., Lapczynska, I., Gillberg, G., *J. Colloid & Interface Sci.*, **56,** 19, (1976).

16. Shinoda, K., and Friberg, S., *Adv. in Colloid and Interface Sci.*, **4,** 193, (1974).

17. Ruckenstein, E., *Chem. Phys. Letters,* **57,** 3517, (1978).

18. Ruckenstein, E., and Chi, J., *J. Chem. Soc., Faraday Trans.*, **2,** 71, 1690, (1975).

19. Ruckenstein, E., *J. Colloid & Interface Sci.*, **66,** 369, (1978).

20. Talmon, Y., and Prager, S., *J. Chem. Phys.*, **69,** 2984, (1978).

21. Talmon, Y., and Prager, S., *Nature (London)*, **267,** 333, (1977).

22. Robbins, M.L., in "*Micellization, Solubilization, and Microemulsions,*" **Vol. 2,** edited by K.L. Mittal, Plenum Press 1977, p. 713-753; also Scriven, L.E., ibid., p. 877-893.

23. Healy, R. N., Reed, R. L., and Stenmark, D. G., *Soc. Petrol. Eng. J.*, **16,** 147, (1967).

24. Winsor, P. A., *Chem. Rev.*, **68,** 1, (1968).

25. Helfrich, W., *Naturforsch. C*, **28,** 693, (1973).

26. Mitchell, D. J., and Ninham, B. W., *J. Chem. Soc., Faraday Trans. 2*, **77,** 601, (1981).

27. Tanford, C., *The Hydrophobic Effect*, John Wiley & Sons, New York, 1973.

28. Tanford, C., *J. Phys. Chem.*, **76,** 3020, (1972).

29. Bancroft, W.D., and Tucker, C.W., *J. Phys. Chem.*, **31,** 1680, (1927).

30. De Gennes, P.G., Taupin, C., *J, Phys. Chem.*, **86,** 2294, (1982).

31. Cavallo, J.L., Rosano, H.L., *J. Phys. Chem.*, **90,** 6817, (1986).

32. Rosano, H.L., Jon, D., Whittam, J.H., *JAOCS*, **59,** 8, 360, (1982).

33. Eicke, H.F., Kubick, R., Hasse, R., Zschokke, I., in "*Surfactant in Solution,*" Edited by Mittal, K., and Lindman, B., Plenum Press, (1984), p. 1533-1558.

34. Cazabat, A.M., Langevin, D., Meunier, J., Pouchelon, A., *J. Phys. Lett.*, **43,** 189, (1982).

35. Kim, M.W., Huang, J.S., *Phys. Rev.*, **A34,** 719, (1986).

36. Bhattachacharaya, S., Stokes, J., Kim, M.W., Webman, I., *Phys. Rev. Lett.*, **55,** 1884, (1985).

37. Van Dijk, H.A., *Phys. Rev. Lett.*, **55,** 1003, (1985).

38. Chan, S.Y., Rosano, H.L., *J. Dispersion Science Tech.*, **9,** 5 & 6, 523, (1988-1989).

39. Lindman, B., Kamenke, N., Kathopoulis, T.M., Brun, B., Nilsson, P.G., *J. Phys. Chem.*, **84,** 2485, (1980).

40. Stilbs, P., Moseley, M.E., and Lindman, B., *J. Magn. Resonance*, **40,** 401, (1980).

41.Stilbs, P., *Progr. N.M.R. Spectrosc., in press.*

42. Stilbs, P., and Moseley, M.E., *Chem. Scripta,* **15,** 176, (1980).

43. Stilbs, P., and Moseley, M.E., *Chem. Scripta,* **15,** 215, (1980).

44. Lindman, B., Stilbs, P., and Moseley, M.E., *J. Colloid Interface Sci.,* **83,** 569, (1981).

45. Lindman, B., Stilbs, P., and Moseley, M.E., in "*Microemulsions,*" Friberg, S.E., and Botherel, P., eds., CRC Press, Cleveland, Ohio, in press.

46. Lindman, B., Ahlonas, T., Soderman, O., Waldenhaug, H., Rapacki, K., and Stilbs, P., *Faraday Disc., Chem. Soc.,* **76,** 317, (1983).

47 Stilbs, P., Rapacki, K., and Lindman, B., *J. Colloid Interface Sci.,* **95,** 583, (1983(.

48. Ceglie, A., Das, K.P., and Lindman, B., *J. Colloid Interface Sci., in press.*

49. Guering, P., and Lindman, B., *Langmuir,* **1,** 464, (1985).

50. Nilsson, P.G., and Lindman, B., *J. Phys. Chem.,* **86,** 271, (1982).

Chapter Two

1. Stoekenius, W., Schulman, J.H., and Prince, L.M., *Kolloid-Z.,* **169,** 170, 1960.

2. Shinoda, K., and Kuneida, H., *J. Colloid Interface Sci.,* **42,** 381, 1973.

3. Adamson, A.W., *J. Colloid Interface Sci.,* **29,** 261, 1969.

4. Gerbacia, W.E., Rosano, H.L., and Zajac, M., *J. Am. Oil Chem. Soc.,* **53,** 101, 1976.

5. Robbins, M.L., in "*Micellization, Solubilization, and Microemulsions,*" Mittal, K.L., Ed., Plenum Press, New York, 1977; Vol. 2, pp 713-753; See also Scriven, L.E., ibid., pp. 877-893.

6. Rosano, H.L., Lan, T., Weiss, A., Whittam, J.H., Gerbacia, W.E., *J. Phys. Chem.,* **85,** 468-473, 1981.

7. Hoar, T.P., and Schulman, J.H., *Nature (London),* **152,** 102, 1943.

8. Friberg, S.E., *Colloids Surf.*, **4, 201, 1982.**

9. Rosano, H.L., Lan, T., Weiss, A., Gerbacia, W.E.F., and Whittam, J.H., *J. Colloid Interface Sci.*, **72a (2), 1979.**

10.Rosano, H.L., Jon, D., and Whittam, J.H., *J. Am. Oil Chem. Soc.*, **59,** 360, 1982.

11.Rosano, H.L., *U.S. Patent* 4 146 499, 1979.

12.Gerbacia, W., Rosano, H.L., and Whittam, J.H., in "Colloid and Interface Science"; Kerker, M., Ed.; Academic Press: New York, 1976, Vol. II, pp 245-256.

13.Overbeek, J.Th., *Discuss. Faraday Soc.*, **65,** 7, 1978.

14.Podzimek, M., Friberg, S.E., *J. Dispersion Sci. Technol.*, **1,** 34, 1980.

15.Rosano, H.L., *J. Soc. Cosmet. Chem.*, **25,** 609, 1974.

16.Scriven, L.E., in *"Micellization, Solubilization, and Microemulsions";* Mittal, K.L.. Ed.; Plenum Press: New York, 1977; p. 277.

17.Schulman, J.H., McRoberts, M., *Trans. Faraday Soc.*, **42,** 165, 1946.

18.Di Meglio, J.M., Dvolaitsky, M., Ober, R., and Taupin, C., *J. Phys. Lett. (Orsay, Fr.),* **44,** L229-L234, 1983.

19.Hill, A.E., and Malisoff, W.M., *J. Am. Chem. Soc.*, **48,** 918, 1926.

20.Ruckenstein, E., Chi, J., *J. Chem. Soc., Faraday Trans.* **2,** 71, 1690, 1975.

21.Talmon, Y., Prager, J., *J. Chem. Phys.*, **69,** 2984, 1978.

22.De Gennes, P.G., Taupin, C., *J. Phys. Chem.*, **86,** 2294, 1982.

Chapter Three

1. Tadros, Th. F., in *"Structure/Performance Relationships in Surfactants,"* Rosen, M. J., editor, **253rd ACS Symposium Series,** ACS, Washington, D.C., 1984, p. 154.

2. Rosano, H. L., Lan, T., Weiss, A., Whittam, J. H., and Gerbacia, W. E., *J. Phys. Chem.*, **85,** 468, (1981).

3. Bowcott, J.E., and Schulman, J.H., *Z. Electro-Chem.*, **59,** (4), 283, (1955).

4. 4. Schulman, J.H., and Montague, J.H., *Ann. N.Y. Acad. Sci.*, **92,** 366, (1961).

5. Gerbacia, W.E., and Rosano, H.L., *J. Colloid Interface Sci.*, **44,** 242, (1973).

6. Gerbacia, W.E., Rosano, H.L., and Whittam, J.H., *J. Colloid Interface Sci.*, Kerker, M., editor, Academic Press, New York, 1976, **Vol. II,** pp. 245-256.

7. Rosano, H.L., Lan, T., Weiss, A., Gerbacia, W.E.F., and Whittam, J.H., *J. Colloid Interface Sci.*, **72a,** (2), 1979.

8. Rosano, H. L., *J. Soc. Cosmet. Chem.*, **25,** 609, (1974).

9. Rosano, H. L., *U. S. Patent* 4,146,499, (Mar. 27, 1979).

10. Rosano, H. L., Weiss, A., and Gerbacia, W. E., in " *Proceedings the VIIth International Congress on Surface Active Substances,*" Moscow, September 12-16, 1976, **Vol. 1,** p. 453.

11. Rosano, H. L., Jon, D., and Whittam, J. H., *J. Am. Oil Chem. Soc.*, **59,** (8), 360, (1982).

12. Bellocq, A. M., Bourbon, D., and Lemmcean, B., *to be published.*

13. Healy, R. N., Reed, R. L., and Stenmark, D. G., *SPE J.*, **16,** 147, (1976).

14. Robbins, M., *private communication.*

14. Di Meglio, J. M., Dvolaitzky, M., and Taupin, C., *to be published.*

16. Chatenay, D., Guering, P., Urback, W., Cazabat, A. M., Langevin, P., Meuiner, J., Leger, L., and Lindman, B., *to be published.*

17. Di Meglio, J. M., Paz, L., Dvoalaitzky, M., and Taupin, C., *J. Phys. Chem.*, **88,** 6036, (1984).

18. Shinoda, K., *Progr. Colloid Polymer Sci.*, **68,** 1, (1983).

19. Shinoda, K., Kunieda, H., Arai, T., and Saijo, H., *J. Phys. Chem.*, **88,** 5126, (1984).

20. Kahlweit, M., Lessner, E., and Strey, R., *J. Phys. Chem.*, **87,** 5032, (1983)

21.Lindman, B., Stilbs, P., and Moseley, M., *J. Colloid Interface Sci.*, **83,569, (1981)**

22.Di Meglio, J. M., Dvolaitzky, M., Ober, R., and Taupin, C., *J. Phys. Lett.*, **44,** L229, (1983).

23.De Gennes, P. G., and Taupin, C., *J. Chem. Phys.*, **86,** 2294, (1982).

24.Stoekenius, W., Schulman, J.H., and Prince, L.M., *Kolloid Z.*, **169,** 170, (1960).

25.Lagues, M., Ober, R., and Taupin, C., *J. Phys. Lett.*, **39,** 487, (1978).

26.Scriven, L. E., in "*Micellization, Solubilization, and Microemulsions,*" Mittal, K. L., editor, Plenum Press, New York, 1977, **Vol. 2,** p. 877.

27.Talmon, Y., and Prager, S., *J. Chem. Phys.*, **69,** 517, (1978).

28.Friberg, S., Lapezynska, I., and Gillberg, G., *J. Colloid and Interface Sci.*, **56,** 19, (1976).

29.Robbins, M. L., *Preprints, 48th National Colloid Symposium, 1974, p. 174.*

30.Cavallo, J. L., and Rosano, H. L., *J. Phys. Chem.*, **90,** 6817, (1986).

31.Weatherford, W. D., *J. Dispersion Sci. Technol.*, **6,** 467, (1985).

31.Hoar, T.P., and Schulman, J.H., *Nature,* **152,** 102, (1943).

Chapter Four

1. Rosano, H.L., and Lyons, G.B., *J. Phys. Chem.*, **89,** 363, (1985).

2. Rosano, H.L., Cavallo. J.L., and Lyons, G.B.; Presented at the 5th International Conference on Colloid and Surface Science, Potsdam, New York, June 25th-28th, 1985.

3. Rosano, H.L., Cavallo, J.L., and Lyons, G.B., in "*Microemulsion Systems,*" **Proceedings of the 59th Colloid and Surface Science Symposium and 5th International Congress on Colloid and Surface Science,** Marcel Dekker, New York, (1987), Chapt. 16, pp. 265-279.

4. Shinoda, K., Friberg, S., *Adv. Coll. Inter. Sci.*, **4,** 281, (1978).

5. Reed, R.L., Nealy, R.W., in "*Improved Oil Recovery by Surfactant and Polymer Flooding*," Academic Press, New York, 1977.

6. De Gennes, P.G., Taupin, C., *J. Phys. Chem.*, **86**, 2294, (1982).

7. Di Meglio, J.M., Dvolaitsky, M., Leger, L., Ober, R., Paz, L., Taupin, C., Presented at the 5th International Congress on Surface and Colloid Science, Potsdam, New York, June 25-28, 1985,; ibid., in "*Microemulsion Systems*," **Proceedings of the 59th International Congress on Surface and Colloid Science**, Marcel Dekker, New York, 1987.

8. Di Meglio, J.M., Dvolaitsky, M., Taupin, C., *J. Phys. Chem.*, **88**, 6036, (1983).

9. Di Meglio, J.M., Dvolaitsky, M., Ober, R., Taupin, C., *J. Phys. Lettres*, **44**, L-229, (1983).

10. Di Meglio, J.M., Dvolaitsky, M., Taupin, C., to be published, **J. Phys. Chem.**

11. "*Microemulsions*," L.M. Prince, Ed., Academic Press, New York, 1977.

12. Scriven, L.E., in "*Micellization, Solubilzation, and Microemulsion*," **Vol. 2**, K.L. Mittal, Ed., Plenum Press, New York, 1977, pg. 877.

13. Mackay, R.A., Dixit, N., Agarwal, R., and Seiders, P., *J. Dispersion Sci. Technol.*, **4**, 397, (1983).

14. Mackay, R.A., in "*Microemulsions*," I.D. Robb, Ed., Plenum Press, New York, 1982, pp. 207-219.

15. Mackay, R.A., Dixit, N.S., Hermansky, C., and Kertes, A.S., *Colloids and Surfaces*, **2**, 27, (1986).

16. Mackay, R.A., *Advances in Colloid Interface Sci.*, **15**, 131, (1981).

17. Zana, R., Mackay, R.A., *to be published in J. Coll. Inter. Sci.*

18. R.A. Mackay, *private communication.*

19. Rosano, H.L., *U.S. Patent No. 4*, 146, 499, March 27, 1979.

20. Rosano, H.L., *J. Cosmetic Chem.*, **25**, 609, (1974).

21.Macero, D.J., Ruffs, C.L., *J. Electroanal.*, **7,** 328, (1964).

22.Hoyer, H., Novodoff, J., *J. Coll. Inter. Sci.*, **26,** 490, (1968).

23.Novodoff, J., Rosano, H.L., Hoyer, H., *J. Coll. Inter. Sci.*, **38,** 426, (1972).

24.Meites, L., in "*Polarographic Techniques,*" Interscience Puublishing, 2nd Edition, New York, (1963).

25.Hoar, T.P., Schulman, J.H., *Nature (London),* **152,** 102, (1943).

26.Stoekenius, W., Schulman, J.H., and Prince, L.M., *Kolloid Z.*, **169,** 170, (1960).

27.Schulman, J.H., and Riley, D.P., *J. Colloid Sci.*, **3,** 383, (1948).

28.Schulman, J.H., and Friend, J.A., *J. Colloid Sci.*, **4,** 497, (1949).

29.Kim, M.W., Dozier, W.D., and Klein, R., *J. Chem. Phys.*, **84,** 5919, (1986).

30.Huang, J.S., and Kim, M.W., *Phys. Review Letters,* **47,** 1462, (1981).

31.Fourche, G., Belloco, A.M., Brunetti, S., *J. Colloid Interface Sci.*, **88,** 302, (1982).

32.Cazabat, A.M., and Langevin, D., *J. Chem. Phys.*, **4,** 3148, (1981).

33.Bowcott, J.E.L., and Schulman, J.H., *Z. Electrochem.*, **59,** 283, (1955).

34.Dvolaitsky, M., Guyot, M., Lagues, M., Le Pesant, J.P., Ober, R., Sauterey, C., and Taupin, C., *J. Chem. Phys.*, **69,** 3279, (1978).

35.Cavallo, J.L., and Rosano, H.L., *J. Phys. Chem.*, **90,** 6817, (1986).

36.Huang, J.S., Safran, S.A., Kim, M.W., Grest, G.S., Kotlarchyk, M., and Quirke, N., *Phys. Rev. Letters,* **53,** 592, (1984).

37.Ober, R., and Taupin, C., *J. Phys. Chem.*, **84,** 2418, (1980).

38.Kotlarchyk, M., Chen, S.H., Huang, J.S., and Kim, M.W., *Physical Review A,* **29,** 2054, (1984).

39.Zana, R., Lang, J., *Colloids and Surfaces,* **48,** 153, (1990).

40.Lianos, P., Lang, J., Strzielle, C., Zana, R., *J. Phys. Chem.*, **86,** 1019, (1982).

41.Almgren, M., Greieser, F., Thomas, J.K., *J. Am. Chem. Soc.*, **102,** 3188, (1980).

42.Cannon, P.L., Jr., Garlick, S.M., Christeson, S.D., Wong, N.M., Novelli, A.C., Longo, F.R., Mackay, R.A., *to be published.*

43.Chokshi, K., Qutubuddin, S., Hassam, A., *J. Coll. Inter. Sci.*, **129,** 315, (1989).

44.Lindman, B., Stilbs, P., in "*Microemulsion Systems,*" **Proceedings of the 59th Colloid and Surface Science Symposium and 5th International Congress on Colloid and Surface Science,** Marcel Dekker, New York, 1987, Chapt. 7, pp. 129-144.

45.Lindman, B., Stilbs, P., Moseley, M.E., *J. Coll. Inter. Sci.*, **83,** 569, (1981).

46.Langevin, D., *Adv. Coll. Inter. Sci.*, **34,** 583, (1991).

47.Shinoda, K., Lindman, B., *Langmuir*, **3,** 135, (1987).

50.Mackay, R.A., Dixit, N., and Agarwal, R., "*Inorganic Reactions in Organized Media,*" **ACS Symposium Series No. 177,** S.H. Holt, Ed., 1982, pp. 179-198.

51.Mackay, R.A., Hermansky, C., and Agarwal, R., *Colloid and Surfaces*, **2,** 27, (1986).

52.Mackay, R.A., and Agarwal, R., *J. Colloid Interface Sci.*, **65,** 225, (1978).

53.Mackay, R.A., and Agarwal, R., *J. Colloid Interface Sci.*, **65,** 225, (1978).

54.Rosano, H.L., Nixon, A.L., and Cavallo, J.L., *J. Phys. Chem.*, **93,** 4536, (1989); also, to be published in "*The Proceedings of the 2nd World Surfactants Congress,*" *ASPA, Paris, France, March 24th-28th, 1988.*

55.Rosano, H.L., Lan, T., Weiss, A., Gerbacia, W.E.E., and Whittam, J.H., *J. Colloid Interface Sci.*, **72,** 233, (1979).

Chapter Five

1. Hoar, T.P., Schulman, J.H., *Nature (London),* **152,** 102, (1943).

2. De Gennes, P.G., Taupin, C., *J. Phys. Chem.*, **82,** 2294, (1982).

3. Rosano, H.L., Lyons, G.B., *J. Phys. Chem.*, **89,** 363, (1985).

4. Rosano, H.L., Cavallo, J.L., Lyons, G.B., *Presented at the 5th International Conference on Surface and Colloid Science,* Potsdam, N.Y., June 25-28, 1975; Rosano, H.L., Cavallo, J.L., Lyons, G.B., in "*Microemulsion Systems,*" **Proceedings of the 59th Colloid and Surface Science Symposium and 5th International Congress on Colloid and Surface Science,** Marcel Dekker, New York, (1987), Chapt. 16, pp. 265-279.

5. Scriven, L.E., in "*Micellization, Solubilization, and Microemulsions,*" **Vol. 2,** K.L. Mittal, Ed., Plenum Press, New York, 1977, pg. 877.

6. Langevin, D., *Advances in Coll. Inter. Sci.,* **34,** 583, (1991).

7. Shinoda, K., Lindman, B., *Langmuir,* **3,** 135, (1987).

8. Schulman, J.H., Matalon, R., Cohen, M., *Discuss. Faraday Soc.,* **11,** 117, (1951).

9. Stoekenius, W., Schulman, J.H., Prince, L.M., *Kolloid-Z.,* **169,** 170, (1960).

10. Schulman, J.H., Riley, D.P., *J. Colloid Sci.,* **3,** 383, (1948).

11. Schulman, J.H., Friend, J.A., *J. Colloid Sci.,* **4,** 497, (1949).

12. Kim, M.W., Dozier, W.D., Klein, R., *J. Chem. Phys.,* **84,** 5919, (1986).

13. Huang, J.S., Kim, M.W., *Phys. Review Letters,* **47,** 1462, (1981).

14. Fourche, G., Belloco, A.M., Brunetti, S., *J. Colloid Interface Sci.,* **88,** 302, (1982).

15. Cazabat, A.M., Langevin, D., *J. Chem. Phys.,* **4,** 3148, (1981).

16. Bowcott, J.E.L., Schulman, J.H., *Z. Electrochem.,* **59,** 283, (1955).

17. Dvolaitsky, M., Guyot, M., Lagues, M., Le pesant, J.P., Ober, R., Sauterey, C., Taupin, C., *J. Chem. Phys.,* **9,** 3279, (1978).

18. Mackay, R.A., *Advances in Colloid Interface Sci.,* **15,** 131, (1981).

19. Mackay, R.A., Dixit, N., Agarwal, R., Seiders, P., *J. Dispersion Sci. Technol.,* **4,** 397, (1983).

20. Mackay, R.A., in "*Microemulsions,*" I.D. Robb, Ed., Plenum Press, New York, 1982, pp. 207-219.

21. Mackay, R.A., Dixit, N., and Agarwal, R., in *"Inorganic Reactions in Organized Media,"* **ACS Symposium Series No. 177,** S.H. Holt, Ed., 1982, pp. 179-198.

22. Mackay, R.A., Dixit, N.S., Hermansky, C., and Kertes, A.S., *to be published, J. Colloid Interface Sci.*

23. Mackay, R.A., Hermansky, C., Agarwal, R., in *"Colloid and Interface Science,"* **Vol. II,** M. Kerker, Ed., Academic Press, New York, 1976, pp. 289-303.

24. Hwang, J.S., Cummins, H.Z., *J. Chem. Phys.*, **77,** 616, (1982).

25. Huang, J.S., Safran, S.A., Kim, M.W., Grest, G.S., Kotlarchyk, M., Quirke, N., *Phys. Rev. Letters*, **53,** 592, (1984).

26. Ober, R., Taupin, C., *J. Phys. Chem.*, **84,** 2418, (1980).

27. Kotlarchyk, M., Chen, S.H., Huang, J.S., Kim, M.W., *Physical Review A*, **29,** 2054, (1984).

28. Cavallo, J.L., Rosano, H.L., *J. Phys. Chem.*, **90,** 6817, (1986).

29. Lyons, G.B., Rosano, H.L., *to be published.*

30. Zana, R., Lang, J., *Colloids and Surfaces*, **48,** 153, (1990).

31. Almgren, M., Greieser, F., Thomas, J.K., *J. Am. Chem. Soc.*, **102,** 3188 ,(1980).

32. Cannon, P.L., Jr., Garlick, S.M., Christeson, S.D., Wong, N.M., Novelli, A.C., Longo, F.R., Mackay, R.A., *to be published.*

33. Chokshi, K., Qutubuddin, S., Hassam, A., *J. Coll. Inter. Sci.*, **129,** 315, (1989).

34. **Rosano,** H.L., *J. Cosmetic Chem.*, **25,** 609, (1974).

35. **Rosano,** H.L., Nixon, A.L., Cavallo, J.L., *J. Phys. Chem.*, **93,** 4536, (1989); also, to be published in **"The Proceedings of the 2nd World Surfactants Congress,"** ASPA, Paris, France, March 24th-28th, 1988.

36. Rosano, H.L., Lan, T., Weiss, A., Gerbacia, W.E.F., Whittam, J.H., *J. Coll. Inter. Sci.*, **72,** 233, (1979).

37. Weatherford, W.D., *J. Dispersion Sci. Technol.*, **6,** 467, (1985).

38. Lagues, M., Sauterey, C., *J. Phys. Chem.*, **384,** 3503, (1980).

39. Bennett, K.E., Hatfield, J.C., Macosko, C.W., Scriven, L.E., in "*Microemulsions,*" Robb, I.D., Ed., Plenum Press, pp. 65-94, (1982).

40. Van Dijk, H.A., *Phys. Rev. Lett.*, **55,** 1003, (1985).

41. Eicke, H.F., Kubick, R., Hasse, Zschokke, I., in "*Microemulsions,*" Ed. by Robb, I.D., Plenum Press, 65, (1982).

42. Cazabat, A.M., Langevin, D., Meunier, J., Pouchelon, A., *J. Phys. Lett.*, **43,** L89, (1982).

43. Kim, M.W., Huang, J.S., *Phys. Rev.*, **A34,** 719, (1986).

44. Bhattachavharaya, S., Stokes, J., Kim, M.W., Webman, I., *Phys. Rev. Lett.*, **55,** 1884, (1985).

45. Bug, A.L.R., Safran, S.A., Grest, G.S., Webman, I., *Phys. Rev. Letters,* **350,** 1930, (1983).

46. Safran, S.A., Turkevich, L.A., *Discuss. Faraday Soc.*, **11,** 1117, (1951).

47. Safran, S.A., Grest, G.S., Bug, A.L.R., Webman, I., in "*Microemulsion Systems,*" **Proceedings of the 59th Colloid and Surface Science Symposium and 5th International Congress on Colloid and Surface Science,** Rosano, H.L., and Clausse, M., Marcel Dekker, New York, (1987), Chapt. 7, pp. 129-144.

48. Schulman, J.H., *N.Y. Acad. Sci.*, **92,** 366, (1961).

49. Rosano, H.L., Jon, D., Whittam, J.H., *J. Am. Oil Chem. Soc.*, **59,** 8, 360, (1982).

50. Di Meglio, J.M., Dvolaitsky, M., Leger, L., Ober, R., Paz, L., Taupin, C., **Presented at the 5th International Congress on Surface and Colloid Science,** Potsdam, New York, June 25-28, 1985.

51.Di Meglio, J.M., Paz, L., Dvolaisky, M., Taupin, C.; *J. Phys. Chem.*, **88,** 6036, (1983).

52.Di Meglio, J.M., Dvolaisky, M., Ober, R., Taupin, C., *J. Phys. Lett.*, **44,** L-229, (1983).

53.Zulauf, M., Eicke, H.F., *J. Phys. Chem.*, **83,** 480, (1982).

54. Eicke, H.F., Rehak, J., *Helv. Chim. Acta,* **59,** 2883, (1976).

55. Bellocq, *to be published.*

56. Gerbacia, W.E., Rosano, H.L., *J. Colloid Interface Sci.*, **44,** 242, (1973).

57. Bowcott, J.E., Schulman, J.H., *Z. Elektrochem.*, **59,** 4, 283, (1955).

58. Schulman, J.H., Stoeckenius, W., Prince, I.M., *J. Phys. Chem.*, **63,** 1677, (1959).

59. Goddard, E.D., Schulman, J.H., *J. Colloid Sci.*, **8,** 309, (1953). (1973).